HISTOVARIABILITY AND GROWTH IN THE BASAL CERATOPSIAN DINOSAUR *PSITTACOSAURUS MONGOLIENSIS* FROM THE LOWER CRETACEOUS KHULSANGOL FORMATION, CENTRAL MONGOLIA

by

Badamkhatan Zorigt

A dissertation submitted in partial fulfillment
of the requirements for the degree

of

Doctor of Philosophy

in

Earth Sciences

MONTANA STATE UNIVERSITY
Bozeman, Montana

April 2016

©COPYRIGHT

by

Badamkhatan Zorigt

2016

All Rights Reserved

DEDICATION

For my parents Zorigt Sanjdorj and Altantuya Natsagdorj who have always given me unconditional love and support.

ACKNOWLEDGEMENTS

This research was funded by Gerry Ohrstrom, Elizabeth Moore, David Swingle, and Matt Morse, and the Mongolian Student Scholarship Program from the Rio Tinto Inc. I thank Dr. Jack Horner, the Museum of the Rockies and the Department of Earth Sciences and Cell Biology & Neuroscience for multiple years of graduate student funding. I express my gratitude to Ellen-Therese Lamm for histology training and specimen preparations. I appreciate the time, patience, and guidance given by my committee members Dr. Jack Horner, Dr. David Varricchio, Dr. David Bowen, and Susan Gibson. My deepest gratitude goes to my advisor Dr. Jack Horner for supporting me all these years and helping me to understand the paleobiology of dinosaurs. My gratitude is extended to all my fellow graduate students (past and present) Dr. J. Scannella, Dr. E. F. Fowler, Dr. D. Fowler, Dr. H. Woodward, C. Woodruff, Dr. A. Bailleul, and Katie Tremaine for providing invaluable resources for memorable discussions, ideas, and helpful criticisms. I also thank Dr. Tsogtbaatar Khishigjav (Institute of Paleontology and Geology, Mongolian Academy of Sciences) and Dr. Bolortsetseg Minjin for their invaluable support. I would like express my gratitude to Dr. John Scannella and Tiffany Ranalli for spending their invaluable time for reviewing the earlier drafts of this dissertation. Special thanks to Bob Harmon, Carrie Ancell, and Jamie Jette for supporting me all these years. This dissertation could not be possible without the endless support and love of my family, S. Zorigt, N. Altantuya, Z. Khatanbaatar, Z. Khatantuul, Ch. Oyunnomin, E. Dulamsuren and my beautiful daughter B. Mongoljin.

TABLE OF CONTENTS

1. A BRIEF HISTORY OF PALEOBIOLOGIC RESEARCH ON THE DINOSAURS OF MONGOLIA 1

Abstract 1
Introduction 2
Stratigraphy of Lower and Upper Cretaceous Formations in Mongolia 4
Overview 4
Lower Cretaceous Formations 5
Tsagaantsav and Ondorukhaa Formations 5
Andaikhudag (Ondai Sair) Formation 6
Khulsangol Formation 6
Upper Cretaceous Formations 6
Bayanshiree Formation 6
Djadokhta Formation 7
Baruungoyot Formation 7
Nemegt Formation 7
Taxonomic Diversity of the Dinosaurs of Mongolia 8
Studies on the Dinosaur Behavior 15
Parental Care 15
Life Habit 17
Tracks from the Cretaceous Dinosaur Sites 18
Physiology of Mongolian Dinosaurs 20
Morphological Studies on Dinosaur Ontogeny 20
Histological Studies on Dinosaur Ontogeny 21
Molecular Studies 22
Conclusions 23
Summary of Dissertation 25
Literature Cited 33

2. TAPHONOMY AND DEPOSITIONAL ENVIRONMENT OF A MONODOMINANT *PSITTACOSAURUS* BONEBED FROM THE LOWER CRETACEOUS KHULSANGOL FORMATION OF CENTRAL MONGOLIA 46

Contribution of Authors and Co-Authors 46
Manuscript Information Page 47
Abstract 48
Introduction 49
Methods 49
Geologic Setting 50

TABLE OF CONTENTS - CONTINUED

Sedimentology of the Builst Khudag Site....52
Lithofacies....52
Matrix-Supported Boulder Conglomerate (Gmg)....52
Matrix-Supported, Stratified, Pebble-Cobble Conglomerate (Gmm)....53
Horizontally Stratified, Mottled Sandstone (Sh)....54
Horizontally Stratified, Homogeneous, Massive Sandstone (Sm)....54
Horizontally Stratified, Homogeneous Mustone (Fm)....55
Facies Association....55
Matrix-Supported Boulder Conglomerate (Gmg)....55
Horizontally Stratified, Mottled Sandstone (Sh) and Pebble-Cobble Conglomerate (Gmm)....56
Horizontally Stratified, Mudstone (Fm) and Structureless, Massive Sandstone (Sm)....56
Interpretation of Depositional Environment....57
Taphonomic Features....58
Taxonomic Composition of the BLK Bonebed....58
P. mongoliensis Skeletal Representation and Minimum Number of Individuals (MNI)....58
Spatial Occurrence and the Bone Preservation at the BLK Locality....59
Size Distribution of Individuals....61
Taphonomic Modification....61
Taphonomic Interpretation....63
Discussion....64
Conclusions....66
Acknowledgements....67
Literature Cited....85

3. INTRASKELETAL HISTOVARIABILITY IN THE HIND LIMB OF *PSITTACOSAURUS MONGOLIENSIS*....91

Contribution of Authors and Co-Authors....91
Manuscript Information Page....92
Abstract....93
Introduction....94
Methods....95
Results....96
Descriptions of MPC-D100/618-001....96
Femur....96

TABLE OF CONTENTS – CONTINUED

Tibia 96
Fibula 97
Descriptions of MPC-D100/620-015 97
Femur 97
Tibia 97
Fibula 98
Descriptions of MPC-D100/618-005 98
Femur 98
Tibia 98
Fibula 99
Descriptions of MPC-D100/619 99
Femur 99
Tibia 100
Fibula 100
Discussion 100
Conclusions 103
Acknowledgements 104
Literature Cited 114

4. ONTOGENETIC HISTOVARIABILITY IN A POPULATION OF *PSITTACOSAURUS MONGOLIENSIS* FROM THE LOWER CRETACEOUS KHULSANGOL FORMATION, UVURKHANGAI PROVINCE, MONGOLIA 117

Contribution of Authors and Co-Authors 117
Manuscript Information Page 118
Abstract 119
Introduction 120
Methods 122
Results 124
Growth Phase A 124
Growth Phase B 125
Growth Phase C 126
Growth Phase D 127
Discussion 129
Histological Analysis of *P. mongoliensis* 129
Regression and Growth Curves 133
Age Frequency 135
Conclusions 136
Acknowledgements 138
Literature Cited 162

TABLE OF CONTENTS – CONTINUED

5. CONCLUSIONS 166

Literature Cited 169

REFERENCES CITED.....170

LIST OF TABLES

Table Page

2.1. Lithofacies of the Khulsangol Formation in the study area 81

2.2. Identifiable skeletal elements recovered from the BLK bonebed 82

2.3. *P. mongoliensis* skeletal materials recovered from the BLK locality 83

2.4. Taxa recovered from the BLK locality. *P.mongoliensis* MNI was determined by using most common elements including femur, tibia, fibula, humerus, radius, and ulna 84

2.5. *P. mongoliensis* aggregate consists of five individuals 84

2.6. Bone modification data observed from the total of 544 skeletal elements of *P. mongoliensis* recovered from the Builst Khudag site 84

3.1. Data collected from the four *P. mongoliensis* individuals that used in this study 105

4.1. Total specimen (tibiae) list used in this study 139

4.2. Data collected from 58 histologically sectioned *P. mongoliensis* tibiae 140

4.3. Average daily bone apposition rate for each year of growth based on 365 days to compare modern vertebrates 141

4.4. Estimates of *P. mongoliensis* femur length, body length, and body mass based on regression equation and the Developmental Mass Extrapolation method 143

LIST OF FIGURES

Figure Page

1.1. Composite stratigraphic column of the Mesozoic strata in Mongolia....31

1.2. Cretaceous dinosaur sites in the Gobi Basin....32

2.1. Location map of the Early Cretaceous Builst Khudag (BLK) dinosaur site in central Mongolia....68

2.2. Simplified geologic map of the Lower Cretaceous Builst Khudag area....68

2.3. Composite stratigraphic section of the Builst Khudag (BLK) locality....69

2.4. Matrix-supported, unsorted, boulder conglomerate facies (Gmg)....70

2.5. Matrix-supported, stratified, pebble-cobble conglomerate lense (Gmm) contacts with underlying horizontally stratified, mottled sandstone facies (Sh). 71

2.6. Horizontally stratified, mottled sandstone facies (Sh) with red mudstone interbeds 72

2.7. Close-up photo of horizontally stratified, mottled sandstone facies (Sh). 72

2.8. Horizontally stratified, massive sandstone (Sm) is overlying mudstone facies (Fm)....73

2.9. Caliche from the horizontally stratified mudstone (Fm)....74

2.10. Horizontally stratified, mottled sandstone (Sh) is overlain by pebble conglomerate (Gmm). 74

2.11. Unidentified bones collected as a surface float from the BLK locality....75

2.12. Location map of BLK site showing three locations of the bonebed exposures and bone distribution....76

LIST OF FIGURES – CONTINUED

Figure Page

2.13. The panoramic view of the Ulaan shavar location at the BLK locality....77

2.14. *Psittacosaurus* skeleton preservation in the BLK site....78

2.15. Vertebrae collection from the surface float at the Ulaan shavar location at BLK site....79

2.16. Histogram, showing estimated body length distribution of the *P. mongoliensis* bone assemblage from the BLK site....79

2.17. Taphonomic map of seven articulated *P. mongoliensis* individuals from three separate quarries at the BLK site....80

2.18. Partially prepared *P. mongoliensis* femur from mottled sandstone unit....81

3.1. Transverse sections of the *P. mongoliensis* hind limb elements from the specimen MPC-D100/618-001....106

3.2. Transverse sections of the *P. mongoliensis* hind limb elements from the specimen MPC-D100/620-015....108

3.3. Transverse sections of the *P. mongoliensis* hind limb elements from the specimen MPC-D100/618-005....110

3.4. Transverse sections of the *P. mongoliensis* hind limb elements from the specimen MPC-D100/619....112

4.1. Relationship graphs between tibia length and A) diphyseal perimeter, B) diaphyseal area, and C) cortical thickness....145

4.2. Relationship graphs between tibia length and A) medullary cavity perimeter, and B) medullary cavity area....146

4.3. Ontogenetic growth curves for ten *P. mongoliensis* individuals....147

4.4. Growth curve for *P. mongoliensis*....148

LIST OF FIGURES – CONTINUED

Figure Page

4.5. Transverse sections from the four *P. mongoliensis* tibiae representing growth Phase A 149

4.6. Transverse section of the smallest *P. mongoliensis* tibia (NT002) representing growth Phase A in this study.....150

4.7. Transverse section of the *P. mongoliensis* tibia (NT003) representing growth Phase A. 151

4.8. Transverse sections from the ten *P. mongoliensis* tibiae representing growth Phase B 152

4.9. Transverse section of the *P. mongoliensis* tibia (NT009) representing growth Phase B 153

4.10. Transverse section of the *P. mongoliensis* tibia (NT017) representing growth Phase B. 154

4.11. Transverse sections from the five *P. mongoliensis* tibiae representing growth Phase C 155

4.12. Transverse section of the *P. mongoliensis* tibia (NT027) representing growth Phase C 156

4.13. Transverse sections from the eighteen *P. mongoliensis* tibiae representing growth Phase D 157

4.14. Transverse section of the *P. mongoliensis* tibia (NT034) representing growth Phase D 159

4.15. Transverse section of the *P. mongoliensis* tibia (NT071) representing growth Phase D. 160

4.16. An age frequency chart for 36 *P. mongoliensis* individuals 161

ABSTRACT

Large datasets are required in order to study the details of growth in non-avian dinosaurs. The Cretaceous dinosaur sites in Mongolia offer tremendous opportunities to collect a sufficient data for such study. This dissertation introduces a brief history of dinosaur research in Mongolia. As a result of many expeditions since the 1920s, numerous new dinosaurs were named and many new dinosaur localities have been discovered. Whereas the majority of studies of Mongolian dinosaurs have focused on the fossils of Late Cretaceous taxa, dinosaur fossils are also abundant in the Early Cretaceous dinosaur sites. One of the richest Early Cretaceous dinosaur sites is Builst Khudag (BLK) in central Mongolia. Sedimentologic and taphonomic studies of the BLK site suggest that the depositional environment of the locality indicates the occurrence of a debris flow and sheet-flood in an alluvial setting. The fossils of the parrot-beaked, herbivorous dinosaur *Psittacosaurus* is the most common taxon from the BLK site. A *Psittacosaurus* aggregation consisting of juveniles reflects a catastrophic mortality event. Previously, the humerus, femur, tibia, and fibula were suggested to represent the ideal bones for growth determination studies. Since various elements grow in different developmental regimes, it is necessary to further determine an ideal element for *Psittacosaurus* growth assessment. Associated femora, tibiae, and fibulae from four individuals were examined. The femur and tibia show comparable bone tissues in all individuals; the tibia and fibula present comparable numbers of growth lines. Based on this finding, the tibia appears to provide the most comprehensive view of growth in *Psittacosaurus*. The *Psittacosaurus* growth strategy was further assessed using 58 tibiae collected from the BLK site. The *Psittacosaurus* growth rate reaches its peak (3.19 μm/day) after passing the threshold size at the age of two. During the ages of 10-13, the body size reaches 170.3 cm in length and the growth rate is considerably slowed down. This study confirms that *Psittacosaurus* growth fits in a sigmoidal shaped curve.

CHAPTER ONE

A BRIEF HISTORY OF PALEOBIOLOGIC RESEARCH ON THE DINOSAURS OF MONGOLIA

Abstract

After the pioneering reconnaissance by the 1924 Central Asiatic Expedition led by Roy Chapman Andrews, the dinosaur fossils of Mongolia have been studied intensely by many researchers from various countries including Mongolians. Along with paleontological research, the stratigraphy of the dinosaur producing rock formations has been studied; however, the terrestrial sequences in the Gobi Basin hinder stratigraphic correlation with the International Cretaceous marine stages. A number of new dinosaur taxa including some of the rarest taxa (e.g. *Deinocheirus, Mononykus*) have been named as a result of various joint expeditions. The Gobi Basin of Mongolia offers not only a plethora of dinosaur fossils in a superb preservational state reflecting life-like postures. An abundance of herbivorous dinosaur fossils from the Mongolian Cretaceous formations widens our view of dinosaur physiology and behavior of these extinct organisms, providing insights into population growth strategy and parental care. Most of these amazing discoveries were made in early 80s. In the last two decades, the dinosaur research has been advanced using various modern techniques such as a histologic analysis, detailed morphologic studies using high resolution CT scanners, and molecular studies. Inevitably, the use of modern technology on the Mongolian fossils will aid us in understanding the life of dinosaurs in depth.

Introduction

Mongolia has been an important focus for paleontologists for many years. The abundance of dinosaur fossil and dinosaur fossils bearing rock formations still intrigue paleontologists throughout the world.

It started in 1924, when Roy Chapman Andrews led the Central Asiatic Expedition (CAE) from the American Museum of Natural History (AMNH). The CAE discovered and described the first dinosaur species from central Asia including ceratopsians (*Protoceratops andrewsi*, *Psittacosaurus mongoliensis*) and theropods (*Velociraptor mongoliensis, Saurornithoides mongoliensis,* and *Oviraptor philoceratops*). The CAE not only discovered new dinosaur taxa but also the very first dinosaur eggs and one of the world's largest collections of dinosaur ontogenetic stages from the Flaming Cliffs (late Cretaceous Djadokhta Formation). The very first geological reconnaissance work in Mongolia was also conducted by the CAE (Berkey and Morris, 1927), which resulted in stratigraphic subdivision of Cretaceous sequences in Mongolia.

Subsequent paleontological research was carried out by the Mongolian Paleontological Expedition (MPE) of the Academy of Sciences of the USSR (1946-1949; Kurochkin et al., 2000). Many new dinosaur fossil localities were discovered such as Nemegt, Altan Uul, Bugiin tsav, Bayan Shiree etc., making an invaluable contribution to Mongolian paleontology. Along with paleontological research, the geology of the dinosaur bone-bearing rock formations was studied as well.

From 1963-1971, the next wave of major paleontological research was conducted by the Polish-Mongolian Paleontological Expedition (PMPE; Kurochkin et al., 2000).

One of the most famous findings from PMPE was the discovery of a *Velociraptor* and *Protoceratops* in a "fighting" posture (Barsbold, 1974). Also, they discovered and named *Deinocheirus* (Osmólska and Roniewicz, 1970), which remained enigmatic until its recent redescription as a large ornithomimosaur (Lee et al., 2014).

Due to political change in Mongolia, the country was closed to western researchers from 1940s until 1990. Since 1990, the AMNH has resumed its operations in Mongolia (Norell et al., 1994; Novacek, 1996; Webster, 1996). One of its key discoveries was the skeleton of an *Oviraptor* found associated with eggs that contained fossilized embryos suggesting that the individual was incubating its own eggs rather than stealing those of other dinosaurs (Norell et al., 1994; Norell et al., 1995). The AMNH expedition discovered a new dinosaur-rich site in the Upper Cretaceous Nemegt Basin which was named Ukhaa Tolgod in the Late Cretaceous Nemegt Basin (Dashzeveg et al., 1995). Consequently, many new expeditions started to conduct paleontological research in Mongolia such as the Japan-Mongolia Joint Expedition (1993-2010) (Watabe and Suzuki, 2000; Watabe et al., 2008) and the Korea-Mongolia International Dinosaur Project (2001-present; Currie et al., 2003).

Recently, extensive paleontological research has been carried out by the Museum of the Rockies and the Institute of Paleontology and Geology (Mongolian Academy of Sciences). The primary aims of this expedition are 1) to train young Mongolian paleontologists and allow them to conduct their own research without any dependence on outside factors, 2) to collect adequate specimens/data for dinosaur population studies. This expedition has been actively working since 2005.

This chapter will review the history of Mongolian dinosaur paleontology including the Cretaceous formations in Gobi Basin, dinosaur taxa discovered by joint expeditions in Mongolia with an emphasis on the dinosaur behavior and physiology research resulting from these expeditions.

Stratigraphy of Lower and Upper Cretaceous Formations in Mongolia

Overview

The Cretaceous of Mongolia represents an extensional inland basin (Jerzykiewicz, 2000). The Cretaceous stratigraphic record of Mongolia is discontinuous due to localized, tectonically controlled, and episodic sedimentation in the Late Cretaceous (Jerzykiewicz, 2000). The Mongolian dinosaur-producing Cretaceous is divided into six stages: Tsagaantsav (Berriasian-Valanginian), Shinekhudag (Hauterivian-Barremian), Huhteeg (Aptian-Albian), Bayanshiree (Late Cenomanian-Coniacian to early Santonian), Djadokhta (Mid-Campanian), Baruungoyot (Mid-Late Campanian), and Nemegt (Late Campanian-Early Maastrichtian) (Gradziński et al., 1977; Fox, 1978; Lillegraven and McKenna, 1986; Jerzykiewicz and Russell, 1991).

Berkey and Morris (1927) subdivided the Cretaceous deposits of the Gobi Basin into the Ondai Sair, Oshih, Iren Dabasu, and Djadokhta formations. The authors stated that determining these formations' detailed structures and age was impossible due to their discontinuous sedimentation.

Jerzykiewicz (2000) compiled an extensive review of the upper Cretaceous formations of Mongolia that produce most of the terrestrial faunas, and produced a

composite stratigraphic column of the Mesozoic of Mongolia (Fig. 1.1). He listed the Andaikhudag (Ondaisair), Khulsangol, and Doshuul Formations in the Lower Cretaceous, and the Saynshand, Baynshiree, Djadokhta, Baruungoyot, and Nemegt formations in the Upper Cretaceous. The following dinosaur-bearing formations are distinguished by the majority of researchers: the Tsagaantsav, Andaikhudag, and Khulsangol formations in the Lower Cretaceous and the Bayanshiree, Djadokhta, Baruungoyot, and Nemegt formations in the Upper Cretaceous (Shuvalov, 2000).

Lower Cretaceous Formations

Tsagaantsav and Ondorukhaa Formations: The Tsagaantsav Formation occurs mostly in the eastern Gobi. The formation consists of conglomerates (at the base), sandstone, clays, limestone, and marls and reaches up to 150-200m in thickness. The Tsagaantsav Formation was dated at 119-141 Myr by using fossil vertebrates and invertebrates (Solovyev et al., 1977; Verzilin, 1979a; Devyatkin et al., 1990; Shuvalov, 1994). This formation is distributed at the Gurvan Ereen range, Hara-Hutul, Hamaryn Hural, Ulaan Oosh, Tsahiurt, and Gashuuny Hudag localities. The Tsagaantsav Formation produces psittacosaurid, iguanodontid, and small carnivorous dinosaurs, and pterosaurs (Kalandadze and Kurzanov, 1974).

The Tsagaantsav and Ondorukhaa formations are stratigraphically coeval (Shuvalov, 1975b). The Ondorukhaa Formation occurs in the central Mongolia. Fossil materials are scarcer than the Tsagaantsav Formation (Shuvalov, 2000).

Andaikhudag (Ondai Sair) Formation: This formation is widely distributed in central Mongolia. The Andaikhudag Formation is composed of sandstone, argillites, marls, and bituminous shales ("fish shale") (Shuvalov, 1975b). The most abundant dinosaur fossil in the Andaikhudag Formation is *Psittacosaurus.* Based on ostracod, this formation is dated as Hauterivian-Barremian age (Shuvalov, 1975b, 2000).

Khulsangol Formation: The Khulsangol Formation is richer in dinosaur fossils. The grey-colored sandstone dominates in this formation. The most common dinosaurs in the Khulsangol Formation are *Psittacosaurus*, small theropods, and sauropods. The Khulsangol Formation occurs at the Builst Khudag, Andaikhudag, Hoovor (central Mongolia); Huren Dukh, Khamar khural, Huhteeg (eastern Gobi); and Ih Ereen (south Gobi) localities (Shuvalov, 1975b, 1975a).

Upper Cretaceous Formations

Bayanshiree Formation: The Bayanshiree Formation consists of grey sandstones and gravels with isolated layers of clays and conglomerates in the lower part and multicolored clays and sandstones in the upper part. The total thickness of the formations is 150-200 m. Various horizons of the Bayanshiree Formation produce dinosaurs including ankylosaurs, ornithomimosaurs, and segnosaurs. The age of the Bayanshiree Formation has been determined to be Cenomanian to lower Santonian. A layer of basalt which overlies the formation was dated as 101-92 Myr (Shuvalov and Nikolaeva, 1985; Harland et al., 1990).

Djadokhta Formation: The Djadokhta Formation consists of red colored, very fine to fine grained, poorly sorted sandstones (Hasegawa et al., 2009). This formation is distributed in the Bayan Zag area. The thickness of the Djadokhta Formation at Bayan Mandahu is 80 m (Jerzykiewicz and Russell, 1991). The Djadokhta Formation produces many dinosaur taxa including *Protoceratops, Velociraptor, Oviraptor,* and *Pinacosaurus* (Berkey and Morris, 1927; Shuvalov, 2000).

Baruungoyot Formation: The Baruungoyot Formation is widely distributed in the Altan uul, Nemegt, Khulsan, Bugiin tsav, Hermiin tsav, Bambuu hudag, Ingenii hoovor, Shireegiin gashuun, and Ukhaa tolgod localities (Jerzykiewicz and Russell, 1991). The type section of the Baruungoyot Formation at Khulsan reaches 110 m in thickness (Gradziński and Jerzykiewicz, 1974). The lithology of the formation consists of brownish-red, fine grained, poorly cemented sandstone (Gradziński et al., 1977). The Baruungoyot Formation is relatively less fossiliferous compared to the Nemegt Formation.

Nemegt Formation: The Nemegt Formation is most famously exposed at the Nemegt and Altan Uul localities (Gradziński, 1970; Gradziński and Jerzykiewicz, 1972; Verzilin, 1979b). This formation occurs also in the Tsagaan hoshuu, Nogoon tsav, Ingenii tsav, Bambuu hudag, Bugiin tsav, Gurilin tsav, Huren tsav (Gradziński, 1970; Gradziński et al., 1977; Verzilin, 1979b; Martinson, 1982). The total thickness of the Nemegt Formation is 320 m (Gradziński, 1970). The Nemegt Formation consists mainly of grey

and yellow-brown sandstones, mudstones with interlayers of red mudstones, and intraformational gravels and conglomerates (Sochava, 1975; Verzilin, 1980, 1982).

Taxonomic Diversity of the Dinosaurs of Mongolia

Every paleontological expedition conducted in Mongolia made important discoveries in their time. The very first dinosaur species described from Mongolia was *Protoceratops andrewsi* (Granger and Gregory, 1923). The holotype consisted of a skull, lacking the occiput. In the same year, two Lower Cretaceous dinosaurs were described (Osborn, 1923), *Psittacosaurus mongoliensis* and *Protiguanodon mongoliense*. The type specimen of *Psittacosaurus* was recovered from the Oshih (Oosh) Formation at Ooshiin Nuruu range (Fig. 1.2). The type specimen was an almost complete skull and jaws of an adult animal, with the skeleton including the backbone, tail, pelvis, and limbs (Osborn, 1923). The other species, *P. mongoliense*, consisted of a nearly complete, articulated skeleton. However *P. mongoliense* is now considered as a juvenile stage of *P. mongoliensis* (Sereno, 2010).

In 1924, subsequent new dinosaur species were classified from the collection of the Central Asiatic Expedition. In the first publication resulting from the this work, Osborn (1924b) named the sauropod dinosaur *Asiatosaurus mongoliensis* and the theropod *Prodeinodon mongoliense*, both based on teeth collected from the Lower Cretaceous Oshih Formation. In the second publication, Osborn et al. (1924) described three new theropod species; *Velociraptor mongoliensis*, *Saurornithoides mongoliensis, and Oviraptor philoceratops*. The *V. mongoliensis* type specimen consisted of a skull and

jaws, one ungual and articulated phalanges. The *S. mongoliensis* specimen was a skull and jaws with teeth, series of vertebrae with pelvis, and partial hindlimbs. The type specimen of *O. philoceratops* was comprised of a skull, jaws, cervical vertebrae, and one forelimb. All three theropods were collected from the Upper Cretaceous Djadokhta Formation.

Charles Gilmore (1933) described the first ankylosaur species from the Upper Cretaceous Djadokhta Formation. The type specimen of *Pinacosaurus granger* consisted of a poorly preserved skull, jaws, and a few scattered dermal bones. E.A. Maleev (1952) described the next ankylosaur species *Talarus plicatospineus* from the Upper Cretaceous Bayan Shireh Formation. The type specimen consisted of fragmentary skull and the postcranial elements.

In the same year, the hadrosaurid *Saurolophus angustirostris* was described by Rozhdestvensky (1952). This new species was distinguished based on its cranial crest which is long, spike-like and projects upward and backward at a 45 degree angle (Rozhdestvensky, 1952; Maryanska and Osmólska, 1981).

In 1954, an article titled “A new turtle-like reptile from Mongolia” was published by Maleev. In that article Maleev (1954) described a new reptile species called *Therizinosaurus cheloniformis* that consisted of several giant claws, metacarpals, and ribs. The author thought that the appearance of this animal was turtle-like and its giant claws probably used for harvesting seaweed. Later, Rozhdestvensky (1970) properly identified that this animal as a theropod dinosaur.

Another theropod dinosaur, *Tarbosaurus bataar,* was described by Maleev (1955). The holotype of this species was found from the Nemegt Formation at the Altan Uul locality. The holotype consists of a skull and cervical vertebrae. This species is considered smaller than *Tyrannosaurus rex* from North America and it differs from *T. rex* in its more elongated snout and a greater number of maxillary and dentary teeth.

One of the most mysterious dinosaurs from Mongolia is *Deinocheirus mirificus* (Osmólska and Roniewicz, 1970). During the Polish-Mongolian Paleontological Expedition of 1965, an unusual incomplete carnosaurian dinosaur skeleton was discovered. The specimen consisted of a shoulder girdle, forelimbs, and other incomplete bone fragments. The new species was described based on the long slender scapula, long fore limbs, and manus with three uniformly developed fingers, ending in strong, large claws. Recently, Lee et al. (2014) described the nearly complete skeleton of *Deinocheirus* (MPC-D 100/127) as an ornithomimosaur. The authors suggested this animal lived near ponds or lakes and fed on fish.

Another interesting theropod dinosaur that was found during the course of the Polish – Mongolian Paleontological Expedition was *Gallimimus bullatus* (Osmólska et al., 1972). This species presents an interesting bulbous structure in the skull. The holotype was found in the locality of Tsagaan Khushuu in the Nemegt basin (Fig. 1.2). The cranium exhibits a very long, broad and dorsoventrally flattened snout. The lower jaw is shovel-like anteriorly, with elongated external mandibular fenestra.

The Polish-Mongolian Paleontological Expedition discovered four new pachycephalosaurids [*Prenocephale prenes*, *Tylocephale gilmorei*, *Homalocephale*

calathoceros, Goyocephale lattimorei (Maryanska and Osmolska, 1974; Perle et al., 1982)], two new ankylosaurids [*Saichania chulsanensis* and *Tarchia gigantea* (Maryanska, 1977)] and one ceratopsid [*Bagaceratops rozhdestvenskyi* (Maryanska and Osmólska, 1975)]. All four pachycephalosaurids were recovered from the Baruungoyot and Nemegt formations at the Khulsan and Nemegt localities (Maryanska and Osmolska, 1974; Perle et al., 1982). *B. rozhdestvenskyi* was found from the Nemegt Formation at the Khermen tsav locality (Fig. 1.2).

A subsequent major paleontological study was carried out by the Soviet-Mongolian Paleontological Expedition (SMPE) in 1969 (Kurochkin et al., 2000). Kurzanov (1976) described a new tyrannosaurid, *Alioramus remotus,* from the Nemegt Formation at Nogoon Tsav locality. A smaller body, a row of bony crests along the top of the snout, a greater number of teeth, and lower skull profile distinguish this animal from other tyrannosaurids. After thirty three years, another *Alioramus* species, *A. altai* was described by Brusatte et al. (2009).

SMPE discovered an interesting therizinosaurid theropod from the Bayan Shireh Formation at Amtgay khudag. The new species, *Segnosaurus galinensis*, was described by Perle (1979). Another therizinosaurid from the same formation was *Enigmosaurus mongoliensis* (Barsbold, 1979). Other theropod dinosaur species that were collected and described during the course of SMPE include *Garudimimus brevipes* (Barsbold, 1981), *Erlikosaurus andrewsi* (Perle, 1981), *Avimimus portentosus* (Kurzanov, 1981), *Adasaurus mongoliensis* (Barsbold, 1983), and *Harpymimus okladnikovi* (Barsbold and Perle, 1984).

In the 1980s, Maryanska and Osmolska (1981) described the first lambeosaurine from the Nemegt Formation. The holotype consisted of vertebrae, the left ilium, a partial pubis, ribs, and fragmentary hind limbs. The authors erected a new species, *Barsboldia sicinski*, based on the distinctive characters of neural spines (Maryanska and Osmólska, 1981). However this species is now included in subfamily Saurolophinae instead of Lambeosaurinae (Prieto-Márquez, 2011).

Between 1980-2009, many new dinosaur species were described from the collections of Polish-Mongolian and SMPE. The Polish-Mongolian and SMPE described the following new dinosaur species: ankylosaurids *Shamosaurus scutatus* (Tumanova, 1983), *Tsagantegia longicranialis* (Tumanova, 1993); ornithopod *Altirhinus kurzanovi* (Norman, 1998); theropods *Elmisaurus rarus* (Osmólska, 1981), *Borogovia gracillicrus* (Osmólska, 1982), *Conchoraptor gracilis* (Barsbold, 1986), *Archaeornithoides deinosauriscus* (Elzanowski, 1983), *Anserimimus planinychus* (Barsbold, 1988), *Tochisaurus nemegtensis* (Kurzanov and Osmólska, 1991), *Parvicursor remotus* (Karhu and Rautian, 1996), *Nomingia gobiensis* (Barsbold et al., 2000), *Ceratonykus oculatus* (Alifanov and Barsbold, 2009); ceratopsids *Udanoceratops tschizhovi* (Kurzanov, 1992), *Bainoceratops efremovi* (Tereschenko and Alifanov, 2003), *Gobiceratops minutus* (Alifanov, 2008).

The paleontological expeditions of the American Museum of Natural History resumed in 1990 (Novacek et al., 1994; Novacek, 1996; Webster, 1996). One of the first publications from the joint expedition was about the new theropod dinosaur *Mononykus olecranus* from the Nemegt Formation at Bugiin Tsav locality (Perle et al., 1994). This

new species differs from other alvarezsaurids in exhibiting a triangular pubis and different proportions of toe bones (Perle et al., 1994). Subsequent theropods were also described in following years including *Shuvuuia deserti* (Chiappe et al., 1998), *Achillobator giganticus* (Perle et al., 1999), *Khaan mckennai* (Clark et al., 2001), *Citipati osmolskae* (Clark et al., 2001), *Tsaagan mangas* (Norell et al., 2006), *Mahakala omnogovae* (Turner et al., 2007b), *Shanag ashile* (Turner et al., 2007a), *Zanabazar junior* (Norell et al., 2009), *Kol ghuva* (Turner et al., 2009), and *Albinykus baatar* (Nesbitt et al., 2011). The joint expedition largely focused on the new locality of Ukhaa Tolgod (Djadokhta Formation). The locality is well known by producing the aforementioned species of *C. osmolskae., K. mckennai, K. ghuva, S. deserti, T. mangas* etc. Not only were many new theropods described, but also other dinosaur species; Ksepka and Norell (2006) described a new long-necked sauropod, *Erketu ellisoni*, based on the elongated cervical vertebrae with camellae and reduced neural arch laminations. In the same year, a new neoceratopsid, *Yamaceratops dornogobiensis*, was also described (Makovicky and Norell, 2006). The holotype consisted of a partial skull missing premaxillae, rostral, predentary, much of the frill, left cheek, and posterior part of left mandible. Another ornithopod, *Haya griva,* was found in the Javkhlant Formation and was described by Makovicky et al. (2011). The holotype of this basal ornithopod consisted of a complete skull with anterior cervical vertebrae. The autapomorphies are this small ornithopod's five homodont, bulbous, and unserrated premaxillary teeth.

The Japan-Mongolia Joint Paleontological expedition started in 1997 (Watabe and Suzuki, 2000). As a result of the joint expedition, many new localities were discovered as

well as many new dinosaur species. Watabe et al. (2011) described a new pachycephalosaurid, *Amtocephale gobiensis*, from Bayan Shireh Formation. The authors stated that *A. gobiensis* could be the oldest pachycephalosaurid (Watabe et al., 2011). Recently, Tsuihiji et al. (2014) described the exceptionally well-preserved troodontid theropod *Gobivenator mongoliensis*. The holotype specimen was collected from the Djadokhta Formation at the Zamiin Khond locality.

In 1996, a team from the Mongolian Highland International Dinosaur Project collected an interesting oviraptorid skeleton from the Nemegt Formation. Later, the specimen was described by Lu et al. (2004) as a new oviraptorid species, *Nemegtomaia barsboldi*.

Sereno (2000) redescribed a small ceratopsian, *Graciliceratops mongoliensis*, that was described previously as *Microceratops gobiensis* by Maryanska and Osmolska (1975). Sereno (2000) argued that previous description of *M. gobiensis* was not enough to assign this specimen to *M. gobiensis* (Bohlin, 1953).

The legacy of previous paleontological expeditions in Mongolia is represented by more than 50 genera of the world's dinosaur treasury (Barsbold, 1997). Mongolia has contributed to the dinosaur paleontology by producing many different taxa that have been filling the gaps in the evolutionary record of the dinosaurs. Most of the dinosaur species were found mainly in Upper Cretaceous formations and represented by a single or fewer individuals consisting of almost complete material. Some dinosaur taxa (such as *Psittacosaurus* and *Protoceratops*) are represented by many individuals; larger sample

sizes are important in that they provide an opportunity to conduct population-level research.

Studies on the Dinosaur Behavior

Mongolia has been providing data on the dinosaur social behavior (Osborn, 1924a; Norell et al., 1995; Weishampel et al., 2008). Completeness and specificity of the data are crucial to interpretations of dinosaur behavior (Horner and Makela, 1979; Horner et al., 1997). The exceptional preservation of the fossil materials (e.g. "fighting dinosaur specimen of *Velociraptor* and *Protoceratops*", 3D preservation of *Protoceratops*, *Oviraptor* egg nest) in the Mongolian dinosaur beds has been providing a unique opportunity to study the behavioral aspects of dinosaur species.

Parental Care

The first discovery of the theropod dinosaur *Oviraptor* was associated with nests and eggs thought to belong to *Protoceratops andrewsi* (Osborn et al., 1924) with Osborn suggesting that *Oviraptor* fed on the eggs of *Protoceratops*. Norell et al. (1995) found an *Oviraptor* embryo within the same type of egg associated with the *Oviraptor* holotype suggesting that the holotype's proximity to the nests was related to parental care rather than to predation. The fifteen eggs in the nest are arranged in a circular pattern. Norell et al. (1995) stated that there is no nesting strategy similarity between *Maiasaura* and *Oviraptor*.

A subsequent study on oviraptorid embryos was published by Weishampel et al. (2008). The authors studied three separate oviraptorid embryos and associated eggshells

from the Nemegt Formation at the Bugin Tsav locality. The eggshells were sampled from three eggs containing embryonic remains and studied microscopically. The structure exhibited the elongatoolithid microstructure that is similar to those of embryonic eggs of the oviraptorid *Citipati osmolskae*. All three embryonic and egg specimens came from one egg clutch, possibly laid by a single female, although the embryos are different sizes (Weishampel et al., 2008). Based on the ascending process of quadratojugal, that borders more than ¾ of infratemporal fenestra, and a laterally everted acromion, the embryos were determined to belong to an oviraptorosaurian. The unfused neural arches and centra of the cervical and dorsal series represented the very latest stages of embryonic development or very close to hatching. The histology of the mid-shaft cross-section of the smaller femur exhibits porous fibro-lamellar bone tissue with weakly developed osteons. The larger femur shows fibrolamellar bone extending nearly to the periosteal surfaces. The histologic examination shows that the larger embryo has more mature tissues than the smaller individuals. The authors concluded that these embryos were in a very active growth stage and had an elevated metabolism at the time of death. Also, the authors proposed that the oviraptorids were altricial animals with asynchronous egg-laying strategy based on the size disparities of the embryos that possibly from same clutch.

Fastovsky et al. (2011) reported that parental care was a basal behavioral characteristic of ceratopsian dinosaurs. The Mongolian-Japanese expedition collected a series of fifteen fully articulated, aligned skeletons of juvenile *Protoceratops*, with the skulls all facing east-southeast. Six complete individuals show juvenile characteristics and are closely positioned along the well-defined margin, showing an originally circular

shape about 70 cm in diameter. The bone-bearing deposit is suggested to have been a sandy aeolian dune field, dominated by west-southwest winds during the Cretaceous. The authors concluded that the *Protoceratops* nest strongly supports that some kind of nest care was involved in the early post-natal developmental stages of *Protoceratops* dinosaurs.

Life Habit

One of the first famous discoveries in Mongolian dinosaur research was the discovery of the *Velociraptor* and *Protoceratops* in "fighting" posture. The specimen was discovered by Polish-Mongolian Paleontological Expedition in 1971 (Colbert, 2000). An articulated *Velociraptor* skeleton was found with hands grasping a *Protoceratops* and the *Protoceratops* exhibits a semi-erect stance with the *Velociraptor*'s right forelimb clutched between its jaws, showing a desperate fight for survival. The sediment that contains the finding consists of structureless sandstone interpreted as an arid environment with fields of sand dunes (Barsbold, 1974, 1998).

A semi-aquatic life habit of dinosaurs has been previously proposed by various workers (Matthew et al., 1915; Mook, 1918; Brown and Schlaikjer, 1940; Colbert, 1961, 1965; Barsbold, 1974; Bakker, 1986; Charig and Milner, 1986; Charig and Milner, 1997; Lacovara et al., 2002). Gregory and Mook (1925) and Tereschenko (2008) suggested that the laterally flattened tail with very high neural spines of protoceratopsids could be adapted for swimming ability. However, paleoenvironmental conditions of the Djadokhta Formation at Bayan Zag and Tugrugiin Shiree exhibit the aeolian and associated facies of a subaerial depositional system (Lefeld, 1971; Gradziński and Jerzykiewicz, 1974;

Jerzykiewicz, 1989; Eberth, 1993; Jerzykiewicz et al., 1993; Fastovsky et al., 1997). Yet the presence of freshwater mollusks, distribution of nests and the character of breaking up the egg shells (Mikhailov, 1997) also support that protoceratops dwelt near ponds. Recently, Ford and Martin (2010) proposed that psittacosaurs also had a semi-aquatic life habit based on their sprawling posture, high nares and orbits, fore and hindlimb anatomy, presence of muscle scars from strong flexor muscle on the back of the metatarsals, presence of a long tail with deep chevrons, and gastroliths.

Longrich (2010) proposed that protoceratops adapted to nocturnal life style based on their large eyes and binocular vision. The author suggested that feeding at night might allow these animals to avoid the heat of the day in their desert environment.

Tracks from the Cretaceous Dinosaur Sites

Studying dinosaur tracks and traces is crucial for determining the abundance, size, speed, ancient environmental condition, and potential population structure of the dinosaurs (Lockley et al., 1989; Lockley et al., 1994). Namnandorzhi (1957) reported the first dinosaur tracks from Mongolia: 20 dinosaur tracks from the Lower Cretaceous sediments at Mt. Saijrakh. Dinosaur tracks were later reported from the Lower Cretaceous Khuren Dukh locality (Obata and Matsukawa, 1996; Matsukawa et al., 1997). Ukhaa Tolgod, the dinosaur locality discovered by the party from the American Museum of Natural History, also produced dinosaur footprints in the eolian sand deposits (Loope et al., 1998).

Extensive research was conducted on footprints from the Nemegt Formation at the Nemegt locality by Currie et al. (2003). The authors differentiated theropod,

sauropod, and hadrosaur footprints. The footprints were preserved in soft, muddy surfaces and then they were buried rapidly by water-borne sand. The overall sedimentology of track-bearing strata indicates the marshy floodplain environments which is similar to the St. Mary River Formation of southern Alberta and other Mesozoic sites worldwide (Nadon, 1993; Currie et al., 2003).

Ishigaki et al. (2010) reported a discovery of 20,000 dinosaur footprints from a total of 18 localities. They classified the footprints into four types based on morphology. Tridactyl or tetradactyl with long, slender, and digital impressions (Type "A") could belong to variously sized theropod dinosaurs, possibly *Avimimus.* Tridactyl (Type "B") footprints with broad digital impressions could belong to *Saurolophus*. Oval or round shaped (Type "C") footprints could belong to the ankylosaurids. Type "D" footprints possibly belong to Nemegtosaurus and Opisthocoelicaudia. The footprints from Djadokhta Formation were preserved in eolian deposits with rare intercalations of fluvio-lacustrine deposits. The footprints from the Bayn Shire Formation were preserved in fluvio-lacustrine deposit. The footprints in the Baruun Goyot and Nemegt Formations were found from fluvio-lacustrine deposits with minor eolian sediments.

Niedzwiedzki et al. (2012) published an interesting paper on a footprint associated with a *Protoceratops* skeleton from the Upper Cretaceous Djadokhta Formation at Bayn Dzak (known also as the Flaming Cliffs). During preparation of the specimen, the authors discovered a footprint with the skeleton. The footprint that was associated with the *Protoceratops* was a tetradactyl, digitigrade, and 9.1 cm wide and 7.8 cm in length. The

track was preserved in reddish-brown sandstone, cemented by carbonate and silica matrix.

Physiology of Mongolian Dinosaurs

Morphological Studies on Dinosaur Ontogeny

In the last decades, the role of dinosaur ontogeny has been considered seriously (e.g., Rozhdestvensky, 1965; Dodson, 1976; Horner and Makela, 1979; Sampson et al., 1997). Collecting larger samples of taxa has been increasing our knowledge of different growth stages for certain dinosaur species and has revealed morphological changes throughout ontogeny (Horner and Goodwin, 2009; Scannella and Horner, 2010; Fowler et al., 2011).

The very first dinosaur ontogenetic study was conducted on the ornithischian dinosaur *Protoceratops*, involving more than 40 skulls collected from the locality of Bayan Dzak (also known as the Flaming Cliffs) by Central Asiatic Expedition (Brown and Schlaikjer, 1940). Brown and Schlaikjer (1940) published a detailed description of *Protoceratops* cranial morphology based on these different ontogenetic stages, with special attention given to "salient growth changes": the parietal-squamosal frill expands; the orbit reduced; and the facial area deepens throughout ontogeny. The authors noted that not a single important feature in the *Protoceratops* skull remains constant throughout its ontogeny.

Another important paper was subsequently published on the ontogenetic variation of theropod dinosaurs by Rozhdestvensky (1965). He proposed that three tyrannosaur

species (*Tyrannosaurus bataar, Tarbosaurus efremovi*, and *Gorgosaurus lancinator*) could be three different growth stages of single tyrannosaur species *T. bataar*. He suggested that these taxa had been differentiated mainly by differences in size, relative robustness of the skull, and the different numbers of teeth.

Tsuihiji et al. (2011) reported the first and most complete juvenile *T. bataar* specimen (MPC-D 107/7) that was collected from the Nemegt Formation. The specimen exhibits juvenile characteristics including elongated antorbital fenestra, lack of interdigitating transverse ridges and grooves that reinforce the suture between nasal and maxilla in adults, thinner labiolingually lateral teeth than adults etc. The histological analysis revealed that this individual died at age 2-3.

Dodson (1976) conducted a biometric study on *Protoceratops andrewsi* concerning relative growth and sexual dimorphism. The author used bivariate plots, measurement ratios, and a principal component analysis. In the result, he distinguished two morphs of *Protoceratops* proposing that they represent male and female. He proposed that important features for sexual discriminators include width of the frill, nasal height of the skull, and height of the skull. However, the length of the orbit, separation of the parietal fenestrae, and thickness of the frill do not function as sexual discriminators.

Histological Studies on Dinosaur Ontogeny

Bone histology provides a unique opportunity to explore the physiology and the life history of dinosaurs. Erickson and Tumanova (2000) performed the first major histological study on *Psittacosaurus mongoliensis*. In this study, the authors utilized seventeen specimens consisting of humeri, femora, and tibiae. However, different skeletal

elements exhibit different histology because of their various remodeling rates (Horner et al., 1999). Based on vascular patterns within the fibrolamellar tissue, the specimens were classified into groups A-G representing ages 3-9. Interestingly, the vascularities of the bones increased rather than decreased as the animal became older. The authors developed the Developmental Mass Extrapolation method to calculate the body mass of *Psittacosaurus* individuals. The femoral diaphysis was used for determining the body mass. They concluded that the estimated mass ranged from 0.94 kg for the smallest (age 3) to 19.87 kg for the largest individual (age 9). A sigmoidal growth curve was produced. This was the first study that used the mass estimates to produce a growth curve from ontogenetic series of *P. mongoliensis* (Erickson and Tumanova, 2000).

P. lujiatunensis experienced a high mortality rate until they reached three years of age (Erickson et al., 2009). Interestingly, *Maiasaura* had a similar mortality rate in the first and third year of development (Woodward et al., 2015). Sexual maturity of *P. lujiatunensis* started in the tenth year of life (Erickson et al., 2009) but at three years of age in *Maiasaura* (Woodward et al., 2015).

A histological study on *Protoceratops* postcranial bones was conducted by Makovicky et al. (2007). The authors used more than 100 specimens collected by the Central Asian Expedition in the 1920's. They concluded that growth of the *Protoceratops* slowed around 9-10 years in age and eventually ceased around 11-13 years.

Molecular Studies

Schweitzer et al. (1999) conducted the first molecular study on the alvarezsaurid *Shuvuuia deserti*. The authors found small fibers in association with specimen (IGM

100/977) that might represent degradation products of the protein beta keratin. The specimen was collected from the Late Cretaceous Ukhaa Tolgod locality in 1993. Small, white fibers of varying lengths and diameters were found around the perimeter of the bones. These fibers were about 200 um in diameter and 0.5 um in cross section. These small fibers contain organic components that are degradation products of the protein beta keratin. The authors proposed that the chemical (beta keratin) and physical (hollowness) characteristics of these fibers could be protofeathers. However, these fibers did not possess morphological similarities that are observed in modern feathers such as complex branching.

Conclusions

Since the AMNH expedition in 1923, numerous dinosaur species from Mongolia have been described along with the discoveries of numerous important dinosaur sites. However, many of the taxa were described from partial skeletons that might not be sufficient to diagnose valid species. Many species were incorrectly determined to represent new species but actually reflect different ontogenetic stages of known taxa. In the early years of paleontology of Mongolia, specimens were collected with insufficient taphonomic and stratigraphic data. Unfortunately, the scientific utility of those specimens is limited. Today, paleontologists tend to use relatively large sample sizes with sufficient stratigraphic and histologic data to assess the ontogenetic state of dinosaurs. Multiple years of fieldwork are necessary at highly fossiliferous sites to obtain adequate samples for such research.

Explorations of paleohistology have been increasing in recent dinosaur ontogenetic research. Past studies using fewer specimens for histological analysis may have led to possible misinterpretation about the dinosaur growth rate because of the individual histological variation that could greatly skew the result. The histology of different skeletal elements also affects the result because the different skeletal elements have different remodeling rates (Horner et al., 1999). To obtain a reliable result, using a large sample size that consists of the same skeletal element is crucial. A large sample size would help us to encompass the individual histologic anomaly that could skew the result. The Cretaceous formations (e.g. Khulsangol, Djadokhta formations) of Mongolia provide a unique opportunity to collect more specimens of multiple growth stages of single dinosaur species that would allow us to draw more reliable conclusions about their growth rate.

Studying dinosaur ontogeny is important to understanding dinosaur biology. Studies on dinosaur cranial variation combined with histological analysis (Horner and Goodwin, 2006; Scannella and Horner, 2010) have been advancing our knowledge in the dinosaur ontogeny. Cranial morphological studies of ceratopsian dinosaurs from Mongolia are meaningless without a thorough ontogenetic histology study. The dinosaur sites (e.g. Tugrikiin Shiree, Bayan Zag, Builst Khudag) in Mongolia offer a great opportunity to collect large cranial and postcranial samples of abundant dinosaur taxa such as *Protoceratops*, *Psittacosaurus* with good stratigraphic and taphonomic data to thoroughly study the intraspecific variation and ontogeny of these basal ceratopsians.

Summary of Dissertation

Previous studies of the dinosaur fossils of Mongolia have focused on the charismatic Upper Cretaceous localities and taxa. However, the fossil abundance of the Early Cretaceous dinosaur sites in the Gobi desert is similar to those of the Upper Cretaceous localities. The stratigraphy and taphonomy of the Early Cretaceous localities [e.g. Khuren Dukh, Khamryn-Us, Oosh, Builst Khudag (BLK)] have been studied briefly, and only a few papers were published on them (e.g., Kalandadze and Kurzanov, 1974; Shuvalov, 1974; Bratseva and Novodvorskaya, 1975; Shuvalov, 1975a; Martinson and Shuvalov, 1976). The Builst Khudag (BLK) dinosaur site is one of the understudied Mongolian localities. Since its discovery in the 1970s, a very few researchers have worked at the BLK site. A framework study of the taphonomy and depositional environment of the dinosaur-bearing rock units of this site is necessary to understand better the paleobiological aspects and the life history of the most common Early Cretaceous dinosaur *Psittacosaurus*.

Today, the spectrum of dinosaur research is not limited only to the conservative morphologic analyses of the bones as it has been in the past. Paleohistology has been playing a major role in the assessment of ontogenetic stages and the growth analysis of the dinosaurs. In the last two decades, the growth strategies of many dinosaur taxa have been determined (e.g., Varricchio, 1993; Chinsamy, 1994; Curry, 1999; Horner et al., 1999; Erickson and Tumanova, 2000; Horner et al., 2000; Sander, 2000; Horner and Padian, 2004; Sander and Klein, 2005; Reizner and Horner, 2006; Erickson et al., 2009; Klein et al., 2009; Werning, 2012). However, most of those studies have used fewer

numbers of various skeletal elements to reconstruct growth curves. There is an evidence suggesting that not all skeletal elements were developed in the same histologic regime (Horner et al., 1999); therefore, using the histologic features (e.g. numbers of growth lines) from various bones could lead to confusion when constructing a growth curve for a particular dinosaur taxon. Moreover, individuals' histologic variations are necessary to be encompassed to determine a population size histologic analysis. In order to resolve this issue, a larger set of samples consisting of same-skeletal elements has been required. The Early Cretaceous dinosaur-rich localities of Mongolia, such as the BLK and Oosh, offer an incredible opportunity to conduct an extensive paleobiologic research on the growth of the Early Createcous herbivorous dinosaur *Psittacosaurus*.

The main purpose of this dissertation is to investigate the life history of the *P. mongoliensis* population by examining the local sedimentology, taphonomy, and a large data set of specimens consisting of a single-skeletal element from each individual. In order to conduct in-depth research, overviewing previous dinosaur studies in Mongolia is important. Chapter One reviews previous paleobiologic studies on the dinosaurs from Mongolia. Since the 1920s, various expeditions have worked in the Gobi Desert of Mongolia. Because of that, a number of new taxa of dinosaur have been named; as well, many new dinosaur localities have been discovered. More than 50 genera of the world's dinosaur treasury were named from the Mongolian Cretaceous formations (Barsbold, 1997). Exceptionally preserved dinosaur fossils have been discovered from many new dinosaur sites such as Ukhaa tolgod (Dashzeveg et al., 1995). On dinosaur behavior, various discoveries have been made from the Cretaceous formations in Mongolia. There

is a world class specimen discovered by the Polish-Mongolian expedition consisting of an association of two dinosaurs suggesting a fight between herbivorous and carnivorous dinosaurs (Barsbold, 1974). Another finding consisting of a close association of theropod dinosaur and its eggs suggests nesting behavior of carnivorous dinosaurs. Moreover, the eggs with the associated embryos were found from the famous Djadokhta and Nemegt formations (Norell et al., 1994; Weishampel et al., 2008). The fossils from the Cretaceous formations in Mongolia have been contributed to dinosaur physiological research. A morphology-based study on the herbivorous ceratopsian dinosaur *Protoceratops* suggested the occurrence of gradual cranial change during its ontogeny (Brown and Schlaikjer, 1940). An ontogenetic histological study on the Early Cretaceous ceratopsian *Psittacosaurus* was carried out as well. The result of this study suggests that vascularity in the *Psittacosaurus* long bones increases as the animal became older (Erickson and Tumanova, 2000). However, the histologic study on *Psittacosaurus* was somewhat incomplete due to a lack of samples for observation of the intra-skeletal histologic variations and individual histologic variations.

Chapter Two discusses the sedimentology and taphonomy of the dinosaur-fossil rich, Early Cretaceous Builds Khudag (BLK) locality in central Mongolia. Since its discovery in 1970s, this site has been known as one of the dinosaur producing Early Cretaceous site. Unfortunately, the geology and paleontology of the site have been poorly studied. The BLK deserves more attention to research due to its richness of dinosaur fossils. A comprehensive sedimentologic study was required to determine the taphonomic mode of the site. The stratigraphic section of the BLK site consists of a boulder

conglomerate bed at the base, stratified-mottled sandstone producing a majority of dinosaur bones, thin mudstone layer and structureless medium sandstone at the top of the section. Based on the sedimentologic data, the depositional environment of the site reflects a combination of the debris flow and sheet-flood deposits that occurred in the alluvial fan. The majority of the bones collected from the site are identified as *P. mongoliensis* suggesting a monodominant *P. mongoliensis* bonebed. The combination of sedimentologic and taphonomic data suggests that the *P. mongoliensis* individuals died and were buried simultaneously. The *P. mongoliensis* aggregation consisting of five individuals supports the idea that this animal lived in a juvenile-only cluster between 2-5 years old. However, the size range of these individuals is larger than the similar juvenile aggregations of different *Psittacosaurus* species from China. This size disparity could be explained as a taxon-specific growth rate of *P. mongoliensis*.

Chapter Three details the intraskeletal histologic variations of the *P. mongoliensis* hind limb. Assessing ideal skeletal element for the skeletochronology prior to constructing the growth curve for *P. mongoliensis* is crucial. However, the femur and tibia were suggested as the best for the age determination (Horner et al., 1999). In previous studies, the *Psittacosaurus* long bones including the humerus, femur, tibia, and fibula have been used in the previous studies (Erickson and Tumanova, 2000; Erickson et al., 2009). The actual use of those bones in the skeletochronologic and ontogenetic assessment of this animal has been vague. In this chapter, we compared the histology of hind limb elements including the femur, tibia, and fibula from four individuals reflecting different ontogenetic stages. The bone tissue combinations in the associated femur and

tibia present similarly in each individual; whereas, the fibula shows a different tissue. Probably, this tissue difference is somewhat related to the weight-bearing function of the bones as the tibia and femur bear the most of the body weight whereas the fibula is responsible for the smaller portion of the gross weight. Skeletochronologically, the tibia and fibula show comparable numbers of growth lines in the cortex. The femur shows a lower number of growth lines compared to the associated tibia and fibula. The innermost growth lines may have been erased due to the extensive expansion of medullary cavity in the femur. The innermost cortices of the all elements including the femur, tibia, and fibula from the largest individual were invaded by the extensive resorption cavities, suggesting the weight-bearing hind limb elements reflect a considerable physiological change (possible initiation of skeletal maturity) simultaneously.

The final study, detailed in Chapter Four, determines the growth strategy of *P. mongoliensis* using a larger sample size (n=58) than previous studies, consisting of various sizes of *P. mongoliensis* tibiae from the same bonebed at the BLK locality. Four ontogenetic growth phases (A, B, C, and D) of *P. mongoliensis* are determined based on the tissue types. In growth phase A, the tibiae (n=4) reflect a fast growing, unorganized bone tissue in the first two years of life. Growth phase B (represented by 10 tibiae) occurs in the next 2-5 years, presenting an extremely fast-growing bone tissue that consisted of a combination of reticular and radial tissues. Growth phase C is represented by an occurrence of the reticular/sub-plexiform vascularization with the parallel-fibered bone matrix. The bones in growth phase D exhibits mostly plexiform vascularization, sometimes combined with the reticular vascularization. The large resorption cavities are

common in the inner cortices. Some tibiae even show a pack of growth line in the periosteum reflecting a possible External Fundamental System (EFS), which indicates the skeletal maturity. However, it was impossible to trace those lines in the entire bone due to patchy preservations of the specimens. For that reason, we hesitate to determine this feature as a positive EFS. During the first two years of life, *P. mongoliensis* reached a threshold body size. After the tenth year (Phase D), the growth considerably slowed down. At this stage, the body mass reached up to 46.6 kg and 170.3 cm in body length. The growth curve of *P. mongoliensis* is comparable to those of *P. lujiatunensis* (Erickson et al., 2009). In general, there is a considerable amount of histologic variation between similarly sized individuals.

Figure 1.1. Composite stratigraphic column of the Mesozoic strata in Mongolia (derived from Jerzykiewicz, 1991, incorporating data from: Gradzinsky, 1970; Gradzinsky and Jerzykiewicz, 1974; Shuvalov, 1975; Sochava, 1975; Jerzykiewicz, 1995).

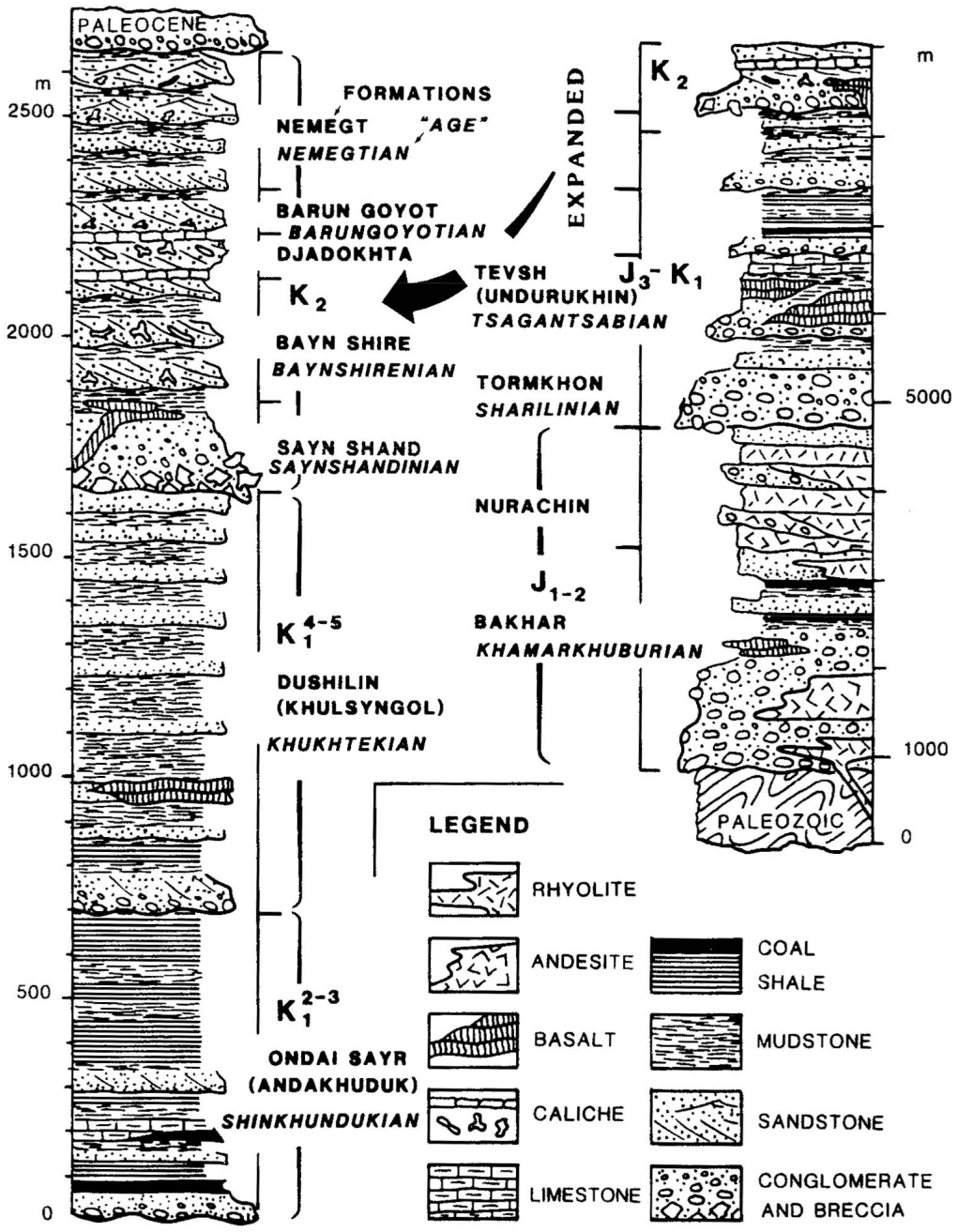
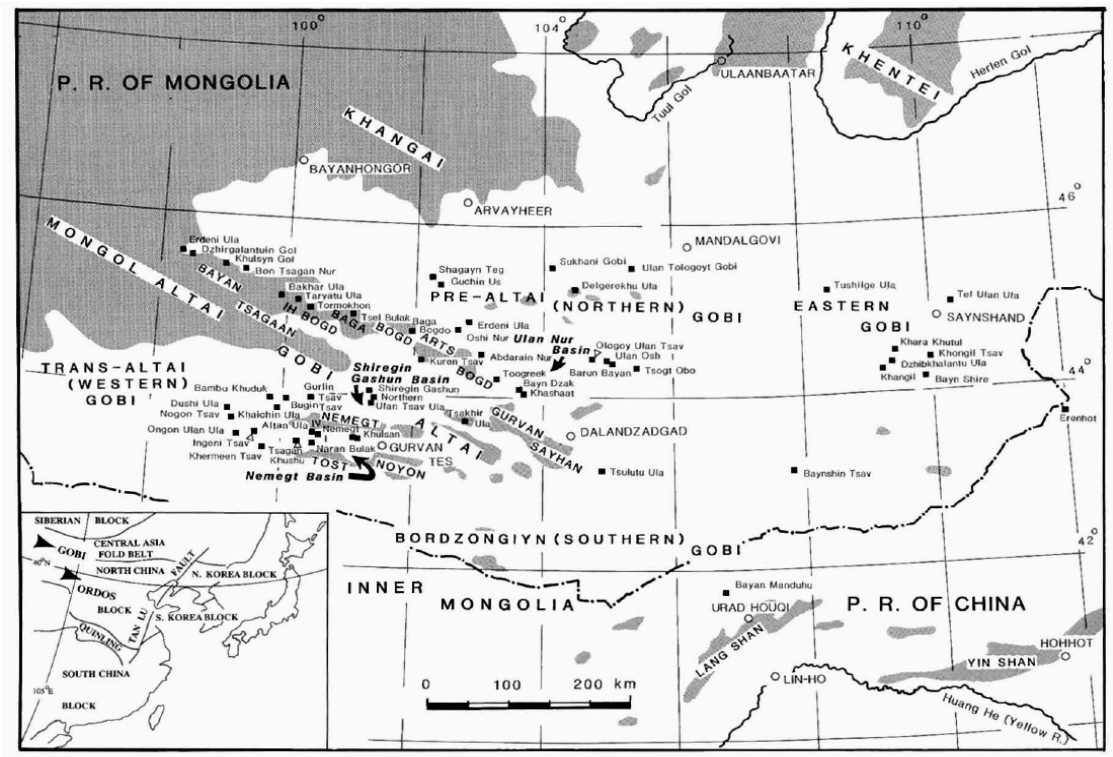


Figure 1.2. Cretaceous dinosaur sites in the Gobi Basin (derived from Jerzykiewicz and Russell, 1991).



Literature Cited

Alifanov, V. R. 2008. The tiny horned dinosaur *Gobiceratops minutus* gen. et sp. nov.(Bagaceratopidae, Neoceratopsia) from the Upper Cretaceous of Mongolia. Paleontological Journal 42: 621-633.

Alifanov, V. R., and R. Barsbold. 2009. *Ceratonykus oculatus* gen. et sp. nov., a new dinosaur (? Theropoda, Alvarezsauria) from the Late Cretaceous of Mongolia. Paleontological Journal 43: 94-106.

Bakker, R. T. 1986. The Dinosaur Heresies, New Theories Unlocking the Mystery of the Dinosaurs and Their Extinction. William Morrow and Co., New York.

Barsbold, R. 1974. Duel of Dinosaurs. Pryroda 2: 81-83.

Barsbold, R. 1979. Opisthopubic pelvis in the carnivorous dinosaurs. Nature 279: 792-793.

Barsbold, R. 1981. Toothless carnivorous dinosaurs of Mongolia. Trudy Sovmestnoi Sovetsko-Mongol'skoi Paleontologicheskoi Ekspeditsii 15: 28-39.

Barsbold, R. 1983. Carnivorous dinosaurs of the Cretaceous of Mongolia. Trudy Sovmestnoi Sovetsko-Mongol'skoi Paleontologicheskoi Ekspeditsii. 13: 50-112.

Barsbold, R. 1986. Raubdinosaurier Oviraptoren. Herpetologische Untersuchungen in der Mongolischen Volksrepublik: 210-223.

Barsbold, R. 1988. A new Late Cretaceous ornithomimid from the Mongolian People's Republic. Paleontological Journal 1: 124-127.

Barsbold, R. 1997. Mongolian dinosaurs; pp. 447-450 *i*n P. J. Currie, and K. Padian (eds.), The encyclopedia of dinosaurs. Academic Press., San Diego.

Barsbold, R. 1998. Fighting dinosaurs—they really fought: In *Encontro Internacional sobre Paleobiologia dos Dinossáurios: Programa de Musealização para Pistas de Dinossáurios em Portugal*, C. M. de Carvalho AMG, Andrade AMPSAF, da Silva CAPFM, dos Santos VAF ed, pp. 74-78. Museu Nacional de História Natural, Lisbon, Portugal.

Barsbold, R., H. Osmólska, M. Watabe, P. J. Currie, and K. Tsogtbaatar. 2000. A new oviraptorosaur [Dinosauria, Theropoda] from Mongolia: the first dinosaur with a pygostyle. Acta Palaeontologica Polonica 45: 97-106.

Barsbold, R., and A. Perle. 1984. On first finding of primitive ornithomimosauria from the Cretaceous of the MPR (Mongolian Peoples-Republic). Paleontologicheskiy Zhurnal: 121-123.

Berkey, C. P., and F. K. Morris. 1927. Geology of Mongolia; pp. 456, Central Asiatic Expeditions. American Museum of the Natural History, New York.

Bohlin, B. 1953. Fossil reptiles from Mongolia and Kansu. Rep. Sino-Swedish Expedition Publication 37: 113.

Bratseva, G. M., and I. M. Novodvorskaya. 1975. Spore and pollen from the Early Cretaceous Khuren Dukh locality. Trudy Sovmetstnoi Sovetsko-Mongol'skoi Paleontologicheskoya Ekspeditsii. 2: 205-209.

Brown, B. B., and E. M. Schlaikjer. 1940. The structure and relationships of *Protoceratops*. Transactions of the New York Academy of Sciences 2: 99-100.

Brusatte, S. L., T. D. Carr, G. M. Erickson, G. S. Bever, and M. A. Norell. 2009. A long-snouted, multihorned tyrannosaurid from the Late Cretaceous of Mongolia. Proceedings of the National Academy of Sciences 106: 17261-17266.

Charig, A. J., and A. C. Milner. 1986. *Baryonyx*, a remarkable new theropod dinosaur. Nature 324: 359-361.

Charig, A. J., and A. C. Milner. 1997. *Baryonyx walkeri*, a fish-eating dinosaur from the Wealden of Surrey. Bulletin - Natural History Museum Geology Series 53: 11-70.

Chiappe, L. M., M. A. Norell, and J. M. Clark. 1998. The skull of a relative of the stem-group bird *Mononykus*. Nature 392: 275-278.

Chinsamy, A. 1994. Dinosaur bone histology: implications and inferences.; pp. 213-227 *i*n D. Rosenberg, and D. L. Wolberg (eds.), Dino Fest. The Paleontological Society Special Publication No. 7.

Clark, J. M., M. A. Norell, and R. Barsbold. 2001. Two new oviraptorids (Theropoda: Oviraptorosauria), Upper Cretaceous Djadokhta Formation, Ukhaa Tolgod, Mongolia. Journal of Vertebrate Paleontology 21: 209-213.

Colbert, E. H. 1961. Dinosaurs: their discovery and their world. New York, Dutton.

Colbert, E. H. 1965. The Age of Reptiles. Weidenfeld & Nicolson, London.

Colbert, E. H. 2000. Asiatic dinosaur rush; pp. 211-234 *i*n M. J. Benton, M. A. Shishkin, D. M. Unwin, and E. N. Kurochkin (eds.), The age of dinosaurs in Russia and Mongolia. Cambridge University Press.

Currie, P., D. Badamgarav, and E. Koppelhus. 2003. The first Late Cretaceous footprints from the Nemegt locality in the Gobi of Mongolia. Ichnos 10: 1-13.

Curry, K. A. 1999. Ontogenetic histology of *Apatosaurus* (Dinosauria: Sauropoda): New insights on growth rates and longevity. Journal of Vertebrate Paleontology 19: 654-665.

Dashzeveg, D., M. J. Novacek, M. A. Norell, J. M. Clark, L. M. Chiappe, A. Davidson, M. C. McKenna, L. Dingus, C. Swisher, and P. Altangerel. 1995. Extraordinary preservation in a new vertebrate assemblage from the Late Cretaceous of Mongolia. Nature 374: 446-449.

Devyatkin, E. V., T. V. Nikolaeva, and V. F. Shuvalov. 1990. [Structural geomorphological position and main stages of activity of the basalt magmatism in Mongolia in Mesozoic and Cenozoic]; pp. 126-134, Geodynamics of Intercontinental Mountain Regions. Nauka, Novosibirsk.

Dodson, P. 1976. Quantitative aspects of relative growth and sexual dimorphism in *Protoceratops*. Journal of Paleontology: 929-940.

Eberth, D. 1993. Depositional environments and fades transitions of dinosaur-bearing Upper Cretaceous redbeds at Bayan Mandahu (Inner Mongolia, People's Republic of China). Canadian Journal of Earth Sciences 30: 2196-2213.

Elzanowski, A. 1983. Birds in Cretaceous ecosystems. Acta Palaeontologica Polonica 28: 75-92.

Erickson, G. M., P. J. Makovicky, B. D. Inouye, C. F. Zhou, and K. Q. Gao. 2009. A Life Table for *Psittacosaurus lujiatunensis*: Initial Insights Into Ornithischian Dinosaur Population Biology (vol 292, pg 1514, 2009). Anatomical Record-Advances in Integrative Anatomy and Evolutionary Biology 292: 1684-1684.

Erickson, G. M., and T. A. Tumanova. 2000. Growth curve of *Psittacosaurus mongoliensis* Osborn (Ceratopsia : Psittacosauridae) inferred from long bone histology. Zoological Journal of the Linnean Society 130: 551-566.

Fastovsky, D., D. Weishampel, M. Watabe, R. Barsbold, K. Tsogtbaatar, and P. Narmandakh. 2011. A nest of *Protoceratops andrewsi* (Dinosauria, Ornithischia). Journal of Paleontology 85: 1035-1041.

Fastovsky, D. E., D. Badamgarav, H. Ishimoto, M. Watabe, and D. B. Weishampel. 1997. The paleoenvironments of Tugrikin-Shireh (Gobi Desert, Mongolia) and aspects of the taphonomy and paleoecology of *Protoceratops* (Dinosauria: Ornithishichia). Palaios: 59-70.

Ford, T. L., and L. D. Martin. 2010: A semi-aquatic life habit for *Psittacosaurus*. Paper presented at the New Perspectives on Horned Dinosaurs: The Royal Tyrrell Museum Ceratopsian Symposium, 2010.

Fowler, D. W., H. N. Woodward, E. A. Freedman, P. L. Larson, and J. R. Horner. 2011. Reanalysis of "*Raptorex kriegsteini*": a juvenile tyrannosaurid dinosaur from Mongolia. PloS one 6: e21376.

Fox, R. C. 1978. Upper Cretaceous terrestrial vertebrate stratigraphy of the Gobi Desert (Mongolian People's Republic) and western North America. Geological Association of Canada Special Paper 18: 571-594.

Gilmore, C. W. 1933. Two new dinosaurian reptiles from Mongolia with notes on some fragmentary specimens. American Museum Novitates 679: 1-20.

Gradziński, R. 1970. Sedimentation of dinosaur-bearing Upper Cretaceous deposits of the Nemegt Basin, Gobi Desert. Palaeontologia Polonica 21: 147-229.

Gradziński, R., and T. Jerzykiewicz. 1972. Additional geographical and geological data from the Polish-Mongolian Palaeontological Expeditions. Palaeontologia Polonica 22: 17-32.

Gradziński, R., and T. Jerzykiewicz. 1974. Dinosaur and mammal-bearing aeolian and associated deposits of the Upper Cretaceous in the Gobi Desert (Mongolia). Sedimentary Geology 12: 249-278.

Gradziński, R., Z. Kielan-Jaworowska, and T. Maryańska. 1977. Upper Cretaceous Djadokhta, Barun Goyot and Nemegt formations of Mongolia, including remarks on previous subdivisions. Acta Geologica Polonica 27: 281-318.

Granger, W., and W. K. Gregory. 1923. *Protoceratops andrewsi*, a pre-ceratopsian dinosaur from Mongolia. American Museum Novitates 42: 1-9.

Gregory, W. K., and C. C. Mook. 1925. On *Protoceratops*, a primitive ceratopsian dinosaur from the Lower Cretaceous of Mongolia. American Museum of Natural History.

Harland, W. B., R. L. Armstrong, A. V. Cox, L. E. Craig, A. G. Smith, and D. G. Smith. 1990. A geologic time scale. Cambridge: Cambridge University Press: 263.

Hasegawa, H., R. Tada, N. Ichinnorov, and C. Minjin. 2009. Lithostratigraphy and depositional environments of the Upper Cretaceous Djadokhta Formation, Ulan Nuur basin, southern Mongolia, and its paleoclimatic implication. Journal of Asian Earth Sciences 35: 13-26.

Horner, J., K. Padian, and A. de Ricqlès. 1997. Histological analysis of a dinosaur skeleton: evidence of skeletal growth variation. Journal of Morphology 232: 267.

Horner, J. R., A. de Ricqles, and K. Padian. 1999. Variation in dinosaur skeletochronology indicators: implications for age assessment and physiology. Paleobiology 25: 295-304.

Horner, J. R., A. de Ricqles, and K. Padian. 2000. Long bone histology of the hadrosaurid dinosaur *Maiasaura peeblesorum*: growth dynamics and physiology based on an ontogenetic series of skeletal elements. Journal of Vertebrate Paleontology 20: 115-129.

Horner, J. R., and M. B. Goodwin. 2006. Major cranial changes during *Triceratops* ontogeny. Proceedings of the Royal Society of London B: Biological Sciences 273: 2757-2761.

Horner, J. R., and M. B. Goodwin. 2009. Extreme cranial ontogeny in the Upper Cretaceous dinosaur *Pachycephalosaurus*. PloS one 4: e7626.

Horner, J. R., and R. Makela. 1979. Nest of juveniles provides evidence of family structure among dinosaurs.

Horner, J. R., and K. Padian. 2004. Age and Growth Dynamics of *Tyrannosaurus*. Proceedings: Biological Sciences 271: 1875-1880.

Ishigaki, S., M. Watabe, K. Tsogtbaatar, and M. Saneyoshi. 2010. Dinosaur footprints from the Upper Cretaceous of Mongolia. Geological Quarterly 53: 449-460.

Jerzykiewicz, T. 1989: Upper Cretaceous dinosaur-bearing eolianites in the Mongolian Basin. Paper presented at the Sixth Symposium on Mesozoic Terrestrial Ecosystems: abstracts, 1989.

Jerzykiewicz, T. 2000. Lithostratigraphy and sedimentary settings of the Cretaceous dinosaur beds of Mongolia.; pp. 279-296 *i*n M. J. Benton, M. A. Shishkin, and D. M. Unwin (eds.), The age of dinosaurs in Russia and Mongolia. Cambridge University Press.

Jerzykiewicz, T., P. Currie, D. Eberth, P. Johnston, E. Koster, and J.-J. Zheng. 1993. Djadokhta Formation correlative strata in Chinese Inner Mongolia: an overview of the stratigraphy, sedimentary geology, and paleontology and comparisons with the type locality in the pre-Altai Gobi. Canadian Journal of Earth Sciences 30: 2180-2195.

Jerzykiewicz, T., and D. A. Russell. 1991. Late Mesozoic stratigraphy and vertebrates of the Gobi Basin. Cretaceous Research 12: 345-377.

Kalandadze, N. N., and S. M. Kurzanov. 1974. Lower Cretaceous localities of terrestrial vertebrates of Mongolia. Trudy Sovmestnoi Sovetsko-Mongol'skoi Paleontologicheskoi Ekspeditsii 1: 9-18.

Karhu, A. A., and A. S. Rautian. 1996. A new family of Maniraptora (Dinosauria: Saurischia) from the Late Cretaceous of Mongolia. Paleontological journal c/c of paleontologicheskii zhurnal 30: 583-592.

Klein, N., T. Scheyer, and T. Tütken. 2009. Skeletochronology and isotopic analysis of a captive individual of *Alligator mississippiensis* Daudin, 1802. Fossil Record 12: 121-131.

Ksepka, D. T., and M. A. Norell. 2006. Erketu ellisoni, a long-necked sauropod from Bor Guvé (Dornogov Aimag, Mongolia). American Museum Novitates: 1-16.

Kurochkin, E. N., R. Barsbold, M. J. Benton, M. A. Shishkin, D. M. Unwin, and E. N. Kurochkin. 2000. The Russian-Mongolian expeditions and research in vertebrate paleontology. The age of dinosaurs in Russia and Mongolia: 235-255.

Kurzanov, S. M. 1976. A new late Cretaceous carnosaur from Nogon-Tsav, Mongolia. Results of the Soviet-Mongolian Paleontological Expedition 3: 93-104.

Kurzanov, S. M. 1981. An unusual theropod from the Upper Cretaceous of Mongolia. Joint Soviet-Mongolian Paleontological Expedition 15: 39-49.

Kurzanov, S. M. 1992. A giant protoceratopsid from the Upper Cretaceous of Mongolia. Paleontologicheskii Zhurnal: 81-93.

Kurzanov, S. M., and H. Osmólska. 1991. *Tochisaurus nemegtensis* gen. et sp. n., a new troodontid (Dinosauria, Theropoda) from Mongolia. Acta Palaeontologica Polonica 36.

Lacovara, K., M. Lamanna, J. Smith, B. Grandstaff, and J. Smith. 2002. Concentration and preservation potential of vertebrate fossils within coastal lithosomes: examples from the Upper Cretaceous Bahariya Formation of Egypt. Journal of Vertebrate Paleontology 22.

Lee, Y.-N., R. Barsbold, P. J. Currie, Y. Kobayashi, H.-J. Lee, P. Godefroit, F. Escuillié, and T. Chinzorig. 2014. Resolving the long-standing enigmas of a giant ornithomimosaur *Deinocheirus mirificus*. Nature 515: 257-260.

Lefeld, J. 1971. Geology of the Djadokhta Formation at Bayn Dzak (Mongolia). Palaeontologia Polonica 25: 101-127.

Lillegraven, J. A., and M. C. McKenna. 1986. Fossil mammals from the" Mesaverde" Formation (late Cretaceous, Judithian) of the Bighorn and Wind River basins,

Wyoming: with definitions of late Cretaceous North American land-mammal" ages". American Museum novitates; no. 2840.

Lockley, M. G., K. Carpenter, K. F. Hirsch, and J. R. Horner. 1994. Dinosaur ontogeny and population structure: interpretations and speculations based on fossil footprints. Dinosaur eggs and babies: 347-370.

Lockley, M. G., D. D. Gillette, D. D. Gillette, and M. G. Lockley. 1989. Dinosaur tracks and traces: an overview. Dinosaur tracks and traces: 3-10.

Longrich, N. 2010: The function of large eyes in *Protoceratops*: a nocturnal ceratopsian. Paper presented at the New perspectives on horned dinosaurs: The Royal Tyrrell Museum Ceratopsian Symposium. Indiana University Press, Bloomington, 2010.

Loope, D. B., L. Dingus, C. C. Swisher, and C. Minjin. 1998. Life and death in a Late Cretaceous dune field, Nemegt basin, Mongolia. Geology 26: 27-30.

Lü, J. C., Y. Tomida, Y. Azuma, Z. M. Dong, and Y.-N. Lee. 2004. New oviraptorid dinosaur (Dinosauria: Oviraptorosauria) from the Nemegt Formation of southwestern Mongolia. Bulletin of the National Science Museum of Tokyo Series C (Geology & Paleontology) 30: 95-130.

Makovicky, P., R. Sadleir, P. Dodson, G. E. Erickson, and M. Norell. 2007. Life history of *Protoceratops andrewsi* from Bayn Zag, Mongolia.: In *67th Annual Meeting, Society of Vertebrate Paleontology. Program and Abstracts*, Austin, TX.

Makovicky, P. J., B. M. Kilbourne, R. W. Sadleir, and M. A. Norell. 2011. A new basal ornithopod (Dinosauria, Ornithischia) from the Late Cretaceous of Mongolia. Journal of Vertebrate Paleontology 31: 626-640.

Makovicky, P. J., and M. A. Norell. 2006. *Yamaceratops dorngobiensis*, a new primitive ceratopsian (Dinosauria: Ornithischia) from the Cretaceous of Mongolia. American Museum Novitates: 1-42.

Maleev, E. A. 1952. A new family of armored dinosaurs from the Upper Cretaceous of Mongolia. Doklady Akademii Nauk SSSR 87: 1-134.

Maleev, E. A. 1954. New turtle-like reptile in Mongolia. Priroda 3: 106-108.

Maleev, E. A. 1955. New carnivorous dinosaurs from the Upper Cretaceous of Mongolia. Doklady Akademii Nauk SSSR 104: 779-782.

Martinson, G. G. 1982. The Upper Cretaceous mollusks of Mongolia; pp. 5-76 *i*n L. A. Nevesskaya (ed.), Sovmestnaya Sovetsko-Mongolskaya Paleontologicheskaya Ekspeditsia.

Martinson, G. G., and V. F. Shuvalov. 1976. Stratigraphy and fossil molluscs of the Lower Cretaceous lacustrine deposits of the Trans-Altai Gobi in Mongolia. Nauka, Leningrad.

Maryanska, T. 1977. Ankylosauridae (Dinosauria) from Mongolia. Palaeontologia Polonica 37: 85-151.

Maryanska, T., and H. Osmolska. 1974. Pachycephalosauria, a new suborder of ornithischian dinosaurs. Palaeontologia Polonica 30: 45-102.

Maryanska, T., and H. Osmólska. 1975. Protoceratopsidae (Dinosauria) of Asia. Palaeontologia Polonica 33: 133-181.

Maryanska, T., and H. Osmólska. 1981. First lambeosaurine dinosaur from the Nemegt formation, Upper Cretaceous, Mongolia. Acta Palaeontologica Polonica 26.

Matsukawa, M., H. Nagata, Y. Taketani, Y. Khanda, P. Khosbajar, D. Badamgarav, and I. Obata. 1997. Dinosaur bearing Lower Cretaceous deposits in the Choir Basin, S.E. Mongolia-Stratigraphy and Sedimentary Environments. Journal of the Geological Society of the Philippines. 52: 99-114.

Matthew, W. D., H. F. Osborn, and B. Brown. 1915. Dinosaurs with Special Reference to the American Museum: Collections. American museum of natural history.

Mikhailov, K. E. 1997. How Dinosaurs Nested. Nauka Zhizn': 73-79.

Mook, C. C. 1918. The habitat of the sauropod dinosaurs. The Journal of Geology: 459-470.

Nadon, G. C. 1993. The association of anastomosed fluvial deposits and dinosaur tracks, eggs, and nests: Implications for the interpretation of floodplain environments and a possible survival strategy for ornithopods. Palaios: 31-44.

Namnandorzhi, O. 1957. Traces of huge lizards in Mongolia. Priroda 44: 110-111.

Nesbitt, S. J., J. A. Clarke, A. H. Turner, and M. A. Norell. 2011. A small alvarezsaurid from the eastern Gobi Desert offers insight into evolutionary patterns in the Alvarezsauroidea. Journal of Vertebrate Paleontology 31: 144-153.

Niedźwiedzki, G., T. Singer, G. D. Gierliński, and M. G. Lockley. 2012. A protoceratopsid skeleton with an associated track from the Upper Cretaceous of Mongolia. Cretaceous Research 33: 7-10.

Norell, M. A., J. M. Clark, L. M. Chiappe, and D. Dashzeveg. 1995. A nesting dinosaur. Nature 378: 774-776.

Norell, M. A., J. M. Clark, D. Demberelyin, B. Rhinchen, L. M. Chiappe, A. R. Davidson, M. C. McKenna, P. Altangerel, and M. J. Novacek. 1994. A theropod dinosaur embryo and the affinities of the Flaming Cliffs dinosaur eggs. Science 266: 779-782.

Norell, M. A., J. M. Clark, A. H. Turner, P. J. Makovicky, R. Barsbold, and T. Rowe. 2006. A new dromaeosaurid theropod from Ukhaa Tolgod (Ömnögov, Mongolia). American Museum Novitates: 1-51.

Norell, M. A., P. J. Makovicky, G. S. Bever, A. M. Balanoff, J. M. Clark, R. Barsbold, and T. Rowe. 2009. A review of the Mongolian Cretaceous dinosaur *Saurornithoides* (Troodontidae: Theropoda). American Museum Novitates: 1-63.

Norman, D. B. 1998. On Asian ornithopods (Dinosauria: Ornithischia). 3. A new species of iguanodontid dinosaur. Zoological Journal of the Linnean Society 122: 291-348.

Novacek, M. J. 1996. Dinosaurs of the Flaming Cliff. 369, Doubleday, New York.

Novacek, M. J., M. Norell, M. C. McKenna, and J. Clark. 1994. Fossils of the Flaming Cliffs. Scientific American 271: 60-69.

Obata, I., and M. Matsukawa. 1996. Kyouryuu no michi (Road of dinosaur). Catalogue for the Special Exhibit. Nakazato Village, Gunma Prefecture, Japan.

Osborn, H. F. 1923. Two Lower Cretaceous dinosaurs of Mongolia. American Museum Novitates 95: 10.

Osborn, H. F. 1924a. *Psittacosaurus* and *Protiguanodon*: two Lower Cretaceous iguanodonts from Mongolia. American Museum Novitates 127: 16.

Osborn, H. F. 1924b. Sauropoda and Theropoda of the Lower Cretaceous of Mongolia. American Museum Novitates 128: 7.

Osborn, H. F., P. C. Kaisen, and G. Olsen. 1924. Three new theropoda, *Protoceratops* zone, central Mongolia. American Museum of Natural History.

Osmólska, H. 1981. Coossified tarsometatarsi in theropod dinosaurs and their bearing on the problem of bird origins. Palaeontologica Polonica 42: 79-95.

Osmólska, H. 1982. *Hulsanpesperlei* ng, n. sp.(Deinonychosauria, Saurischia, Dinosauria) from the Upper Cretaceous Barun Goyot Formation of Mongolia. Neues Jahrbuchfur Geologie und Palaontologie, Monatshefte 1982: 440-448.

Osmólska, H., and E. Roniewicz. 1970. Deinocheiridae, a new family of theropod dinosaurs. Palaeontologica Polonica 21: 5-19.

Osmólska, H., E. Roniewicz, and R. Barsbold. 1972. A new dinosaur, *Gallimimus bullatus* n. gen., n. sp.(Ornithomimidae) from the Upper Cretaceous of Mongolia. Palaeontologia Polonica 27: 103-143.

Perle, A. 1979. Segnosauridae - the new family of Theropoda from Lower Cretaceous of Mongolia. Trudy, Sovmestnaâ Sovetsko− Mongol'skaâ paleontologičeskaâ èkspediciâ 8: 45-55.

Perle, A. 1981. Nova segnozavrid iz verchnego mela Mongolii. Trudy - Sovmestnaya Sovetsko-Mongol'skaya Paleontologicheskaya Ekspeditsiya 15: 50-59.

Perle, A., L. M. Chiappe, and R. Barsbold. 1994. Skeletal morphology of *Mononykus olecranus* (Theropoda: Avialae) from the late Cretaceous of Mongolia. American Museum Novitates/American Museum of natural history.

Perle, A., T. Maryanska, and H. Osmólska. 1982. *Goyocephale lattimorei* gen. et sp. n., a new flat-headed pachycephalosaur (Ornlthlschia, Dinosauria) from the Upper Cretaceous of Mongolia. Acta Palaeontologica Polonica 27.

Perle, A., M. Norell, and J. M. Clark. 1999. A New Maniraptoran Theropod, *Achillobator giganticus* (Dromaeosauridae), from the Upper Cretaceous of Burkhant, Mongolia. Geology and Mineralogy Chair, National University of Mongolia.

Prieto-Márquez, A. 2011. A reapprisal of *Barsboldia sicinskii* (Dinosauria: Hadrosauridae) from the Late Cretaceous of Mongolia. Journal of Paleontology 85: 468-477.

Reizner, J., and J. R. Horner. 2006. An ontogenetic series of the ceratopsid dinosaur *Einiosaurus procurvicornis* as determined by long bone histology.: In *66th Annual Meeting, Society of Vertebrate Paleontology. Program and Abstracts.*, Ottawa, ONT.

Rozhdestvensky, A. K. 1952. A new representative of duckbilled dinosaurs from the Upper Cretaceous deposits of Mongolia. Doklady Akademii SSSR 86: 405-408.

Rozhdestvensky, A. K. 1965. Growth changes in Asian dinosaurs and some problems of their taxonomy. Paleontologičeskij žurnal 3: 95-109.

Rozhdestvensky, A. K. 1970. Giant claws of enigmatic Mesozoic reptiles. Paleontol. J 1970: 117-125.

Sampson, S. D., M. J. Ryan, and D. H. Tanke. 1997. Craniofacial ontogeny in centrosaurine dinosaurs (Ornithischia: Ceratopsidae): taxonomic and behavioral implications. Zoological Journal of the Linnean Society 121: 293-337.

Sander, P. M. 2000. Longbone histology of the Tendaguru sauropods: implications for growth and biology. Paleobiology 26: 466-488.

Sander, P. M., and N. Klein. 2005. Developmental plasticity in the life history of a prosauropod dinosaur. Science 310: 1800-1802.

Scannella, J. B., and J. R. Horner. 2010. *Torosaurus* Marsh, 1891, is *Triceratops* Marsh, 1889 (Ceratopsidae: Chasmosaurinae): synonymy through ontogeny. Journal of Vertebrate Paleontology 30: 1157-1168.

Schweitzer, M., J. Watt, R. Avci, L. Knapp, L. Chiappe, M. Norell, and M. Marshall. 1999. Beta-keratin specific immunological reactivity in feather-like structures of the Cretaceous Alvarezsaurid, *Shuvuuia deserti*. Journal of Experimental Zoology 285: 146-157.

Sereno, P. C. 2000. The fossil record, systematics and evolution of pachycephalosaurs and ceratopsians from Asia. The Age of Dinosaurs in Russia and Mongolia. Cambridge University Press, Cambridge: 480-516.

Sereno, P. C. 2010: Taxonomy, cranial morphology, and relationships of parrot-beaked dinosaurs (Ceratopsia: Psittacosaurus). Paper presented at the New perspectives on horned dinosaurs: The Royal Tyrrell Museum ceratopsian symposium, 2010.

Shuvalov, V. F. 1974. On the geology and age of the Khobur and Khuren Dukh localities in Mongolia. Trudy Sovmetstnoi Sovetsko-Mongol'skoi Paleontologicheskoya Ekspeditsii. 1: 296-304.

Shuvalov, V. F. 1975a. A new Early Cretaceous dinosaur locality Builyasutuin Khuduk; pp. 210-213 *i*n N. N. Kramarenko (ed.), Fossil Fauna and Flora of Mongolia. Trudy Sovmest. Soviet-Mongol. Nauka, Moscow.

Shuvalov, V. F. 1975b. The Stratigraphy of Mesozoic of Central Mongolia. Trudy Sovmestnoi Sovetsko-Mongol'skoi Geologicheskoi Ekspeditsii. 13: 50-112.

Shuvalov, V. F. 1994. Paleogeography of the lakes of Mongolia in the Mesozoic; pp. *i*n D. V. Sevastyanov, V. F. Shuvalov, and I. Neustrueva, Yu (eds.), Limnology and Paleolimnology of Mongolia. Nauka, Leningrad.

Shuvalov, V. F. 2000. The Cretaceous stratigraphy and palaeobiography of Mongolia.; pp. 256-279 *i*n M. J. Benton, M. A. Shishkin, D. M. Unwin, and E. N. Kurochkin (eds.), The age of dinosaurs in Russia and Mongolia. Cambridge University Press.

Shuvalov, V. F., and T. V. Nikolaeva. 1985. On the age and territorial distribution of Cenozoic basalts in the south of Mongolia. Vestnik Leningradskogo Universiteta: Geologiya, Geografiya 7: 52-59.

Sochava, A. V. 1975. Stratigraphy and lithology of the Upper Cretaceous deposits of South Mongolia. Trudy Sovmestnoi Sovetsko-Mongol'skoi Paleontologicheskoi Ekspeditsii. 13: 113-182.

Solovyev, N. S., G. A. Shatkov, and L. N. Yakobson. 1977. [The Pri-Argun Mongolian volcanic belt]. Geology and Geophysics 3: 20-31.

Tereschenko, V. 2008. Adaptive features of protoceratopsoids (Ornithischia: Neoceratopsia). Paleontological Journal 42: 273-286.

Tereschenko, V. S., and V. R. Alifanov. 2003. *Bainoceratops efremovi*, a new protoceratopid dinosaur (Protoceratopidae, Neoceratopsia) from the Bain-Dzak locality (south Mongolia). Paleontological journal c/c of paleontologicheskii zhurnal 37: 293-302.

Tsuihiji, T., R. Barsbold, M. Watabe, K. Tsogtbaatar, T. Chinzorig, Y. Fujiyama, and S. Suzuki. 2014. An exquisitely preserved troodontid theropod with new information on the palatal structure from the Upper Cretaceous of Mongolia. Naturwissenschaften 101: 131-142.

Tsuihiji, T., M. Watabe, K. Tsogtbaatar, T. Tsubamoto, R. Barsbold, S. Suzuki, A. H. Lee, R. C. Ridgely, Y. Kawahara, and L. M. Witmer. 2011. Cranial osteology of a juvenile specimen of *Tarbosaurus bataar* (Theropoda, Tyrannosauridae) from the Nemegt Formation (Upper Cretaceous) of Bugin Tsav, Mongolia. Journal of Vertebrate Paleontology 31: 497-517.

Tumanova, T. A. 1983. The first ankylosaur from the Lower Cretaceous of Mongolia. Transactions from the Joint Soviet–Mongolian Palaeontological Expedition 24: 110-118.

Tumanova, T. A. 1993. On A New Armored Dinosaur from Southeastern Gobi. Paleontologicheskii Zhurnal: 92.

Turner, A. H., S. H. Hwang, and M. A. Norell. 2007a. A small derived Theropod from Oosh, Early Cretaceous, Baykhangor Mongolia. American Museum Novitates 3557: 1-27.

Turner, A. H., S. J. Nesbitt, and M. A. Norell. 2009. A large alvarezsaurid from the Late Cretaceous of Mongolia. American Museum Novitates: 1-14.

Turner, A. H., D. Pol, J. A. Clarke, G. M. Erickson, and M. A. Norell. 2007b. A basal dromaeosaurid and size evolution preceding avian flight. Science 317: 1378-1381.

Varricchio, D. J. 1993. Bone microstructure of the Upper Cretaceous theropod dinosaur *Troodon formosus*. Journal of Vertebrate Paleontology 13: 99-104.

Verzilin, N. N. 1979a. Cretaceous deposits of Khar Hotol and the problem of Sainshand svita. Bulletin Moskovskogo Obshchestva Ispytatelei Prirody, Otdel Geologicheskii 54: 123.

Verzilin, N. N. 1979b. Genesis of the Upper Cretaceous deposits of South Mongolia on the basis of taphonomic observations. Vestnik Leningradskogo Universiteta: Geologiya, Geografiya 12: 7-13.

Verzilin, N. N. 1980. Special features of deposition of sediments in the territory of South Mongolia in Late Cretaceous time. Vestnik Leningradskogo Universiteta: Geologiya, Geografiya 14: 18-27.

Verzilin, N. N. 1982. Palaeolimnological significance of a peculiarity in the texture of the Upper Cretaceous deposits of Mongolia; pp. 81-100 *i*n G. G. Martinson (ed.), Mesozoic Lake Basins of Mongolia. Nauka, Leningrad.

Watabe, M., and S. Suzuki. 2000. Report on the Japan− Mongolia Joint Paleontological expedition to the Gobi desert, 1996. Hayashibara Museum of Natural Sciences Research Bulletin 1: 58-68.

Watabe, M., K. Tsogtbaatar, and R. Barsbold. 2008. First discovery of a theropod (Dinosauria) from the Upper Jurassic in Mongolia and its stratigraphy. Paleontological Research 12: 27-36.

Watabe, M., K. Tsogtbaatar, and R. M. Sullivan. 2011. A new pachycephalosaurid from the Baynshire Formation (Cenomanian-late Santonian), Gobi Desert, Mongolia. Bulletin of the New Mexico Museum of Natural History & Science 53: 489-497.

Webster, D. 1996. Dinosaurs of the Gobi: Buried by desert sandstorms 80 million years ago, wondrous creatures reveal themselves in well-preserved fossils of parents and nestlings. National Geographic 190: 70-89.

Weishampel, D. B., D. E. Fastovsky, M. Watabe, D. J. Varricchio, F. D. Jackson, K. Tsogtbaatar, and R. Barsbold. 2008. New oviraptorid embryos from Bugin-Tsav, Nemegt Formation (Upper Cretaceous), Mongolia, with insights into their habitat and growth. Journal of Vertebrate Paleontology 28: 1110-1119.

Werning, S. 2012. The ontogenetic osteohistology of *Tenontosaurus tilletti*. PloS one 7: e33539.

Woodward, H. N., E. A. F. Fowler, J. O. Farlow, and J. R. Horner. 2015. *Maiasaura*, a model organism for extinct vertebrate population biology: a large sample statistical assessment of growth dynamics and survivorship. Paleobiology 41: 503-527.

CHAPTER TWO

TAPHONOMY AND DEPOSITIONAL ENVIRONMENT OF A MONODOMINANT *PSITTACOSAURUS* BONEBED FROM THE LOWER CRETACEOUS KHULSANGOL FORMATION OF CENTRAL MONGOLIA

Contribution of Authors and Co-Authors

Manuscript in Chapter 2

Author: Badamkhatan Zorigt

Contributions: Conceived the study, obtained and processed specimens, analyzed data, interpreted results, and wrote the manuscript.

Co-author: John R. Horner

Contributions: Provided fieldwork funding, access to laboratory materials, and workspace, and suggested revisions on earlier drafts of the manuscripts.

Co-author: Khatanbaatar Purevdorj

Contributions: Assisted for fieldwork, specimen collection, and preliminary analysis of the data.

Manuscript Information Page

Badamkhatan Zorigt, John R. Horner, Khatanbaatar Purevdorj
Journal of Vertebrate Paleontology
Status of Manuscript:
_x_Prepared for submission to a peer-reviewed journal
___Officially submitted to a peer-reviewed journal
___Accepted by a peer-reviewed journal
___Published in a peer-reviewed journal

Published by Society of Vertebrate Paleontology

Abstract

The relatively understudied the Early Cretaceous Builst Khudag (BLK) locality (Khulsangol Formation) in central Mongolia has produced a large number of fossils referable to the basal ceratopsian dinosaur *Psittacosaurus mongoliensis*. To understand the nature of the BLK bonebed, it is necessary to examine the sedimentology and taphonomy. The stratigraphic section of the BLK locality consists of an unsorted conglomerate underlying unsorted, ungraded, horizontally bedded mottled sandstone; massive sandstone; and a thin mudstone layer. The sedimentologic features reflect a debris flow followed by sheet-flood deposit that formed in the alluvial setting. *P. mongoliensis* skeletal elements were collected from both the bonebed and surface float. The high occurrence of *P. mongoliensis* fossils suggests a monodominant bonebed. The bones collected from the BLK bonebed exhibit minimal taphonomic modification and excellent preservation, suggesting a scenario of simultaneous death and burial. An articulated juvenile *Psittacosaurus* aggregation is consistent with the juvenile-only aggregate behavior in *Psittacosaurus* which has been previously suggested. However, the age and body sizes of the BLK *P. mongoliensis* aggregation differs from those of *Psittacosaurus* aggregates from the Lujiatun Bed in China and may reflect taxon-specific growth rates.

Introduction

Study of the taphonomic and depositional history of a *Psittacosaurus* bonebed from the Early Cretaceous Khulsangol Formation of Mongolia provides new insights into the life history and behavior of this animal. In China, many volcaniclastic debris deposits have been reported to produce an abundance of psittacosaur skeletons in exceptionally preserved conditions (Brinkman et al., 2001; Zhao et al., 2007). However, thus far, psittacosaur specimens from Mongolia have primarily been reported from lacustrine and lacustrine-margin deposits (Osborn, 1923, 1924; Shuvalov, 1974; Bratseva and Novodvorskaya, 1975, 1976; Suslov, 1983; Chen, 1987; Averianov et al., 2006). Some researchers have suggested that the lifestyle of psittacosaur was probably aquatic (Rozhdestvensky, 1955b, 1955a; Suslov, 1983; Currie, 1997; Ford and Martin, 2010). The occurrence of *Psittacosaurus* in other depositional environments (e.g. alluvial, eolian) is rare (Russell and Zhao, 1996; Eberth, 2010). In this study, we examine the taphonomy and sedimentology of a *Psittacosaurus* bonebed at the Lower Cretaceous Builst Khudag (BLK) locality in the central Mongolia.

Methods

Over the course of five field seasons (2010-2015), sedimentologic and taphonomic data were collected from the BLK locality. The stratigraphic measurement was taken by utilizing a Brunton compass, tape meter, and Jacob's staff. To make a composite stratigraphic column, the marker bonebed was traced laterally throughout the BLK locality. All beds were photographed and the thickness, grain size, sedimentary

structures were documented. The colors of the beds were recorded by using the Munsell Color Chart (Munsell Color, 2000). The lithofacies are classified using the terminology of Miall (2006) and Mulder and Alexander (2001).

Psittacosaurus specimens were found either *in situ* or as surface float. The number of identified specimens (NISP) and minimum number of individuals (MNI) were determined. Taphonomic effects, including abrasion (Shipman, 1981), weathering (Fiorillo, 1988), and fracturing (Haynes, 1983) on the bones were assessed. Orientation of the articulated skeletons was measured using a Brunton compass. A 1x1m^2 mapping grid with 10 cm increments was used for taphonomic mapping of the articulated skeletons. The estimated body length of disarticulated *Psittacosaurus* tibiae were calculated based on the measurements obtained from the complete skeletons. Relative ages at death of the articulated individuals were determined by examining the bone histology of associated tibiae (see Chapter 4 for detailed histologic analysis).

Geologic Setting

The Early Cretaceous BLK site is situated at the southwest end of the Ushgig mountain range, about 20 km north of the Baruunbayan-Ulaan township of Uvurkhangai province, Mongolia (Fig .2.1). The site was discovered by Devyatkin in 1969 during the Soviet Paleontological Expedition (Shuvalov, 1975; Bratseva and Novodvorskaya, 1976). Due to its small size, the site has been generally overlooked by subsequent paleontologists. The general geology of the locality was briefly discussed by Tooruul (1986) and Bochkov (1986); although very few research papers (Shuvalov, 1975;

Bratseva and Novodvorskaya, 1976) have been published on the paleontology of the locality.

In the BLK area, the lower member of the Lower Cretaceous Khulsangol Formation occurs in the southwest end of the Ushgug mountain (Martinson, 1982). The formation is represented by unsorted conglomerate lenses and fine to coarse grained sandstone beds with intercalated beds of mudstone layers (Shuvalov, 1975; Bratseva and Novodvorskaya, 1976; Sinitsa, 1993; Khand et al., 2000). The Lower Cretaceous beds dip approximately 10 degrees to the southwest. In the east end of the Ushgig mountain, the Khulsangol Formation overlies the Andaikhudak Formation [previously described as Ondai Sayr Formation by Berkey and Morris (1927)] on an erosional disconformity (Khand et al., 2000). In the south of the BLK area, the Khulsangol Formation is unconformably overlain by the coarse-grained Paleogene sediments (Fig. 2.2). As is hypothesized for the other Early Cretaceous formations in the area, sedimentation at the BLK area occurred episodically and in fault-controlled conditions (Bochkov, 1986; Tooruul, 1986; Jerzykiewicz, 2000).

The age of BLK locality was determined by Bratseva and Novodvorskaya (1976) using the pollen and spore assemblage from the site. The age of Khulsangol Formation is correlative to the dinosaur bearing Aptian-Albian Khukhteeg Formation in the eastern Gobi (Martinson, 1982; Jerzykiewicz and Russell, 1991).

Sedimentology of the Builst Khudag Site

The BLK locality is represented by approximately 100 meters of horizontally bedded fine to medium-grained sandstones interbedded with 0.5-2 cm thick red mudstone layers and pebble to boulder-grained, poorly sorted conglomerates (Fig. 2.3). Throughout the section, five lithofacies are classified: matrix-supported boulder conglomerate (Gmg), matrix-supported pebble-cobble conglomerate (Gmm), horizontally bedded sandstone (Sh), massive sandstone (Sm), and mudstone (Fm) (Table 1).

The matrix-supported boulder conglomerate occurs in the bottom of the section. The pebble-cobble conglomerate lenses often occur in the fine-medium sandstone beds (Sh). In the upper half of the section, these conglomerate lenses produce dinosaur bones. Almost 90 percent of the section consists of the horizontally bedded, mottled sandstone (Sh) that produces dinosaur material. The mudstone bed (Fm) overlies the dinosaur bearing sandstone beds (Sh). This bed contains immature caliches and is the thinnest (0.5-1 m) unit in the section. The horizontally bedded, massive, internally structureless, grey sandstone overlies the top of the mudstone bed.

Lithofacies

Matrix-Supported Boulder Conglomerate (Gmg): This facies occurs in a 1.5-2 m bed and is composed of well-rounded, poorly sorted, unimbricated, light-colored clasts up to 30 cm in diameters (Fig. 2.4). This conglomerate exhibits two phases of slight inverse grading. The upper grading phase consists of larger boulders. This facies is overlain by a pebble-cobble conglomerate bed with abrupt contact. The lower contact with the

underlying horizontally bedded fine-medium grained sandstone (Sh) is abrupt and uneven. The upper surface incises into the overlying bed and exposes sporadically. The bed is exposed at the north end of the Ulaan shavar site of the BLK locality (Fig. 2.12).

Unsorted, inversely graded, matrix-supported boulder conglomerate is interpreted as a debris-flow deposit. The general characteristics of debris-flow deposits are inverse to normal grading, poor sorting, and a weak of internal structure (Ballance, 1984; Shultz, 1984; Smith, 1986; Miall, 2006). Two phases of slight reverse grading could be interpreted as the changes of dispersive pressure amplitudes (Bagnold, 1956; Lowe, 1982).

Matrix-Supported, Stratified, Pebble-Cobble Conglomerate (Gmm): Matrix-supported pebble-cobble conglomerate facies occurs as 0.2-2 m thick cosets throughout the section. This facies is composed of well-rounded pebble and cobble clasts with fine-medium grained sand matrix in which there is weak sorting and no observable grading (Fig. 2.5). Rarely, slight cross-bedding and weak stratification occur in the sandy-pebbly portion of the bed. This lithofacies usually occurs within the horizontally bedded, mottled sandstone beds (Sh) as a lens. Contacts with over- and underlying sandstone beds (Sh) are even and abrupt. At the bottom of the section, the matrix-supported conglomerate (Gmg) facies is overlain by this facies as well. It produces dinosaur bones in the upper part of the section (Fig. 2.3).

Stratified, weakly sorted, ungraded, pebble-cobble conglomerate is typically interpreted to represent sheet-flood deposits (Bull, 1972; Hartley, 1993). The stratified gravel lenses with slight cross-bedding resemble a shallow channel-filling concentrated

density-flow deposit (Ballance, 1984; Mulder and Alexander, 2001). The cross stratification exhibits a slight lateral migration of flow.

Horizontally Stratified, Mottled Sandstone (Sh): Horizontally bedded sandstone occurs as 0.6-50 m thick units in the section (Fig. 2.6). This facies is composed of fine-medium grained, unsorted, ungraded, horizontally bedded, and mottled sandstone. Within the facies, thin, red colored (5YR 4/6), 1-5 cm thick mudstone layers occur in every 0.8-2 meters. The matrix-supported pebble-cobble conglomerate (Gmm) lenses are contained as well. The mudstone units prevail; whereas, pebble conglomerates are less common. The occurrence of the conglomerate lenses decreases in number upwards throughout the BLK section (Fig. 2.3). This facies occurs partially in the lower-most part of the section, overlain by the boulder conglomerate (Gmg). The contact of this facies with the overlying conglomerate (Gmg) bed is abrupt.

Horizontally stratified, ungraded, sharp contacts with over- and underlying beds are interpreted to represent a sheet-flood deposit that formed by multiple depositional events (Blissenbach, 1954; Mulder and Alexander, 2001). Similar deposits exhibiting sharp bed boundaries and the lack of grading were reported in the Yixian Formation in China (Jiang and Sha, 2007). The mottling of the facies (Fig. 2.7) suggests repeated transitions into oxidation with periodic waterlogging during flooding (Stewart, 1981).

Horizontally Stratified, Homogeneous, Massive Sandstone (Sm): This facies is approximately 40 cm thick in the upper-most part of the section (Fig. 2.8). Massive sandstone is medium-grained, structureless, ungraded, moderately sorted, grey colored

(5Y 7/2) sandstone. The contact with the underlying mudstone bed (Fm) is conformable. The characteristics of this facies including medium-coarse grain, a lack of internal structure, and ungradation suggests a grain flow with rapid sediment suspension which may have been formed as a result of liquefied or grain flows (Stauffer, 1967; Middleton and Hampton, 1976; Mulder and Alexander, 2001).

Horizontally Stratified, Homogeneous Mudstone (Fm): This 50 cm thick bed is horizontally stratified, unsorted, internally structureless, and grey colored (5Y 7/2) (Fig. 2.8). This facies contains immature, small sized (2-6 cm) caliche nodules in it (Fig. 2.9) and overlies the horizontal, mottled sandstone bed with an even and sharp contact (Fig. 2.8). The horizontally stratified, internally structureless, homogeneous mudstone represents a suspension settling in a standing water (Miall, 1977). The immature caliche occurrence in this facies may have resulted from occasional subaerial conditions (Esteban and Klappa, 1983).

Facies Association

Matrix-Supported Boulder Conglomerate (Gmg): Matrix-supported boulder conglomerate bed occurs only at the bottom of section (Fig. 2.4). The characters including slight inverse grading, unsorted, matrix-support resembles a debris flow deposit (Ballance, 1984; Shultz, 1984; Smith, 1986; Miall, 2006). This facies contacts with underlying horizontal sandstone unconformably. Due to a lack of paleosol evidence, there was no erosional surface between the conglomerate and the underlying sandstone bed.

The conglomerate facies is overlain by a pebble-cobble conglomerate facies (Gmm) with unconformable contact. The uneven upper surface of this conglomerate suggests possible erosional contact with overlying matrix supported pebble-cobble conglomerate (Dasgupta, 2006).

Horizontally Stratified, Mottled Sandstone (Sh) and Pebble-Cobble Conglomerate (Gmm): The association of horizontally stratified sandstone and pebble-cobble conglomerate is the most common facies association in the section (Fig. 2.10). The occurrence of conglomerate lenses decreases upwards the section as well as the grain size changes from cobble-pebble. The contacts between these facies are predominantly sharp and unconformable. Dinosaur bones are found in the upper most conglomerate lenses.

Stacked sandstone beds intercalated with red mudstone seams represent the deposits from repeated sheet-flood (Miall, 2006). The occurrence of the cobble-pebble conglomerate lenses with slight cross bedding is comparable to the laterally migrated, channel-filled, concentrated density flow deposit (Ballance, 1984; Mulder and Alexander, 2001; Jiang and Sha, 2007). Based on the distribution of this association, a sheet-flood occurred several times throughout the section.

Horizontally Stratified Mudstone (Fm) and Structureless, Massive Sandstone (Sm): The unsorted, structureless, massive mudstone occurs between the underlying horizontal sandstone bed and overlying massive sandstone (Fig. 2.8). Both contacts are conformable and sharp. The mudstone facies is interpreted as a suspension settling in a standing water. This is the only facies producing

caliche, which is a pedogenic product, typically formed as a result of long periods of non-deposition in semi-arid and arid non-marine settings (Leeder, 1975; Wright and Tucker, 1991; Mack et al., 1993; Hasegawa et al., 2009). Caliche has also been described as evidence of an erosional surface (Esteban, 1976). The horizontal, massive sandstone facies (Sm) is interpreted as a grain flow with rapid sedimentation, based on the ungraded, medium coarse grains and lack of internal structure. This facies occurs only in the uppermost part of the section. The contact with the mudstone bed (Fm) is abrupt (Fig. 2.8).

Interpretation of Depositional Environment

The sedimentary sequences in the BLK locality consist of the deposits of debris flow, sheet-flood, and turbidity flow. The lower part of the section consists of a matrix supported, inversely graded boulder conglomerate bed showing a subaerial debris flow as seen in an alluvial fan (Miall, 1977; Shultz, 1984). Two phases of inverse grading in the conglomerate may indicate the occurrence of a flood that had fluctuated dispersive pressure (Bagnold, 1956; Lowe, 1982).

The horizontally stratified, mottled sandstone facies is interpreted to represent a sheet-flood deposit that formed in semi-arid mountainous catchments (Blissenbach, 1954). Multiple depositional phases of sheet-flood are observed throughout the section. The pebble conglomerate lenses with slight cross bedding were formed as a channel-fill deposit.

The association of horizontally-stratified mudstone and the massive, structureless sandstone represents suspension settling mudstone and grain flow deposits. The presence of caliche in the mudstone may be related to an erosional surface (Esteban, 1976).

Taphonomic Features

Taxonomic Composition of the BLK Bonebed

A total of 3,404 catalogued elements were recovered from the BLK locality, excluding articulated and complete specimens. Of the total bone assemblage, 51% (n=1799) were unidentifiable due to fragmentation. Out of all identifiable elements (n=1684, 49%), 96.8% are assignable to psittacosaur (Table 2.2). The identifiable psittacosaur skeletal materials had been identified following Sereno (1987). All articulated and complete psittacosaur skeletons (n=10) were identified as *Psittacosaurus mongoliensis* and it was assumed that all collected psittacosaur elements belong to this species.

The remaining 3.2% of the materials was identified as representing teeth (n=3), claw (n=2; Fig.2.11, B), isolated femur (n=1), and articulated skeleton of an unknown theropod (n=1), and long bone fragments (n=47; Fig. 2.11, A) of an unknown sauropod. No fossil invertebrates were recovered from the locality.

P. mongoliensis Skeletal Representation and Minimum Number of Individuals (MNI)

Based on the identifiable skeletal material list (Table 2.3), the most abundant skeletal elements are the hind limb elements including vertebrae (24.4%), ribs (17%),

tibiae (10.6%), pes (8.9%), and femora (8.3%). The most commonly recovered elements in the collection were vertebrae (n=425) including centra and processes followed by ribs (n=295). The next common skeletal elements were the hind limb including tibia (n=185), femur (n=144), and pes (n=154). Pelvic (n=25) and cranial (n=9) materials (excluding teeth, n=43) are relatively uncommon at the locality. The complete and nearly complete (>70%) hind limb elements (n=306) occur ubiquitously throughout the exposure.

The minimum number of individuals was assessed based on the relatively abundant long bones at BLK (n=477). To avoid overestimation, the sizes (e.g. total length, width of proximal and distal ends) and geographic positions of the collected bones were used as criteria. The minimum number of *P. mongoliensis* individual is 213 including 10 articulated and complete specimens (Table 2.4).

Spatial Occurrence and the Bone Preservation at the BLK Locality

The BLK bonebed consists of two separate bone-bearing rock units: a horizontally bedded, fine to medium grained, unsorted sandstone unit and a pebble conglomerate unit (see Sedimentology section for detail descriptions of the units). The lateral extension of the sandstone unit is continuous and approximately 1.5 km from northeast to southwest (Fig. 2.12). The thickness of this unit reaches approximately 1.7 m. This unit is exposed at three locations: Baruun jalga, Ulaan shavar, and Uvuljoo (Fig. 2.12; 2.13) From the sandstone unit, so far we have collected a total of 661 skeletal elements of *P. mongoliensis* (articulated specimens are counted as one element). Out of which, ten complete skeletons were recovered in a life-like posture (crouching); four

forelimbs consisting of articulated humerus, radius, and ulna; seven hind limbs consisting tibia, fibula, and metatarsals; two articulated caudal vertebrae; five articulated dorsal vertebrae; and four articulated postcranial elements consisting dorsal vertebrae with ribs and hind limbs (Table 2.3). There are some occurrences of isolated single skeletal elements such as a tibia and femur. Presumably, the associated skeletal elements of those were washed away after subaerial exposure. The bones from this unit are fragile and brown-dark brown in color. The surfaces of the bones are encased in a thin (1-2 mm) mudstone layer (Fig. 2.14, A). Some bones (n=13) were crushed, possibly as a result of lithostatic compaction (Rogers, 1990). Overall the morphological details of the bones are well preserved. In general, there is a high probability of finding an articulated and/or complete skeleton from the sandstone unit.

The bone occurrence in the conglomerate unit is relatively rare compared to the sandstone unit. Since the conglomerate unit occurs as small lenses in the sandstone unit, the lateral extensions of this unit are discontinuous, extending 10-20 m. The bone bearing conglomerate lenses reach approximately 0.2-1 m in thickness. The *Psittacosaurs* skeletal elements from this unit are found mostly in a disarticulated state. The bone surfaces are covered with thin layers of hematite and show some level of abrasions (abrasion stage 1). Although the bones are predominantly found disarticulated, the bones are somewhat associated. The conglomerate unit occurs only at the Ulaan shavar location (Fig. 2.14, B).

The majority of disarticulated skeletal elements (n=872) were collected as surface float. Presumably, those elements were washed out from the main bone bearing units including the sandstone and conglomerate units. In the lower topography below the main

bonebed, surface bone is abundant. The bones collected from the surface are primarily pale brown or yellow in color (Fig. 2.15). Most of the bones were taphomically modified, exhibiting moderate weathering and abrasion.

Size Distribution of Individuals

A total of 35 tibiae were measured for the size determination, ten of which were from articulated skeletons, and the remaining 25 tibiae were disarticulated but complete. Tibia length from the BLK bonebed ranges between 63 mm and 267.7 mm (Fig. 2.16). Based on the histologic evidence (see Chapter 4), juveniles (60-140 cm in body length, n=43) are the most common in the collection; individuals with body lengths over 160 cm are relatively rare.

An aggregate of *P. mongoliensis* consisting of five various sized individuals was discovered during the field season of 2012 and collected in 2014 (Fig. 2.17, B). Four (# 1,2,3,5) of which are oriented between 205 and 251 degrees to the southwest, plunging parallel to the bonebed (8 degrees). The orientation of the remaining individual (# 4) is oriented 60 degrees to the northeast. All specimens were buried in a crouching posture and most of them have a southwest preferred direction (Fig. 2.17, D; Table 2.5). Another five articulated individuals were collected from separate quarries at the BLK site: orientation data for two of these individuals is available (Fig. 2.17, A and C; Table 2.5).

Taphonomic Modification

Six weathering stages (0-5) were established by Behrensmeyer (1978) based on the physical alteration of modern bones. Fiorillo (1988) applied this classification system

to fossil bones and produced a four stage classification system which was used in this research: stage 0 –no sign of surface cracking or flaking, stage 1 – cracking parallel to bone fibers, stage 2 – start showing flaking along with cracking, and stage 3 – loss of the outer bone layer. Only the *in situ* bones (n=544) collected from the bonebed were assessed for weathering and abrasion stages due to the potential for a more accurate assessment of pre-burial modification. Of the 544 analyzed elements, over 88% (n=483) of the specimens show a weathering stage 0 (Table 2.6). The remaining specimens (n=61) present weathering stage 1. No signs of the stages 2 and 3 were observed from the analyzed bones. Weathering stages 0 and 1 are usually observed on the bones that have been exposed for no more than two years in subaerial condition (Behrensmeyer, 1978; Fiorillo, 1988).

Abrasion stages were assessed using Shipman's (1981) classification. Abrasion stage 0 was observed in the 501 bones (92%) collected from a sandstone unit. The remaining 8% of the elements exhibit abrasion stage 1. No heavily abraded elements were observed. However, absence of abrasion does not necessarily suggest a lack of transport because fresh bone may be transported without abrasion (Fernandez-Jalvo, 1988). The bones collected as float from the surface exhibit relatively higher abrasion levels (stage 1-2) than those of the *in situ* bones due to recent modification.

Haynes (1983) reported three major fracture types on modern large mammal bone assemblages: transverse (perpendicular to long axis), spiral (diagonal or oblique to the long axis), and longitudinal (parallel to long axis). The majority of bones from the BLK locality show transverse fractures (Fig. 2.18). The transverse factures could have been

formed due to post-burial and post-fossilization damage that occurred by sediment compaction (Behrensmeyer, 1975). No other taphonomic modifications (such as tooth marks and wet rot) were observed in the specimens.

Taphonomic Interpretation

The BLK bonebed shows a poor record of taxonomic diversity. Based on the number of identified specimens, the BLK bonebed is dominated by *P. mongoliensis*. From the bonebed, small theropod dinosaur bones suggest the presence of a predator in the area and some sauropod material indicates that *P. mongoliensis* was not the only herbivorous dinosaur present. The *in situ* collected specimens exhibiting excellent preservation. These bones, from the mottled sandstone unit, present articulated and undisturbed conditions that suggest the bones did not experience environmental or biological effects such as sediment transport and animal scavenging. The evidence of minimal weathering stages suggests that the bones were not damaged in subaerial conditions prior to fossilization. The presence of minimal abrasion on the bones suggests minimal or no post-mortem transport. However, the bones collected as surface float exhibit levels of abrasion that could have been formed by post-burial transport. The dominant form of fracturing present in the observed bones was transverse fracturing which could be a physical effect from the sediment such as sediment compaction (Behrensmeyer, 1975).

The sedimentology of the BLK site is consistent with an alluvial fan. Both sedimentologic and taphonomic data suggest the taphonomic mode of the BLK site is best described as a flash flood that may have been triggered by intense rainfall.

Discussion

Common taphonomic modes in *Psittacosaurus* bonebeds are usually marginal-lacustrine and volcanogenic (lahar) deposits (Shuvalov, 1974; Suslov, 1983; Brinkman et al., 2001; Zhou et al., 2006). The depositional environment of the BLK bonebed is interpreted as a sheet-flood deposit in the alluvial setting based on the sedimentological features including unsorting, ungrading, no internal structure, and horizontal bedding. A lack of the occurrence of the volcanogenic materials in the BLK bonebed suggests the deposition of the BLK bonebed was related to the influx of water and debris from the steep terrain. A rapid sedimentation of bedload that occurred during the catastrophic flood may be a main cause of the three-dimensional preservations of the articulated skeletons from the BLK locality. The Lujiatun Bed of the Yixian Formation in China produces articulated and three-dimensionally preserved *Psittacosaurus* skeletons as well (Meng et al., 2004; Zhou, 2006; Zhao et al., 2007). The depositional environment of the Lujiatun Beds is represented by debris flow, hyperconcentrated flood flow, stream flow, and sheet flood deposits in a volcanic setting (Barrett and Wang, 2007; Jiang and Sha, 2007; Zhao et al., 2007). It appears that a large amount of instant sediment deposition is responsible for the autochthonous three-dimensional preservation of vertebrate skeletons in terrestrial environment. However, the fossils from the marginal lacustrine members (Jianshangou and Dawangzhangzi beds) of the Yixian Formation are preserved two-dimensionally (Xing and Norell, 2006; Zhao et al., 2007).

Monodominant bonebeds are characterized by the occurrence of a single taxon which represents over 50% of total fossil assemblage (Eberth et al., 2010). The BLK

bonebed is determined as a monodominat bonebed represented by the high occurrence (98% of total vertebrate fossil assemblage) of *P. mongoliensis* skeletal elements. The North American Late Cretaceous McPheeters bonebed is also one of the most popular monodominant dinosaur bonebeds producing more than 89% of the total bones assigned to the single dinosaur family, Ceratopsidae (Chiba et al., 2015). However, the depositional environment of the McPheeters bonebed from the Oldman Formation in Alberta was interpreted as humid and coastal (Chiba et al., 2015).

Psittacosaurus aggregations have been reported previously (Meng et al., 2004; Zhao et al., 2007). One of the aggregations from Lujiatun Bed consisting of 34 juveniles with associated adult suggests a parental care in *Psittacosaurus* (Meng et al., 2004). Alternatively, Zhao et al. (2013) argued that the *Psittacosaurus* lived as a juvenile-only aggregate consisting of individuals with 2-3 years old rather than living with "parent". The *P. mongoliensis* aggregation from the BLK bonebed presents individuals ranging from 2-5 years old (see Chapter 4). The histology of the largest specimen (five years old) suggested an actively growing individual rather than skeletally matured. However, the timing of the reproductive maturation might have occurred relatively early in *Psittacosaurus* before reaching the asymptotic body size (Erickson et al., 2009). Interestingly, there is considerable body-size disparity between Lujiatun aggregations and BLK aggregation. The body size ranges between 25-47 cm in *P. lujiatunensis* aggregations from the Lujiatun Bed [body sizes were obtained from the photographs in the corresponding publications (Meng et al., 2004; Zhao et al., 2007)]. The *P. mongoliensis* aggregation from the BLK bonebed contains larger juveniles ranging 65.9 –

102.21 cm in body length. This size difference in the aggregation may reflect taxon-specific growth rates in *Psittacosaurus*. Nevertheless, the *Psittacosaurus* aggregation from the BLK bonebed is evidently supporting the idea that *Psittacosaurus* lived in a juvenile-only cluster suggested by Zhao et al. (2013).

Conclusions

Based on this study of sedimentology and taphonomy at the BLK site, the following conclusions are inferred:

1. The sedimentary succession of the BLK area was deposited in an alluvial setting as a result of a catastrophic debris flow and sheet-flood induced by intense rainfall.
2. The number of *P. mongoliensis* in the BLK bone assemblage is consistent with a monodominant bonebed.
3. The sedimentologic analysis and abundant occurrence of undisturbed, articulated skeletons of *P. mongoliensis* suggests that the individuals perished in a mass mortality event due to a sudden flood.
4. The occurrence of aggregated skeletons supports the hypothesis of gregarious behavior in *Psittacosaurus* (as hypothesized by Meng et al., 2004; Zhao et al., 2007; Zhao et al., 2013). Different *Psittacosaurus* species may have exhibited taxon-specific growth rates.

Acknowledgements

We express our gratitude to Gerry Ohrstrom, Elizabeth Moore, and David Swingle for fieldwork funding. We are grateful to Drs. Tsogtbaatar Khishigjav and Badamgarav Demchig (Mongolian Academy of Sciences) for helping us to obtain fieldwork permit. We thank B. Uranchimeg, Ch. Bayardorj, and E. Zorig (Mongolian Academy of Sciences) for assisting with fieldwork. We also thank Dr. David Varricchio (Montana State University) for reviewing earlier draft of the manuscript.

Figure 2.1. Location map of the Early Cretaceous Builst Khudag (BLK) dinosaur site in central Mongolia.

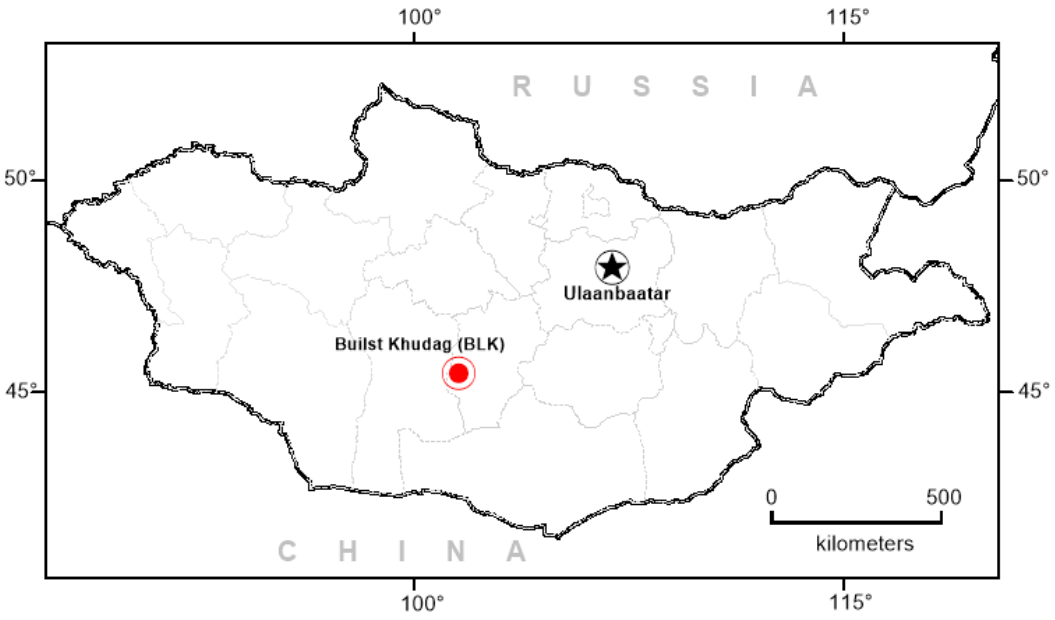


Figure 2.2. Simplified geologic map of the Lower Cretaceous Builst Khudag area (modified from Zabotkin et al., 1988).

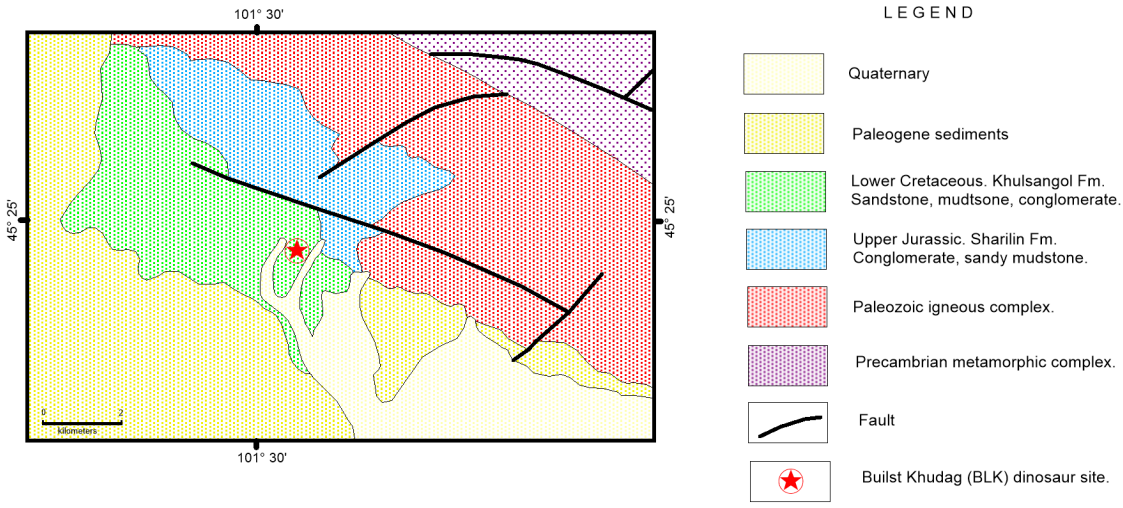


Figure 2.3. Composite stratigraphic section of the Builst Khudag (BLK) locality

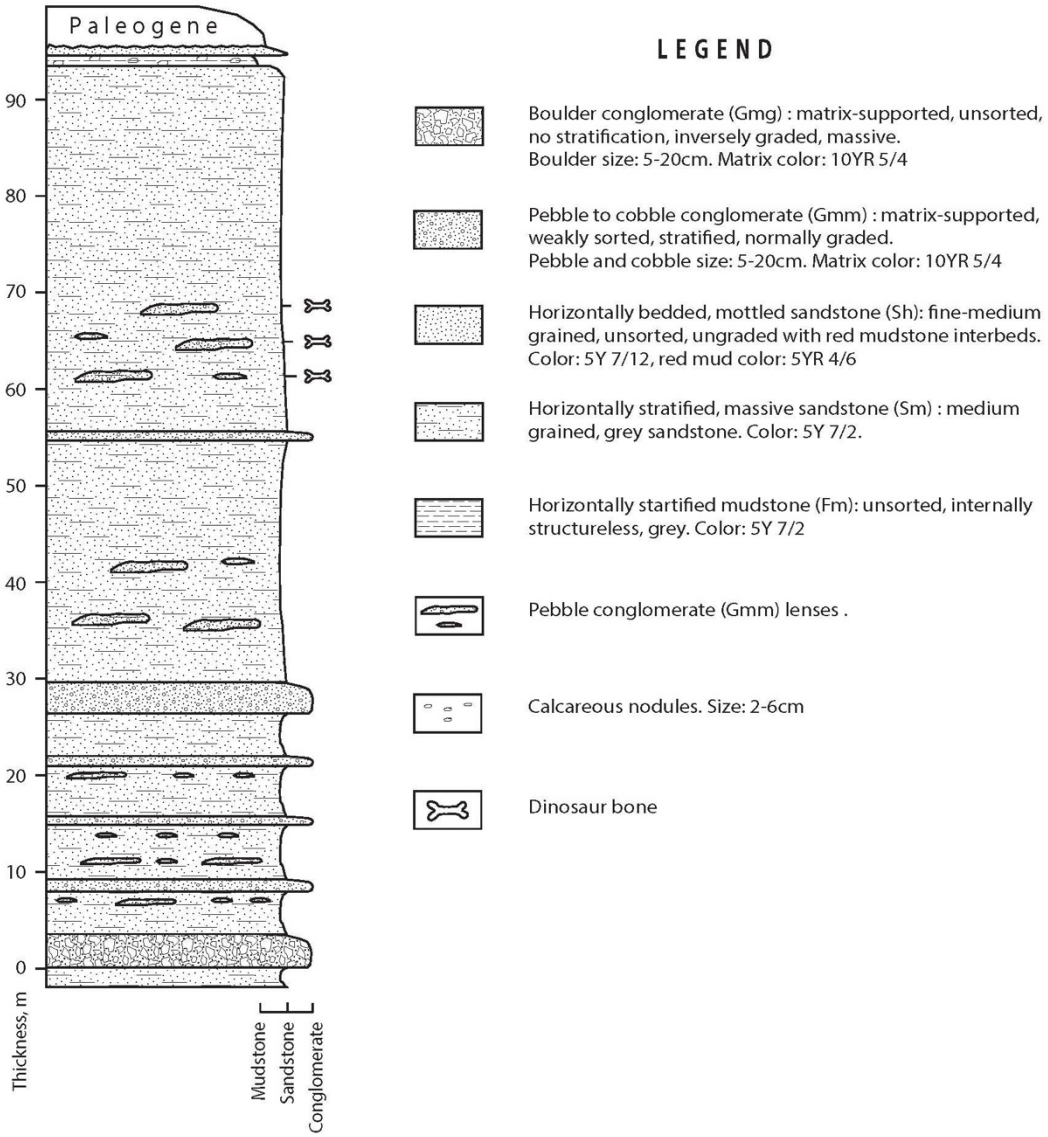


Figure 2.4. Matrix-supported, unsorted, boulder conglomerate facies (Gmg). Jacob's staff is labeled with 10 cm increments.



Figure 2.5. Matrix-supported, stratified, pebble-cobble conglomerate lens (Gmm) contacts with underlying horizontally stratified, mottled sandstone facies (Sh). Scale bar has 1cm increments.

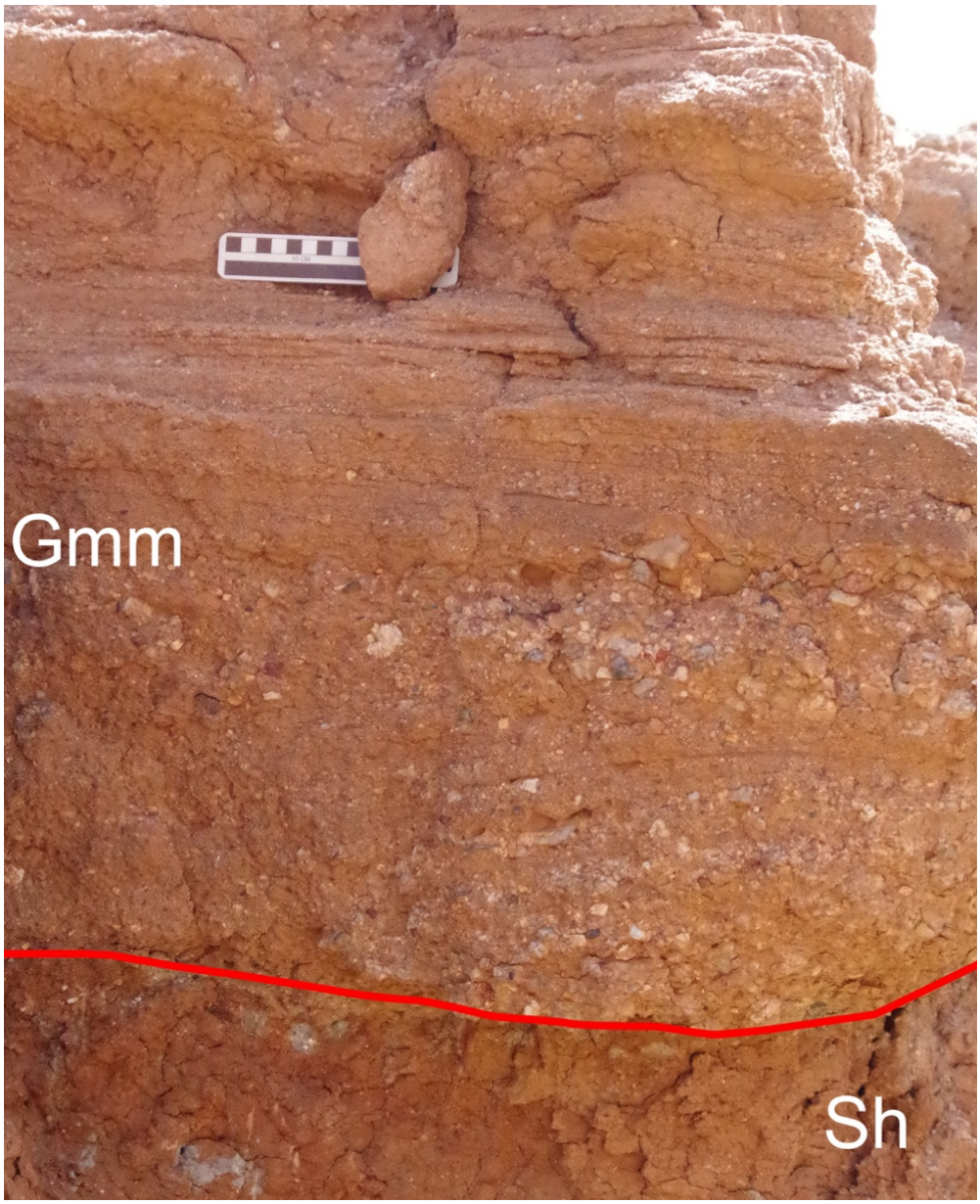


Figure 2.6. Horizontally stratified, mottled sandstone facies (Sh) with red mudstone interbeds. Jacob's staff has 10 cm increments.



Figure 2.7. Close-up photo of horizontally-stratified, mottled sandstone facies (Sh).

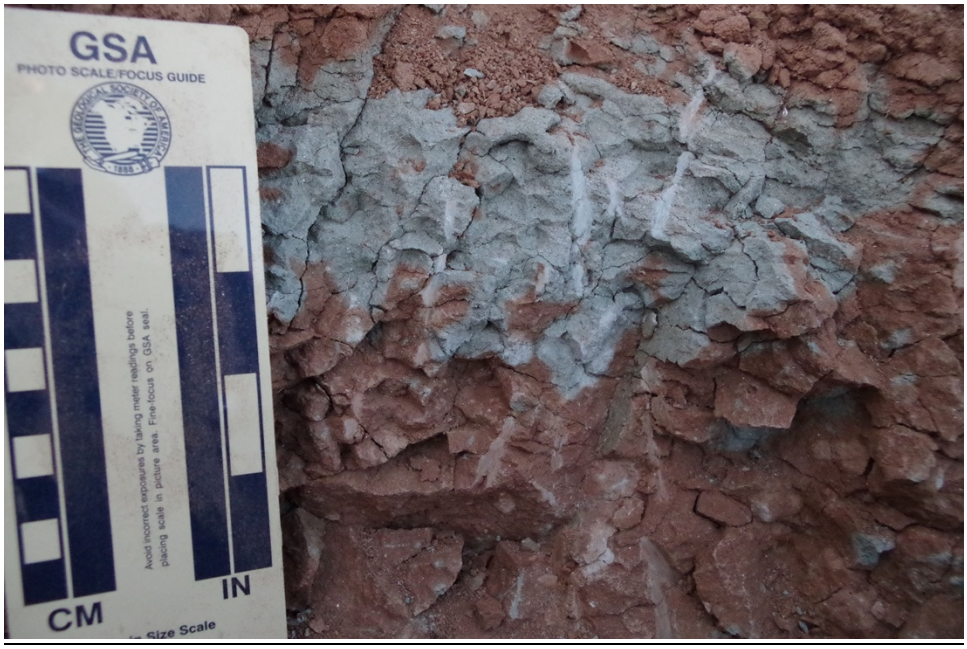


Figure 2.8. Horizontally-stratified, massive sandstone (Sm) is overlying mudstone facies (Fm). Scale bar equals 2 cm.

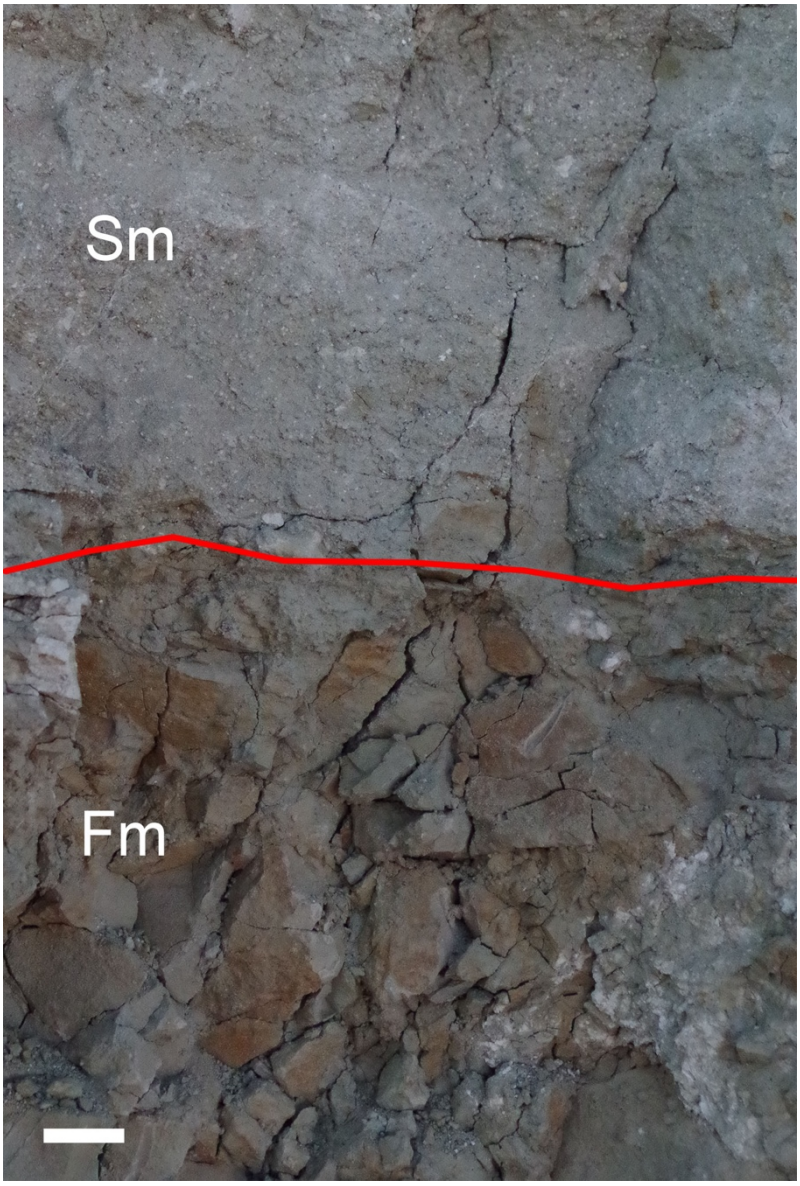


Figure 2.9. Caliche from the horizontally stratified mudstone (Fm). Scar bar is 2 cm.



Figure 2.10. Horizontally stratified, mottled sandstone (Sh) is overlain by pebble conglomerate (Gmm).

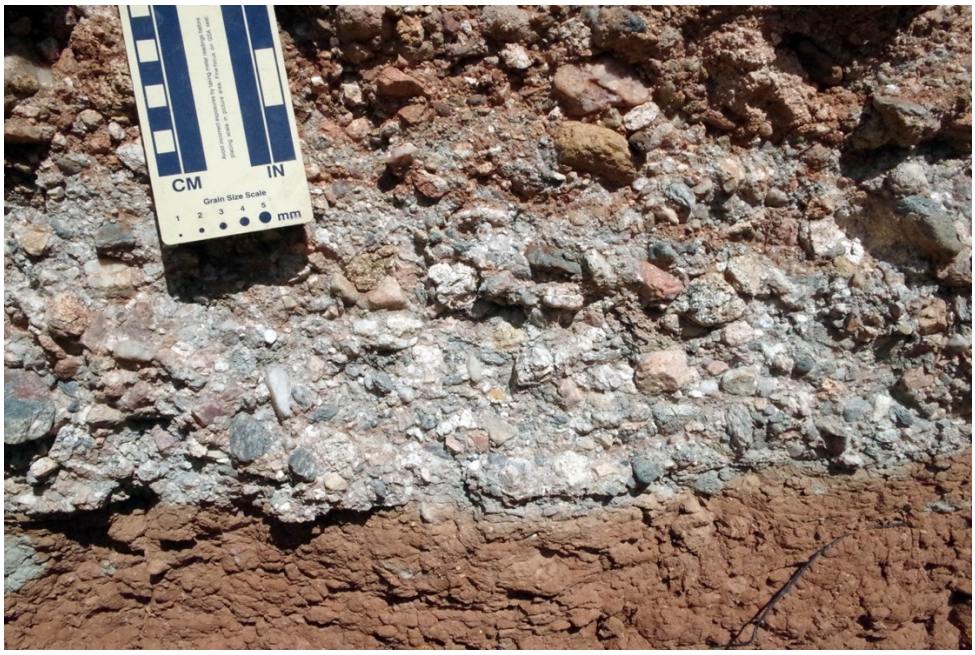


Figure 2.11. Unidentified bones collected as a surface float from the BLK locality. A) Unknown sauropod skeletal materials. B) Undetermined theropod unguals.



Figure 2.12. Location map of BLK site showing three locations of the bonebed exposures and bone distribution.

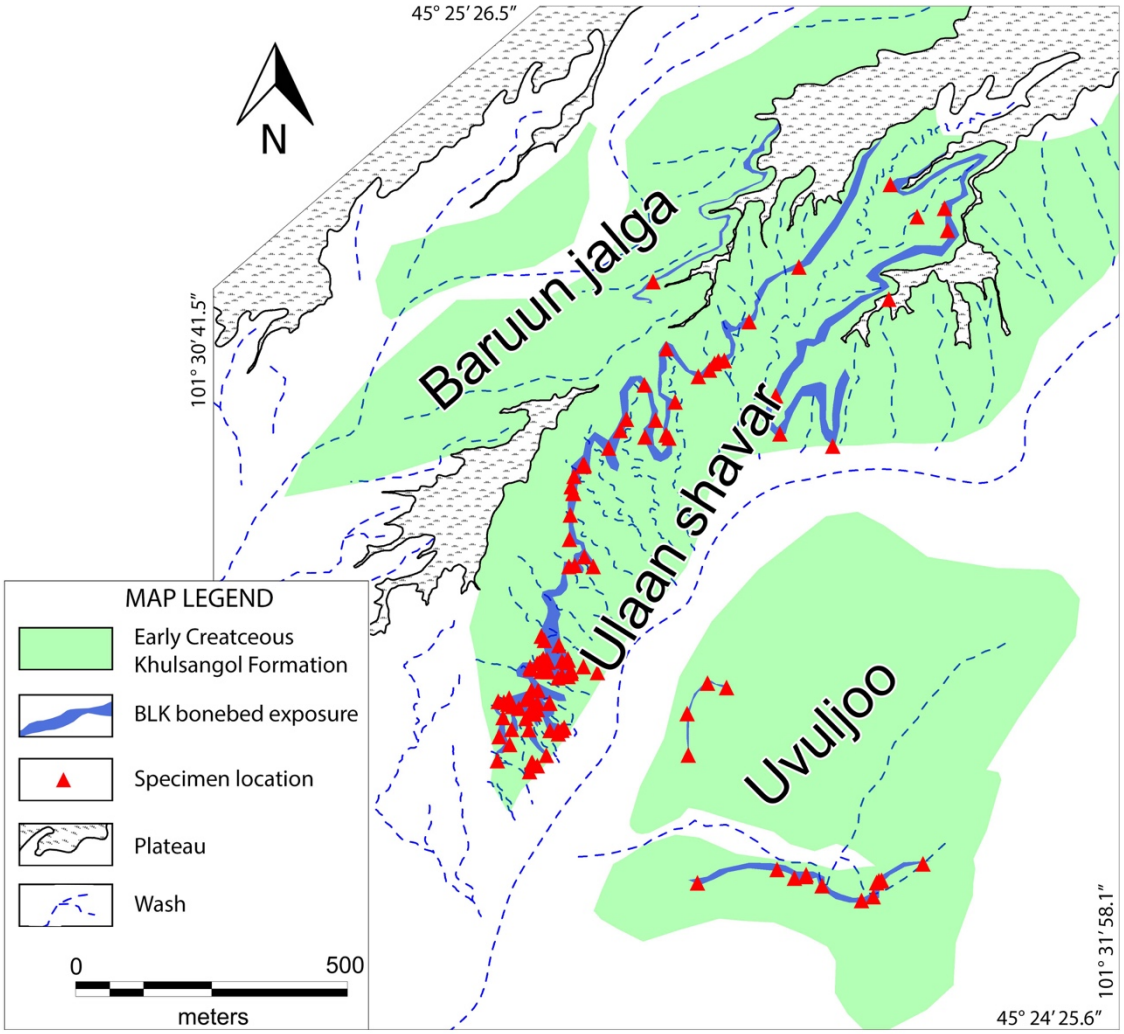


Figure 2.13. The panoramic view of the Ulaan shavar location at the BLK locality. Photos are presenting 180-degree panoramic view of the East coulee of the BLK locality. Photo alignment is in alphabetical order (A to C). Photo A is facing to the south, B is to the west, and C is to the north. The *P. mongoliensis* bonebed is highlighted in blue. Field camp is included in the photo as a scale.

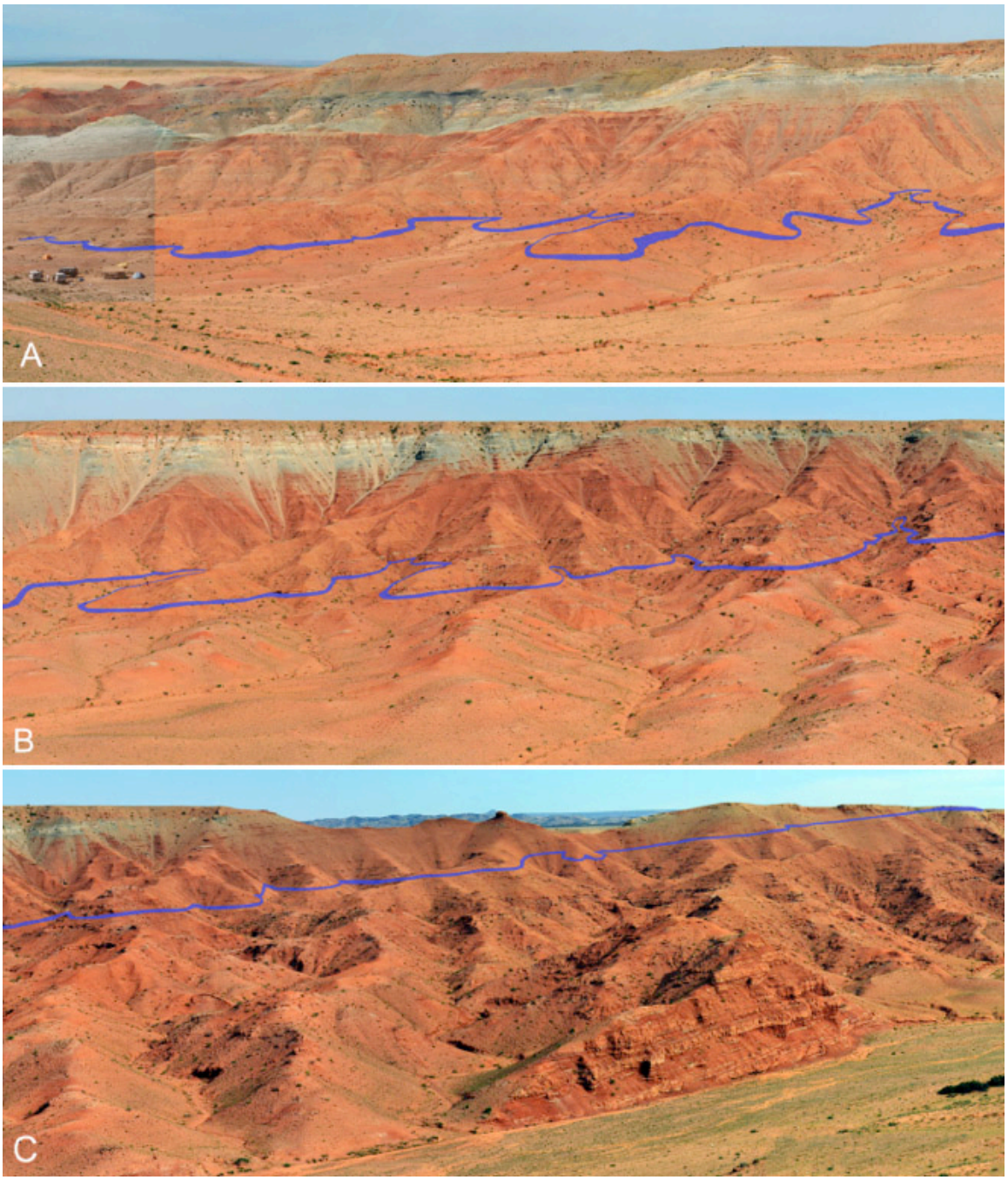


Figure 2.14. Psittacosaurus skeleton preservation in the BLK site. A) preservation of articulated *P. mongoliensis* left hind foot in mottled sandstone, B) preservation of associated vertebral elements and scapula blade in the pebble conglomerate lens.

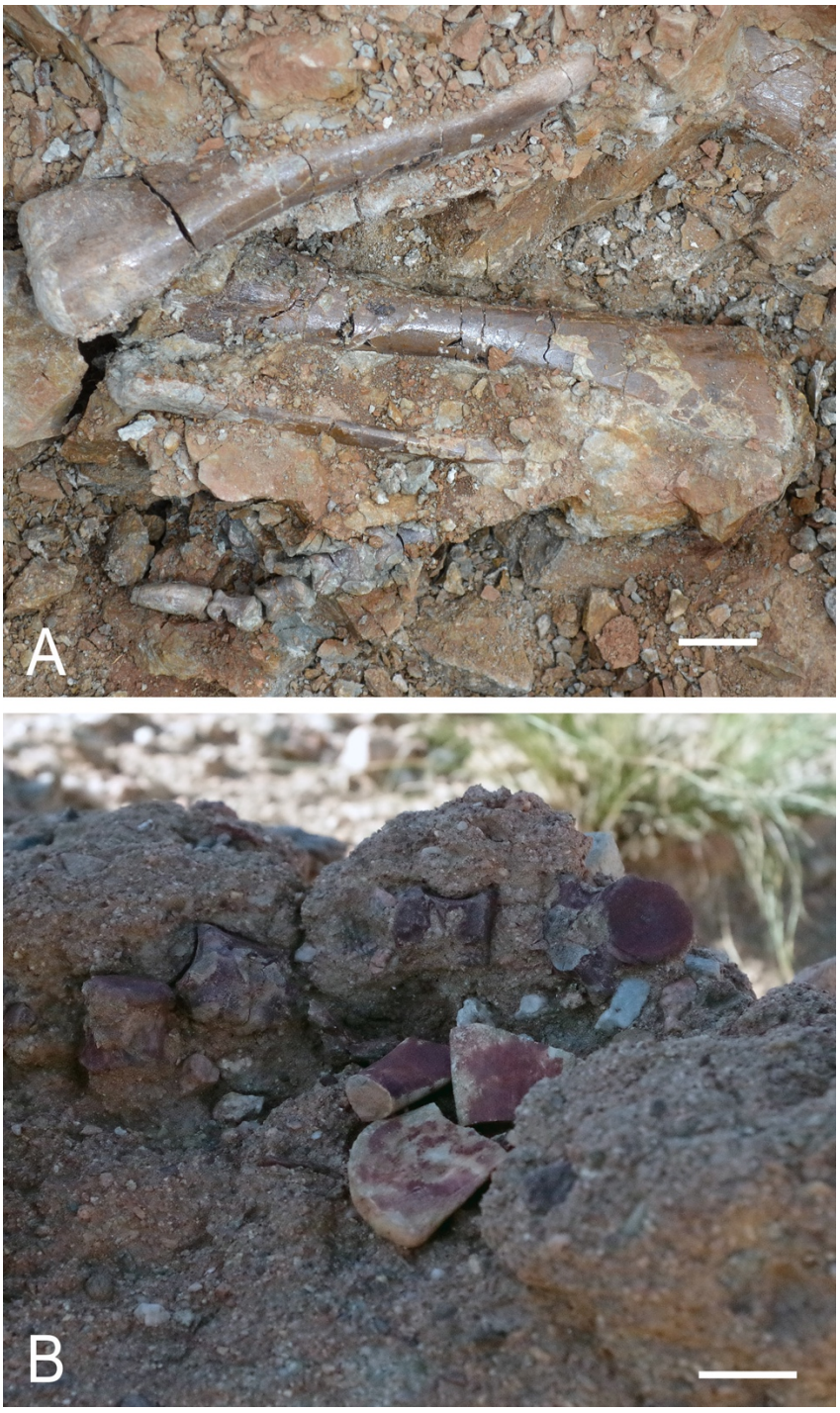


Figure 2.15. Vertebrae collection from the surface float at the Ulaan shavar location at the BLK site.



Figure 2.16. Histogram, showing estimated body length distribution of the *P. mongoliensis* bone assemblage from the BLK site. The body length estimation is based on the ratio of tibia and body length.

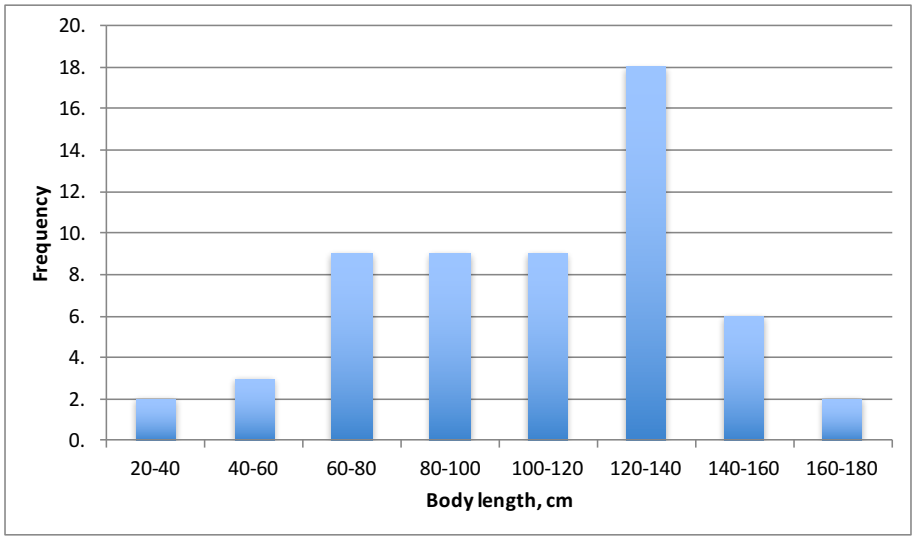


Figure 2.17. Taphonomic map of seven articulated *P. mongoliensis* individuals from three separate quarries at the BLK site. All skeletons have not been prepared completely. A and C present the largest collected individuals in the BLK site. B shows the *P. mongoliensis* aggregate consisting of five individuals preserved together. D presents the orientation data of the psittacosaur individuals, quarry scale, and north arrow. Rose diagram shows the general trends for articulated skeletons of *P. mongoliensis.*

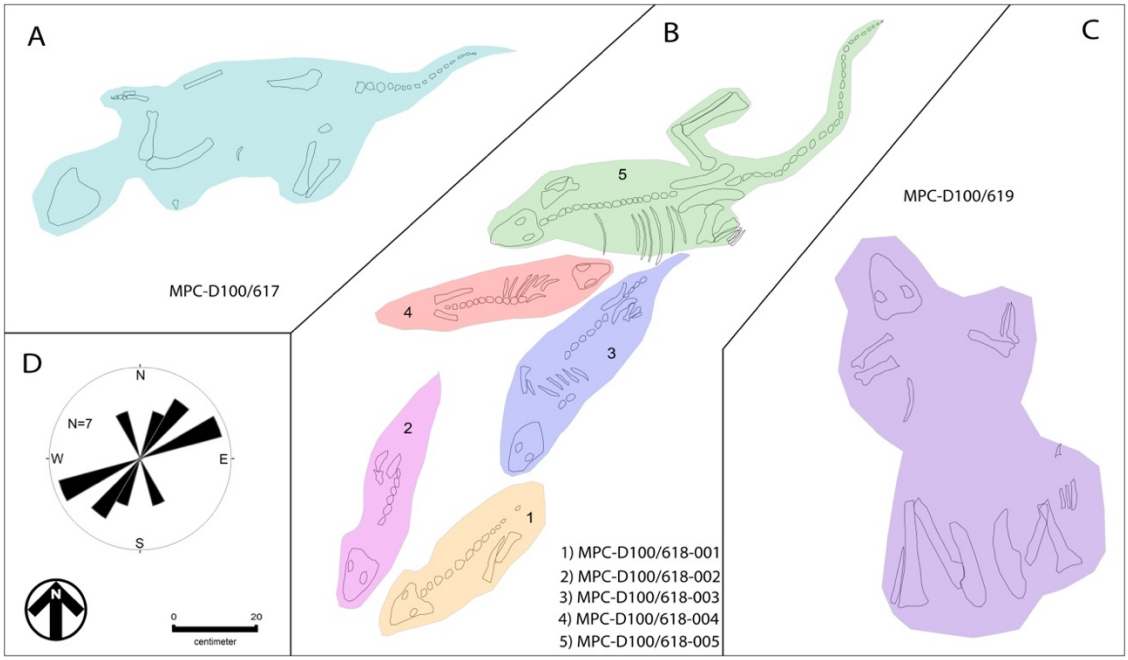


Figure 2.18. Partially prepared *P. mongoliensis* femur from the mottled sandstone unit. The femur shows series of transverse fractures. Scale bar equals 1 cm



Table 2.1. Lithofacies of the Khulsangol Formation in the study area. Facies descriptions and letter codes are based on the Miall (2006) and Mulder and Alexander (2001)

Facies code	Lithofacies	Description	Interpretation
Gmg	Matrix-supported, normal to inverse graded conglomerate	Occurs as a 2 m bed. Contacts with overlaying and overlying beds abruptly. Inversely graded.	Debris-flow deposit
Gmm	Matrix-supported pebble-cobble conglomerate	Occurs as cosets (0.5-3 m). Abrupt contact with underlying beds. Slight cross-bedding andweakly graded.	Channel-fill deposit
Sh	Horizontally bedded sandstone	Occurs as horizontally bedded, fine-medium grained, weakly graded, mottled sandstone with mud layers.	Sheet-flood deposit
Sm	Massive sandstone	Structureless, medium to coarse grained, ungraded sandstone. It occurs at the upper most part of the section.	Sediment gravity flow
Fm	Mudstone	Occurs as a 0.5-1 m bed at top of the section. Contains immature carbonaceous nodules (0.5-2 cm)	Suspension settling in standing water

Table 2.2. Identifiable skeletal elements recovered from the BLK bonebed.

Skeletal elements	Count					
	P. mongoliensis		Unknown theropod		Unknown sauropod	
	Count	%	Count	%	Count	%
Cranial elements (incl. dentaries, teeth)	52	3.0	5	0.3		
Vertebrae (incl. cervical, dorsal, sacral, caudal, all processes)	425	24.4				
Articulated postcranial elements (incl. complete skeleton, articulated dorsal vertebrae, fore and hind limbs)	37	2.1	1	0.1		
Ribs	295	17.0				
Scapulae	62	3.6			13	0.7
Coracoid	37	2.1				
Humeri	71	4.1				
Ulnae	14	0.8				
Radius	12	0.7				
Manus	120	6.9	2	0.1		
Ilium	18	1.0				
Ischium	6	0.3				
Pubis	1	0.1				
Femora	144	8.3	1	0.1	20	1.1
Tibiae	185	10.6			14	0.8
Fibulae	51	2.9				
Pes	154	8.9				
Sub total	**1684**	**96.8**	**9**	**0.5**	**47**	**2.7**
Total	**1740**					

Table 2.3. *P. mongoliensis* skeletal materials recovered from the BLK locality.

	Elements from the BLK bonebed		Surface float	Total number of skeletal elements
	Sandstone unit (Sh)	Conglomerate unit (Gmm)		
Complete skeletons:	10	0	0	**10**
Articulated elements:				
skull with dentary	4	0	1	**5**
forelimb (humerus, radius,ulna)	4	0	0	**4**
hindlimb (tibia, fibula, metatarsal)	7	0	0	**7**
caudal vertebrae	2	0	0	**2**
dorsal vertebrae	5	0	0	**5**
postcranial elements (dorsal vertebrae, ribs, hindlimb)	4	0	0	**4**
Disarticulated elements				
skull bones including dentary, predentary, rostrum, teeth	19	0	33	**52**
Vertebrae (incl. cervical, dorsal, sacral, caudal, all processes)	126	27	272	**425**
rib	127	63	105	**295**
scapula	28	2	32	**62**
coracoid	15	1	21	**37**
humerus	16	6	49	**71**
ulna	9	0	5	**14**
radius	5	0	7	**12**
manus	52	14	54	**120**
ilium	7	0	11	**18**
ischium	2	0	4	**6**
pubis	1	0	0	**1**
femur	38	17	89	**144**
tibia	69	9	107	**185**
fibula	24	7	20	**51**
pes	87	5	62	**154**
Total number of elements from each bone-bearing unit	**661**	**151**	**872**	
Total	**1684**			

Table 2.4. Taxa recovered from the BLK locality. *P.mongoliensis* MNI was determined by using most common elements including femur, tibia, fibula, humerus, radius, and ulna. Articulated and complete *P. mongoliensis* specimens are included in the MNI. * Theropod MNI includes a complete, undescribed specimen.

Taxa	MNI	NISP
P. mongoliensis	213	1684
Unknown theropod	5*	9
Unknown sauropod	2	47

Table 2.5 *P. mongoliensis* aggregate consists of five individuals. Single star (*) denotes the numbers of line of arrested growth (LAGs) used for determining individual's relative age at death based on the preliminary histologic data. Double stars (**) denote that the portion of the elements was destroyed during the field excavation due to an inexperienced crew member.

	Specimen number	Tibia, cm	Body length, cm	Trend	Posture	Completeness	Age at death *
1	MPC-D100/618-001	11.54	73	220	crouching	complete, skull roof is destroyed**	3
2	MPC-D100/618-002	11.6	73.9	205	crouching	complete, skull roof is destroyed**	2
3	MPC-D100/618-003	13.3	76.4	222	crouching	complete	4
4	MPC-D100/618-004	10.4	65.9	60	crouching	complete	2
5	MPC-D100/618-005	16.1	102	251	crouching	complete	5
6	MPC-D100/617	17.5	127.1	250	crouching	complete	5
7	MPC-D100/619	24.2	153.6	330	crouching	Nearly complete, missing partial tail	10

Table 2.6. Bone modification data observed from the total of 544 skeletal elements of *P. mongoliensis* recovered from the Builst Khudag site.

Feature	Stage/Type	Count	Percentage
Weathering	0	468	88.7
	1	76	11.3
	2	0	0
	3	0	0
		n=544	
Abrasion	0	501	92
	1	43	8
	2	0	0
		n=544	
Fracture	Transverse	51	81
	Longitudinal	12	19
	Spiral (helical)	0	0
		n=63	

Literature Cited

Averianov, A. O., A. V. Voronkevich, S. V. Leshchinskiy, and A. V. Fayngertz. 2006. A ceratopsian dinosaur *Psittacosaurus sibiricus* from the Early Cretaceous of West Siberia, Russia and its phylogenetic relationships. Journal of Systematic Palaeontology 4: 359-395.

Bagnold, R. A. 1956. The flow of cohesionless grains in fluids. Philosophical Transactions of the Royal Society of London A: Mathematical, Physical and Engineering Sciences 249: 235-297.

Ballance, P. F. 1984. Sheet-flow-dominated gravel fans of the non-marine middle Cenozoic Simmler Formation, central California. Sedimentary Geology 38: 337-359.

Barrett, P. M., and X.-L. Wang. 2007. Basal titanosauriform (Dinosauria, Sauropoda) teeth from the lower cretaceous Yixian formation of liaoning province, China. Palaeoworld 16: 265-271.

Behrensmeyer, A. K. 1975. The taphonomy and paleoecology of Plio-Pleistocene vertebrate assemblages East of Lake Rudolph, Kenya. Bull. Mus. Compar. Zool., Harvard Univ 146: 473-578.

Behrensmeyer, A. K. 1978. Taphonomic and ecologic information from bone weathering. Paleobiology: 150-162.

Berkey, C. P., and F. K. Morris. 1927. Geology of Mongolia; pp. 456, Central Asiatic Expeditions. American Museum of the Natural History, New York.

Beverage, J. P., and J. K. Culbertson. 1964. Hyperconcentrations of suspended sediment. Journal of Hydraulic Div., ASCE 90: 117-128.

Blair, T. C. 1987. Sedimentary processes, vertical stratification sequences, and geomorphology of the Roaring River alluvial fan, Rocky Mountain National Park, Colorado. Journal of Sedimentary Research 57.

Blissenbach, E. 1954. Geology of alluvial fans in semiarid regions. Geological Society of America Bulletin 65: 175-190.

Bochkov, S. V. 1986. Geological report No.4276. Ministry of Geology, USSR.

Bratseva, G. M., and I. M. Novodvorskaya. 1975. Spore and pollen from the Early Cretaceous Khuren Dukh locality. Trudy Sovmetstnoi Sovetsko-Mongol'skoi Paleontologicheskoya Ekspeditsii. 2: 205-209.

Bratseva, G. M., and I. M. Novodvorskaya. 1976. Burial conditions of Early Cretaceous fauna and flora in the localities of Builyasutuin-Khuduk and Anda-Khuduk. Trudy Sovmetstnoi Sovetsko-Mongol'skoi Paleontologicheskoya Ekspeditsii. 3: 285-290.

Brinkman, D. B., D. A. Eberth, M. Ryan, and P. Chen. 2001. The occurrence of *Psittacosaurus xinjiangensis* Sereno and Chow, 1988 in the Urho area, Junggar Basin, Xinjiang, People's Republic of China. Canadian Journal of Earth Sciences 38: 1781-1786.

Bull, W. B. 1972. Recognition of alluvial fan deposits in the stratigraphic record.

Chen, P. J. 1987. Cretaceous paleogeography in China. Palaeogeography, Palaeoclimatology, Palaeoecology 59: 49-56.

Chiba, K., M. J. Ryan, D. R. Braman, D. A. Eberth, E. E. Scott, C. M. Brown, Y. Kobayashi, and D. C. Evans. 2015. Taphonomy of a Monodominant *Centrosaurus apertus* (Dinosauria: Ceratopsia) Bonebed from the Upper Oldman Formation of Southeastern Alberta. Palaios 30: 655-667.

Currie, P. J. 1997. Gastroliths; pp. 270 *i*n P. J. Currie, and K. Padian (eds.), Encyclopedia of Dinosaurs. Academic Press, San Diego.

Dasgupta, P. 2006. Facies characteristics of Talchir Formation, Jharia Basin, India: implications for initiation of Gondwana sedimentation. Sedimentary Geology 185: 59-78.

Eberth, D. A. 2010. A review of ceratopsian paleoenvironmental associations and taphonomy. New perspectives on horned dinosaurs. Edited by MJ Ryan, BJ Chinnery-Allgeier, and DA Eberth. Indiana University Press, Bloomington, IN: 428-446.

Eberth, D. A., M. Shannon, and B. G. Noland. 2010. A Bonebeds Database: Classification, Biases, and Patterns of Occurrence. Bonebeds: Genesis, analysis, and paleobiological significance: 103.

Erickson, G. M., P. J. Makovicky, B. D. Inouye, C. F. Zhou, and K. Q. Gao. 2009. A Life Table for *Psittacosaurus lujiatunensis*: Initial Insights Into Ornithischian Dinosaur Population Biology (vol 292, pg 1514, 2009). Anatomical Record-Advances in Integrative Anatomy and Evolutionary Biology 292: 1684-1684.

Esteban, M. 1976. Vadose Pisolite and Caliche: GEOLOGIC NOTES. AAPG Bulletin 60: 2048-2057.

Esteban, M., and C. F. Klappa. 1983. Subaerial exposure environment; pp. 1-54, Carbonate depositional environments. American Association of Petroleum Geologists Tulsa, Okla.

Fernandez-Jalvo, Y. 1988. Tafonomia de Microvertebrados en Gran Dolina, Atapuerca (Burgos). Ph. D. Thesis, Facultad de Ciencias Geologicas, Universidad Complutense de Madrid, 1988, unpublished.

Fiorillo, A. R. 1988. Taphonomy of Hazard Homestead Quarry (Ogallala Group), Hitchcock County, Nebraska. Rocky Mountain Geology 26: 57-97.

Ford, T. L., and L. D. Martin. 2010: A semi-aquatic life habit for *Psittacosaurus*. Paper presented at the New Perspectives on Horned Dinosaurs: The Royal Tyrrell Museum Ceratopsian Symposium, 2010.

Hartley, A. J. 1993. Sedimentological response of an alluvial system to source area tectonism: the Seilao Member of the Late Cretaceous to Eocene Purilactis Formation of northern Chile. Alluvial Sedimentation: 489-500.

Hasegawa, H., R. Tada, N. Ichinnorov, and C. Minjin. 2009. Lithostratigraphy and depositional environments of the Upper Cretaceous Djadokhta Formation, Ulan Nuur basin, southern Mongolia, and its paleoclimatic implication. Journal of Asian Earth Sciences 35: 13-26.

Haynes, G. 1983. Frequencies of spiral and green-bone fractures on ungulate limb bones in modern surface assemblages. American antiquity: 102-114.

Jerzykiewicz, T. 2000. Lithostratigraphy and sedimentary settings of the Cretaceous dinosaur beds of Mongolia.; pp. 279-296 *i*n M. J. Benton, M. A. Shishkin, and D. M. Unwin (eds.), The age of dinosaurs in Russia and Mongolia. Cambridge University Press.

Jerzykiewicz, T., and D. A. Russell. 1991. Late Mesozoic stratigraphy and vertebrates of the Gobi Basin. Cretaceous Research 12: 345-377.

Jiang, B., and J. Sha. 2007. Preliminary analysis of the depositional environments of the Lower Cretaceous Yixian Formation in the Sihetun area, western Liaoning, China. Cretaceous Research 28: 183-193.

Khand, Y., D. Badamgarav, Y. Ariunchimeg, and R. Barsbold. 2000. Cretaceous System in Mongolia and its depositional environments. Cretaceous Environments of Asia. 17: 49-79.

Leeder, M. R. 1975. Pedogenic carbonates and flood sediment accretion rates: a quantitative model for alluvial arid-zone lithofacies. Geological Magazine 112: 257-270.

Lowe, D. R. 1982. Sediment gravity flows: II Depositional models with special reference to the deposits of high-density turbidity currents. Journal of Sedimentary Research 52.

Mack, G. H., W. C. James, and H. C. Monger. 1993. Classification of paleosols. Geological Society of America Bulletin 105: 129-136.

Martin, C. A., and B. R. Turner. 1998. Origins of massive-type sandstones in braided river systems. Earth-Science Reviews 44: 15-38.

Martinson, G. G. 1982. The Upper Cretaceous mollusks of Mongolia; pp. 5-76 *i*n L. A. Nevesskaya (ed.), Sovmestnaya Sovetsko-Mongolskaya Paleontologicheskaya Ekspeditsia.

Meng, Q., J. Liu, D. J. Varricchio, T. Huang, and C. Gao. 2004. Palaeontology: Parental care in an ornithischian dinosaur. Nature 431: 145-146.

Meyer, G. A., and S. G. Wells. 1997. Fire-related sedimentation events on alluvial fans, Yellowstone National Park, USA. Journal of Sedimentary Research 67.

Miall, A. D. 1977. Lithofacies types and vertical profile models in braided river deposits: a summary.

Miall, A. D. 2006. The Geology of Fluvial Deposits: Sedimentary Facies, Basin Analysis, and Petroleum Geology. 582 pp., Springer-Verlag.

Middleton, G. V., and M. Hampton. 1976. Subaqueous sediment transport and deposition by sediment gravity waves.

Mulder, T., and J. Alexander. 2001. The physical character of subaqueous sedimentary density flows and their deposits. Sedimentology 48: 269-299.

Munsell Color, C. O. 2000. Munsell soil color charts. Gretabacbeth.

Nemec, W., and R. J. Steel. 1984. Alluvial and coastal conglomerates: their significant features and some comments on gravelly mass-flow deposits.

Osborn, H. F. 1923. Two Lower Cretaceous dinosaurs of Mongolia. American Museum Novitates 95: 10.

Osborn, H. F. 1924. *Psittacosaurus* and *Protiguanodon*: two Lower Cretaceous iguanodonts from Mongolia. American Museum Novitates 127: 16.

Pierson, T. C., and J. E. Costa. 1987. A rheologic classification of subaerial sediment-water flows. Reviews in Engineering Geology 7: 1-12.

Pierson, T. C., and K. M. Scott. 1985. Downstream dilution of a lahar: transition from debris flow to hyperconcentrated streamflow. Water resources research 21: 1511-1524.

Rogers, R. R. 1990. Taphonomy of three dinosaur bone beds in the Upper Cretaceous Two Medicine Formation of northwestern Montana: evidence for drought-related mortality. Palaios: 394-413.

Rozhdestvensky, A. K. 1955a. The first discovery of a dinosaur in the USSR in the indigenous locality. Byuleten' Moskovskogo Obschestva Ispytate lei Prirody, Otdel Geologicheskii 30: 118.

Rozhdestvensky, A. K. 1955b. New data on *Psittacosaurus* - Cretaceous ornithopods. Questions on the Geology of Asia 2: 783-788.

Russell, D. A., and X.-J. Zhao. 1996. New psittacosaur occurrences in Inner Mongolia. Canadian Journal of Earth Sciences 33: 637-648.

Scott, K. M. 1988. Origins, behavior, and sedimentology of lahars and lahar-runout flows in the Toutle-Cowlitz River system, Report 2330-7102.

Sereno, P. C. 1987. The Ornithischian Dinosaur *Psittacosaurus* from the Lower Cretaceous of Asia and the Relationships of the Ceratospia. Columbia University New York.

Shipman, P. 1981. Life History of a Fossil and Introduction To Taphonomy and Paleoecology. 222.

Shultz, A. W. 1984. Subaerial debris-flow deposition in the upper Paleozoic Cutler Formation, western Colorado. Journal of Sedimentary Research 54.

Shuvalov, V. F. 1974. On the geology and age of the Khobur and Khuren Dukh localities in Mongolia. Trudy Sovmetstnoi Sovetsko-Mongol'skoi Paleontologicheskoya Ekspeditsii. 1: 296-304.

Shuvalov, V. F. 1975. A new Early Cretaceous dinosaur locality Builyasutuin Khuduk; pp. 210-213 *i*n N. N. Kramarenko (ed.), Fossil Fauna and Flora of Mongolia. Trudy Sovmest. Soviet-Mongol. Nauka, Moscow.

Sinitsa, S. M. 1993. Jurassic and Lower Cretaceous of Central Mongolia. Trudy Sovmetstnoi Sovetsko-Mongol'skoi Paleontologicheskoya Ekspeditsii. 42: 3-238.

Smith, G. A. 1986. Coarse-grained nonmarine volcaniclastic sediment: terminology and depositional process. Geological Society of America Bulletin 97: 1-10.

Sohn, Y. K., C. W. Rhee, and B. C. Kim. 1999. Debris flow and hyperconcentrated flood-flow deposits in an alluvial fan, northwestern part of the Cretaceous Yongdong basin, central Korea. The Journal of Geology 107: 111-132.

Stauffer, P. H. 1967. Grain-flow deposits and their implications, Santa Ynez Mountains, California. Journal of Sedimentary Research 37.

Stewart, D. J. 1981. A meander-belt sandstone of the Lower Cretaceous of Southern England. Sedimentology 28: 1-20.

Suslov, Y. V. 1983. The burial of psittacosaurs at Khamryn-Us (Eastern Gobi, MPR). Trudy Sovmetstnoi Sovetsko-Mongol'skoi Paleontologicheskoya Ekspeditsii.: 118-120.

Todd, S. P. 1989. Stream-driven, high-density gravelly traction carpets: possible deposits in the Trabeg Conglomerate Formation, SW Ireland and some theoretical considerations of their origin. Sedimentology 36: 513-530.

Tooruul, N. 1986. Geological report N. 3912. Ministry of Geology and Mining, Mongolia.

Wan, Z., Z. Wang, and P. Julien. 1994. Hyperconcentrated flow. Journal of Hydraulic Engineering 120: 1234-1234.

Wright, V. P., and M. E. Tucker. 1991. Calcretes. Blackwell Scientific Publications.

Xing, X., and M. A. Norell. 2006. Non-avian dinosaur fossils from the Lower Cretaceous Jehol Group of western Liaoning, China. Geological Journal 41: 419-437.

Zhao, Q., P. M. Barrett, and D. A. Eberth. 2007. Social behaviour and mass mortality in the basal ceratopsian dinosaur *Psittacosaurus* (Early Cretaceous, People's Republic of China). Palaeontology 50: 1023-1029.

Zhao, Q., M. J. Benton, X. Xu, and P. M. Sander. 2013. Juvenile-only clusters and behaviour of the Early Cretaceous dinosaur *Psittacosaurus*. Acta Palaeontologica Polonica 59: 827-833.

Zhou, C.-F., K.-Q. Gao, R. C. Fox, and S.-H. Chen. 2006. A new species of *Psittacosaurus* (Dinosauria: Ceratopsia) from the Early Cretaceous Yixian Formation, Liaoning, China. Palaeoworld 15: 100-114.

Zhou, Z. 2006. Evolutionary radiation of the Jehol Biota: chronological and ecological perspectives. Geological Journal 41: 377-393.

CHAPTER THREE

INTRASKELETAL HISTOVARIABILITY IN THE HIND LIMB OF *PSITTACOSAURUS MONGOLIENSIS*

Contribution of Authors and Co-Authors

Manuscript in Chapter 3

Author: Badamkhatan Zorigt

Contributions: Conceived the study, obtained and processed specimens, analyzed data, interpreted results, and wrote the manuscript.

Co-author: John R. Horner

Contributions: Provided fieldwork funding, specimen processing facilities and equipment, microscope and photograph equipment. Assisted with the study design, discussed implications of results, and edited earlier drafts of the manuscript. earlier drafts of the manuscripts.

Manuscript Information Page

Badamkhatan Zorigt, John R. Horner
Journal of Vertebrate Paleontology
Status of Manuscript:
_x_Prepared for submission to a peer-reviewed journal
___Officially submitted to a peer-reviewed journal
___Accepted by a peer-reviewed journal
___Published in a peer-reviewed journal

Published by Society of Vertebrate Paleontology

Abstract

Since the discovery of the lines of arrested growth in dinosaur bones, skeletochronology has been explored in numerous dinosaur taxa. Various skeletal elements have been used for the relative age assessment of dinosaur individuals. However, each element exhibits a different histological developmental pattern. In the past, the tibia and femur have been sectioned for histologic analyses for many dinosaur taxa. In previous studies of *Psittacosaurus* skeletochronology, the humerus, femur, tibia, and fibula have been utilized. Determining an ideal skeletal element for *Psittacosaurus* skeletochronology and tissue typing is necessary to study the growth strategy of this animal. We sectioned associated femora, tibiae, and fibulae from four individuals reflecting different ontogenetic stages in this study. The femur and tibia show similar vascularization throughout the specimens. The fibulae exhibit mostly longitudinal vascularizations in all individuals. The tibia and fibula present the same numbers of lines of arrested growth whereas the femur appears to have lost its innermost preserved growth lines due to an extensive expansion of the medullary cavity in the bone. Extensively distributed resorption cavities are observed in all elements including the femur, tibia, and fibula from the larger individual. This may reflect a simultaneous effect in all weight-bearing hind limb elements due to a considerable physiologic change such as initiation of skeletal maturity. However, this hypothesis needs to be tested in other hind limb elements including the metatarsals of *Psittacosaurus*.

Introduction

Bone histology has been utilized as an important tool to decipher the physiology of extinct organisms such as dinosaurs. Many researchers have conducted histological analyses on the growth strategies of different groups of dinosaurs using various skeletal elements (e.g., Varricchio, 1993; Chinsamy, 1994; Curry, 1999; Horner et al., 1999; Erickson and Tumanova, 2000; Horner et al., 2000; Sander, 2000; Horner and Padian, 2004; Sander and Klein, 2005; Reizner and Horner, 2006; Erickson et al., 2009; Klein et al., 2009; Werning, 2012).

Horner et al. (1999) conducted a comparative histologic study on the hadrosaurid dinosaur *Hypacrosaurus* using various bones from a single individual. The result of this study suggested that the weight-bearing elements, including the femur and tibia preserved the greatest number of the lines of arrested growth (LAGs) in the cortices with the least amount of bone remodeling (Horner et al., 1999). In contrast, a skeletochronogical study on the modern *Alligator* revealed that less weight-bearing elements such as the pubis and fibula preserved the greatest number of LAGs (Erickson and Brochu, 1999; Erickson et al., 2004; Garcia, 2011).

The growth rates of the basal ceratopsian dinosaur *Psittacosaurus* have been studied using various elements including the fibula, humerus, tibia, and femur (Erickson and Tumanova, 2000; Erickson et al., 2009). Since there has been found to be a considerable amount of histologic variations in the bones from a single individual of hadrosaur (Horner et al., 1999), a study of intraskeletal histologic in *Psittacosaurus* is necessary to attain a more robust result regarding the growth strategy of this animal. The

purpose of this study is to identify the ideal skeletal element for the tissue typing and the relative age determination for the *P. mongoliensis* growth analyses.

Methods

We used the associated femur, tibia, and fibula of four specimens of *P. mongoliensis* that were collected from the Early Cretaceous Builst Khudag locality in Mongolia. All skeletons were found in an articulated state. Based on a taphonomic study, these individuals had died and were buried simultaneously and experienced minimal taphonomic modifications such as weathering and abrasion (see Chapter 2).

The body lengths of the individuals were measured using a tape measure. The lengths of the femora, tibiae, and fibulae were obtained using a digital calipers (Table 3.1). The mid-shafts of the elements were sampled for histologic analysis. The specimens were prepared and thin sectioned following Lamm (2013). The slides were examined using a Nikon Optiphot-Pol polarizing petrographic microscope. The entire bone cross-section was photographed using a combination of Nikon DS-Fi1 camera and NIS-Elements BR 3.0 software. Adobe Photoshop CC 2015 was used for tracing the perimeters of the diaphysis, medullary cavity, and LAGs. The areas of the whole transverse section of the bone and the medullary cavity were quantified by using NIH ImageJ v.1.49 software.

Results

Descriptions of MPC-D100/618-001

Femur: The transverse sectional area of the left femur of MPC-D100/618-001 is comprised of the medullary cavity (representing 33.6% of the area) and the bone wall (representing 66.4%) (Fig. 3.1, A-B). The cortex mainly consists of reticular and longitudinal vascular canals with parallel fibered bone matrix. There is a dense concentration of the osteocyte lacunae in the inner half of cortex. A distinct zoning is observed between the LAGs. The zone starts with highly vascular tissue and then the density of the vascularization is decreases outward. In the inner half of the zone, the bone matrix is disorganized but not to the degree that defines woven tissue described by Francillon-Vieillot et al. (1990). The bone tissue is parallel-fibered. Two LAGs are preserved in the cortex.

Tibia: The transverse sectional area of the tibia of MPC-D100/618-001 is comprised of the medullary cavity (representing 23.8% of the area) and the bone wall (representing 76.2%) (Fig. 3.1, C-D). The vascularization of the tibia cortex consists of a combination of reticular and radial vascular canals and this bone preserves a zoning pattern similar to that observed in the associated femur. The bone matrix organization shifts from the disorganized fibers (but not to the degree of woven tissue) to the parallel-fibered matrix in the inner 2/3 of the each zone. The density of the vascularization and of osteocyte lacunae becomes reduced in outer in the outer third of each zone (Fig. 3.1, D). Two LAGs are preserved.

Fibula: The transverse sectional area of the fibula of MPC-D100/618-001 is comprised of the medullary cavity (representing 17.4% of the area) and the bone wall (representing 82.6%) (Fig. 3.1, E-F). The fibula cortex mainly consists of reticular and longitudinal vascular canals with parallel-fibered bone matrix. In general, the density of vascularity in the fibula is greatly reduced compare to the associated femur and tibia. The longitudinal canals exhibit a slightly anastomosing pattern in the outer cortex. The zoning pattern is somewhat similar to those of the associated femur and tibia but the outer third of the zone becomes nearly avascular. Three LAGs are preserved in the cortex.

Descriptions of MPC-D100/620-015

Femur: The transverse sectional area of the left femur of MPC-D100/620-015 is comprised of the medullary cavity (representing 17.4% of the area) and the bone wall (representing 82.6%) (Fig. 3.2, A-B). The femur cortex primarily exhibits a combination of reticular and longitudinal vascularization with parallel-fibered matrix. The density of the osteocyte lacunae is evenly distributed. There is a vague zoning pattern observed in this specimen (Fig. 3.2, B). The preserved LAGs were increasingly difficult to trace due to the uniformed tissue organization of the cortex. Three LAGs are preserved in the cortex.

Tibia: The area of medullary cavity in the transverse section of the tibia of this specimen is relatively small (representing 17.4% of the area) (Fig. 3.2, C-D). The cortex is composed of a combination of reticular and sub-plexiform bone tissue. The sub-

plexiform tissue with parallel-fibered matrix is predominant in the outer 1/3 of the cortex. The osteocyte lacunae are distributed evenly. Three to four LAGs are preserved.

Fibula: The expansion area of the medullary cavity is relatively small (17.4%) (Fig. 3.3, E-F) in the fibula of MPC-D100/620-015, somewhat similar to what was observed in the associated tibia. The fibula cortex largely consists of longitudinally oriented vascular canals in the cortex. The density of the vascularity is greatly decreased and uniform compared to the femur and tibia. The bone matrix becomes more organized presenting parallel-fibered tissue. The zoning pattern was difficult to observe. Three LAGs were preserved in the cortex.

Descriptions of MPC-D100/618-005

Femur: Reticular vascularization with a parallel-fibered matrix is observed in the transverse section of the femur mid-shaft of MPC-D100/618-005 (Fig. 3.3, A-B). The medullary cavity comprises 29.1 % of the total area of the transverse section of the bone. A slight decrease of vascularization bearing a narrow LAG is observed in the outer rim of each zone. In the outer fifth of each zone, the density of vascularity decreases. Groups of radial canals occur locally in the mid cortex. Two LAGs are observed in the cortex.

Tibia: The area of the medullary cavity is 17.2% of the total sectional area of the tibia of this individual. The cortex exhibits a combination of reticular and sub-plexiform vascularity with parallel-fibered bone matrix (Fig. 3.3, C-D). There are common occurrences of radial canals in the cortex that are mostly terminated by LAGs. The inner

half of the each zone consists of reticular vascularity with poorly organized bone fibers (but not to the degree of woven tissue). The vascularity shifts to sub-plexiform with parallel-fibered bone tissue in the outer half of each zone. This zoning pattern is sequentially repeated at least 2-3 times in the cortex. Three LAGs are counted.

Fibula: The area of medullary cavity in the fibula is 15.5% of the total sectional area (Fig. 3.3, E-F). The fibula cortex mostly consists of reticular vascularization with a parallel-fibered bone matrix. A distinctive zoning pattern is observed consisting of densely vascularized reticular and less vascular longitudinal tissues. Some resorption cavities are visible in the inner half of the cortex.

Descriptions of MPC-D100/619

Femur: The femur cortex contains a combination of reticular, weakly developed sub-plexiform, and longitudinal canals (Fig. 3.4, A-B). The area of the medullary cavity represents 32.6% of the total transverse sectional area of the femur. The bone tissue mainly consists of parallel-fibered matrix. The weakly developed sub-plexiform tissues occur in the outer cortex. Some locally developed, longitudinally oriented vascular canals occur in the anterior side of the cortex. Development of resorption cavities is observed in the inner half of the cortex. Parallel radial vascularization is locally developed in the posterior side of the mid-cortex. The density of vascularity is considerably decreased in the outer cortex. A total of three LAGs are identified.

Tibia: The area of the medullary cavity in the tibia is considerably decreased (15.7 %) relative to other elements (Fig. 3.4, C-D). The tibia cortex is mainly composed of reticular and sub-plexiform bone tissue. The bone tissue of the tibia is parallel-fibered. The density of vascularity greatly decreases in the outer cortex. Some locally developed radial vascularization is present. The resorption cavities commonly occur in the inner half of the cortex. Some of the cavities are partially filled with lamellae. The periosteum is not preserved in this specimen. Five LAGs are preserved in the cortex.

Fibula: The density of the vascularization is greatly decreased in the fibula. The vascularity is composed mainly of longitudinal and some locally developed reticular canals with parallel-fibered matrix (Fig. 3.4, E-F). The longitudinal vascularization is dominated in the outer two-thirds of the cortex. A large number of resorption cavities are present in the inner half of the cortex. The area of the medullary cavity is as low as only 11.1 % of the total area in the mid-shaft. Five LAGs are preserved.

Discussion

The histology of a smaller *P. mongoliensis* individual (MPC-D100/618-001; body length = 73 cm) exhibits a different vascularity in each of the hind limb elements. The transverse section of the femur exhibits densely developed reticular vascular canals whereas the cortex of the tibia has a combination of reticular and radial vascular canals. The vascular density of the fibula is much lower and the longitudinal vascularization with a slight anastomosis is predominant (Fig. 3.1, A-B). The histologic features of all bones represent fast growth, however the fibula growth appears to have been mostly

longitudinal. The bone area percentage in the mid-shaft was higher in the tibia (76.2%) and fibula (82.6%). Interestingly, radial vascularity has not been observed in the hind limb elements (femur, tibia, and fibula) of *P. lujiatunenesis* (Zhao et al., 2013). There are two LAGs preserved in the cortices, except in the fibula which preserves three LAGs.

Another individual (MPC-D100/620-015, 94.83 cm in body length) shows nearly similar bone tissues in the femur and tibia. The femur of this individual exhibits mostly reticular vascularization; whereas, the tibia shows a combination of reticular and sub-plexiform tissues (Fig. 3.2, A-D). The histology of the femur and tibia suggest fast growth, but the tibia possesses more organized bone tissue. Interestingly, the fibula is composed of strictly longitudinally oriented, less dense vascularization reflecting slow and longitudinal growth (Fig. 3.2, E-F). The tibia has the least medullary expansion, and the bone area percentage is as high as 93.1% whereas femur and fibula are 82% and 82.6% respectively (Table 3.1.). There are four preserved LAGs in the tibia and three in both the femur and fibula.

The thin sections from a larger individual (MPC-D100/618-005; 102.2 cm in body length) exhibit nearly similar histology in all elements including the femur, tibia, and fibula. All hind limb elements present a reticular vascularization with parallel-fibered bone matrix (Fig. 3.3, A-F). However, the vascularization in the outer cortex of the tibia shifts to sub-plexiform akin to what was observed in the tibia from MPC-D100/620-015 (Fig. 3.2, C-D). The vascularization density of the fibula is considerably greater compared to the two smaller individuals. Both the tibia and fibula show three LAGs in the cortices. The LAG count in the femur is lower than in the tibia and fibula,

representing two LAGs in the cortex. The reduced number of LAGs preserved in the femur relative to other bones could be related to expansion of the medullary cavity producing a thin bone wall.

The tibia and femur from the largest individual (MPC-D100/619) in this study show a combination of reticular and sub-plexiform tissues in the cortex. In general, the vascularization density is greatly reduced in all elements. The tibia exhibits predominantly of sub-plexiform tissue in the cortex; whereas, the fibula has mostly longitudinal vascularization. Interestingly, all elements exhibit a development of the resorption cavities in the inner half of the cortex. In the tibia cortex, some of the resorption cavities are partially filled with lamellae forming secondary osteons. Similar intracortical osteoclastic resorption cavities were reported in a larger sized *P. mongoliensis* tibia (from an 8 year old individual) (Erickson and Tumanova, 2000). Apparently, the development of these resorption cavities is simultaneous in the weight-bearing hind limb elements of *P. mongoliensis* (including the femur, tibia, and fibula; Fig. 3.4, A-F). These resorption cavities may be related to the onset of slowed growth in *P. mongoliensis*, possibly marking the beginning of skeletal maturity (see Discussion in Chapter 3). Similar resorption cavities are developed in the juvenile stage of *Maiasaura* (Horner et al., 2000). Generally, the bone remodeling is associated with higher mechanical stress (Enlow, 1962; Carter, 1984; Currey, 1984; Frost, 1990; Bouvier and Hylander, 1996) and/or intense calcium demands (Parfitt, 1994; Schweitzer et al., 2007). However Francillon-Viellot et al. (1990) suggested that the bone resorption is primarily a result of aging rather than biomechanical processes. In this individual, the medullary

cavity represents a greater percentage of the cross sectional area of the femur (32%) compared to the tibia and fibula. The femur preserves three LAGs; whereas, five are preserved in both tibia and fibula.

Conclusions

The main weight-bearing elements, the tibia and femur exhibit similar histologic features which may reflect physiologic changes in the individual. The femur of *Psittacosaurus* exhibits a relatively thin bone wall compared to the tibia and fibula, due to extensive medullary cavity expansion. The innermost growth lines in the femur may have been erased by this medullary cavity expansion before the coeval LAGs in the tibia and fibula. The tibia and fibula have a higher potential to preserve a greater number of the LAGs that formed during the ontogeny of *P. mongoliensis*. However, the fibula shows a little change in tissue types that may not reflect physiological changes of the individual. We propose that the use of the tibia is the ideal hind limb element for both relative age assessment and bone tissue typing in *P. mongoliensis.* The result of this research partially supports the previous study which suggested that the choice of bones for the skeletochronologic analysis should be the tibia and femur (Horner et al., 1999).

The timing of extensive osteoclastic activity in the inner cortex appears to have been simultaneous in weight-bearing hind limb elements from a single individual. In *Psittacosaurus*, it appears that a major physiological change such as skeletal maturity has been reflected in all weight-bearing limb bones regardless of the bone tissue composition.

Acknowledgements

We thank Gerry Ohrstrom, Elizabeth Moore, and David Swingle for fieldwork funding. We are grateful to Dr. Tsogtbaatar Khishigjav (Mongolian Academy of Sciences) for supporting us to obtain fieldwork permit. We thank E.-T. Lamm (Museum of the Rockies) for thin section preparation. We also thank D. Sengee (Mongolian University of Science and Technology) for fieldwork assistance.

Table 3.1. Data collected from the four *P. mongoliensis* individuals that used in this study.

No	MPC number	Field number	Element	Length, mm	Bone area, %	Medullary cavity area, %	Histologic features	LAG count	Body length, cm
1	MPC-D100/618-001	BLK12010-1	Femur	106.81	66.4	33.6	reticular, longitudinal	2	73.0
			Tibia	115.35	76.2	23.8	reticular, radial	2	
			Fibula	111.99	82.6	17.4	reticular, longitudinal	3	
2	MPC-D100/620-015	BLK11-44-1	Femur	138.71	82.0	18.0	reticular, longitudinal	3	94.8
			Tibia	149.81	93.1	6.9	reticular, sub-plexiform	4	
			Fibula	145.45	82.6	17.4	longitudinal	3	
3	MPC-D100/618-005	BLK12010-5	Femur	149.51	70.9	29.1	reticular	2	102.2
			Tibia	161.47	82.8	17.2	reticular, sub-plexiform	3	
			Fibula	156.77	84.5	15.5	reticular	3	
4	MPC-D100/619	BLK12025	Femur	224.69	67.4	32.6	reticular, sub-plexiform; resorption	3	153.6
			Tibia	242.66	84.3	15.7	reticular, sub-plexiform; resorption	5	
			Fibula	235.59	88.9	11.1	longitudinal; resorption cavities	5	

Figure 3.1. Transverse sections of the *P. mongoliensis* hind limb elements from the specimen MPC-D100/618-001. **A)** the femur preserved two LAGs in the cortex; **B)** diaphysis of femur consist of a combination of reticular and longitudinal vascularizations with parallel-fibered bone matrix; **C)** the tibia presents two LAGs; **D)** the tibia cortex is composed of a tissue combination consisting of reticular and radial vascularization with parallel-fibered matrix; **E)** three LAGs were preserved in the fibula; **F)** the fibula cortex shows mainly longitudinal vascularization in decreased density. Red square indicates enlarged views from A) in B), from C) in D), from E) in F). The enlarged views were observed through a full lambda (530nm) plate with polarized light to reveal fiber orientation but this tends to obscure growth marks. White arrows point LAGs. The scale bars in A), C), and E) equal to 1mm; B), D), and F) equal to 0.5mm.

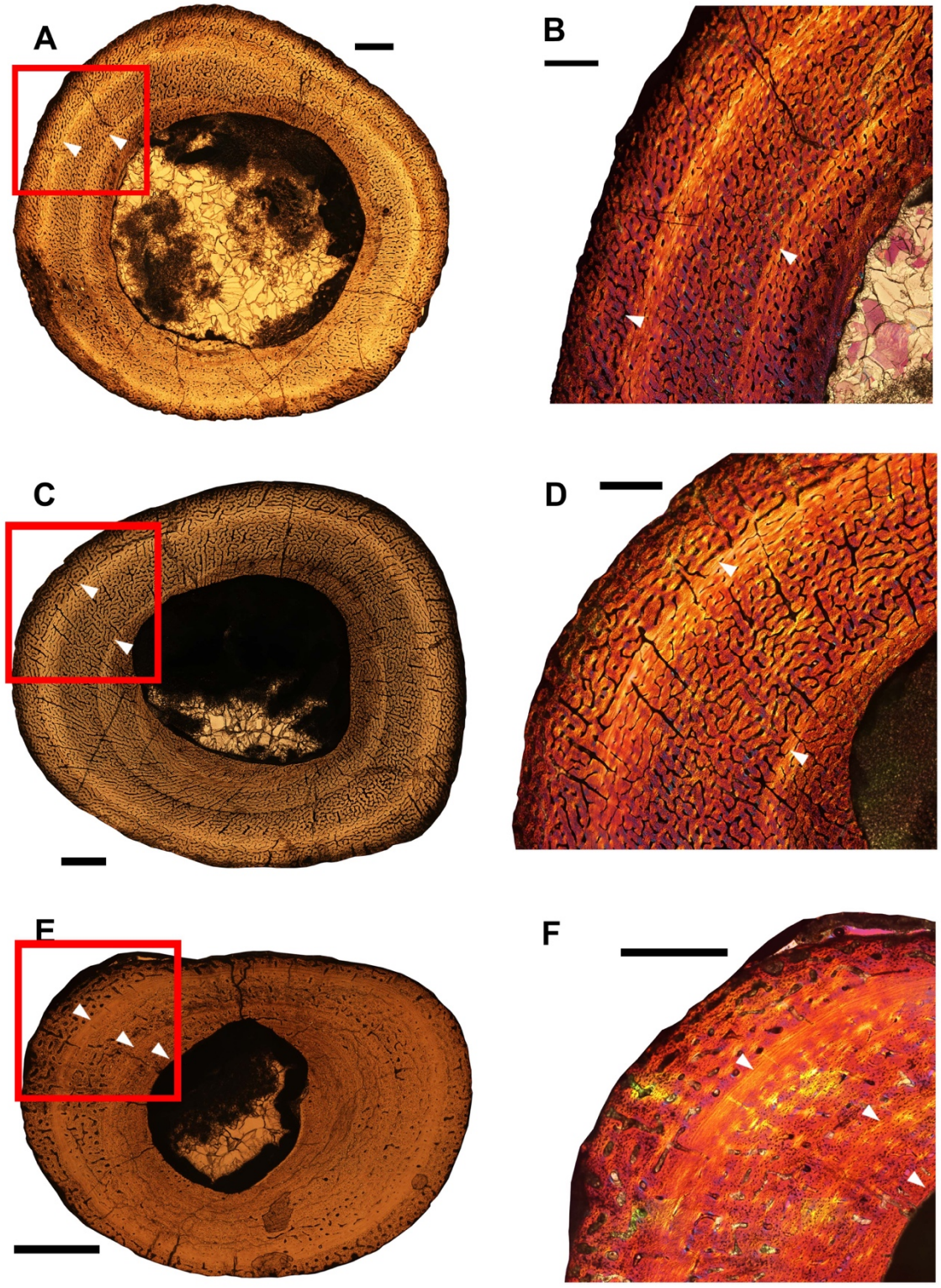

A
B
C
D
E
F

Figure 3.2. Transverse sections of the *P. mongoliensis* hind limb elements from the specimen MPC-D100/620-015. **A)** femur preserved three LAGs in the cortex; **B)** diaphysis of the femur consists of a combination of reticular and longitudinal vascularizations with parallel-fibered bone matrix, the vascularization somewhat shifted to the sub-plexiform in the outer cortex; **C)** tibia has four preserved LAGs; **D)** the tibia cortex is composed of more organized tissues consisting of mainly sub-plexiform and small amount of reticular tissue in the inner 1/3 of the cortex; **E)** The preserved number of LAGs in fibula is three; **F)** the fibula cortex shows mainly longitudinally oriented vascular canals, and the vascularization density is decreased. Red square indicates enlarged views from A) in B), from C) in D), from E) in F). The enlarged views were observed through a full lambda (530nm) plate with polarized light to reveal fiber orientation, but this tends to obscure growth marks. White arrows point preserved LAGs in the cortex. The scale bars in A), C), and E) equal to 1mm; B), D), and F) equal to 0.5mm.

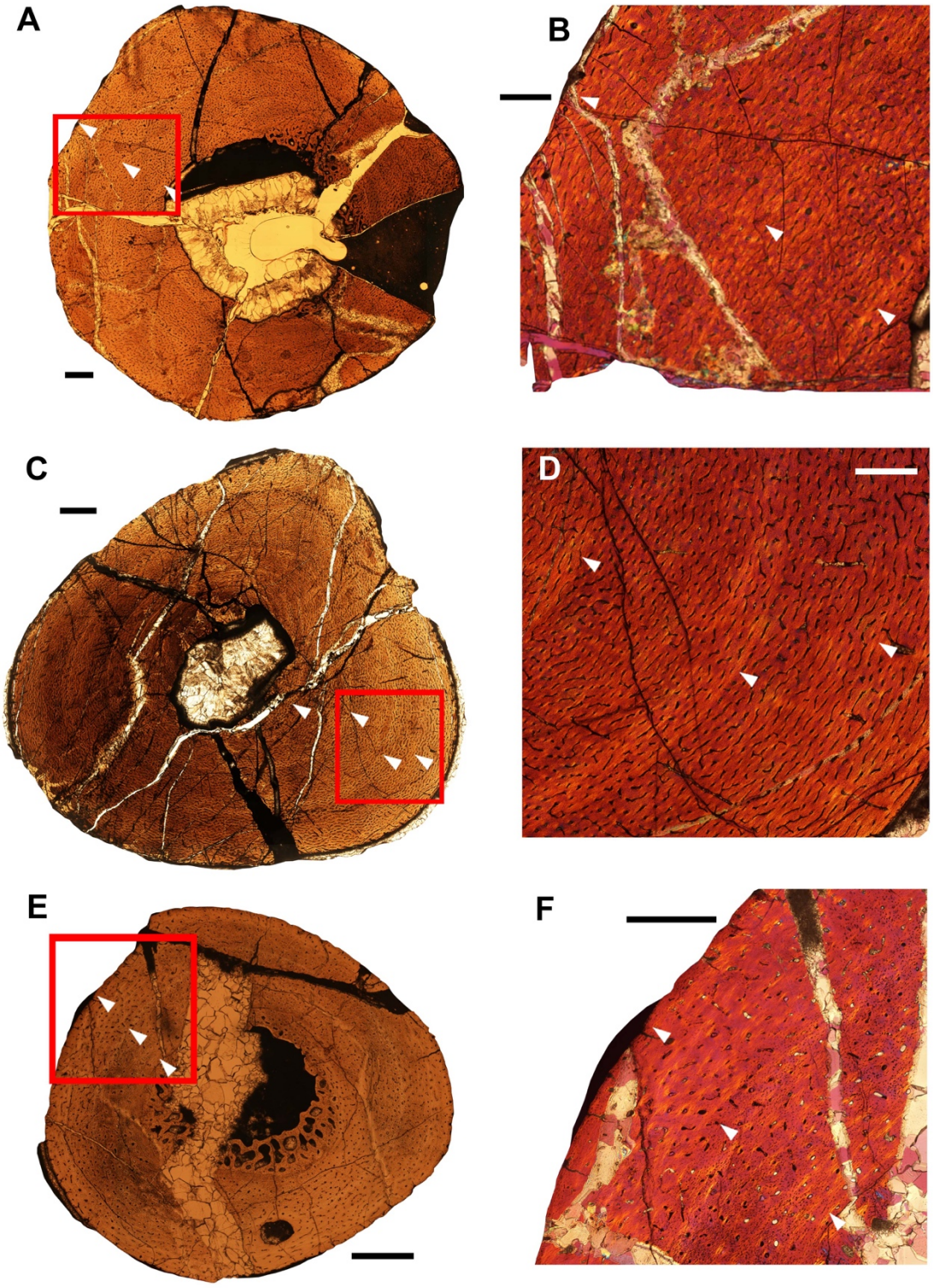

A
B
C
D
E
F

Figure 3.3. Transverse sections of the *P. mongoliensis* hind limb elements from the specimen MPC-D100/618-005. **A)** femur preserved two LAGs in the cortex; **B)** diaphysis of the femur consist of mainly reticular vascularizations with parallel-fibered bone matrix; **C)** tibia has three preserved LAGs; **D)** the tibia cortex consists of reticular, radial, and sub-plexiform tissues with parallel-fibered matrix; **E)** The preserved number of LAGs in the fibula is three; **F)** the fibula cortex shows mainly reticular vascularizations with parallel-fibered bone matrix. The density of the vascularization is somewhat increased. Red square indicates enlarged views from A) in B), from C) in D), from E) in F). The enlarged views were observed through a full lambda (530nm) plate with polarized light to reveal fiber orientation but this tends to obscure growth marks. White arrows point preserved LAGs in the cortex. The scale bars in A), C), and E) equal to 1mm; B), D), and F) equal to 0.5mm.

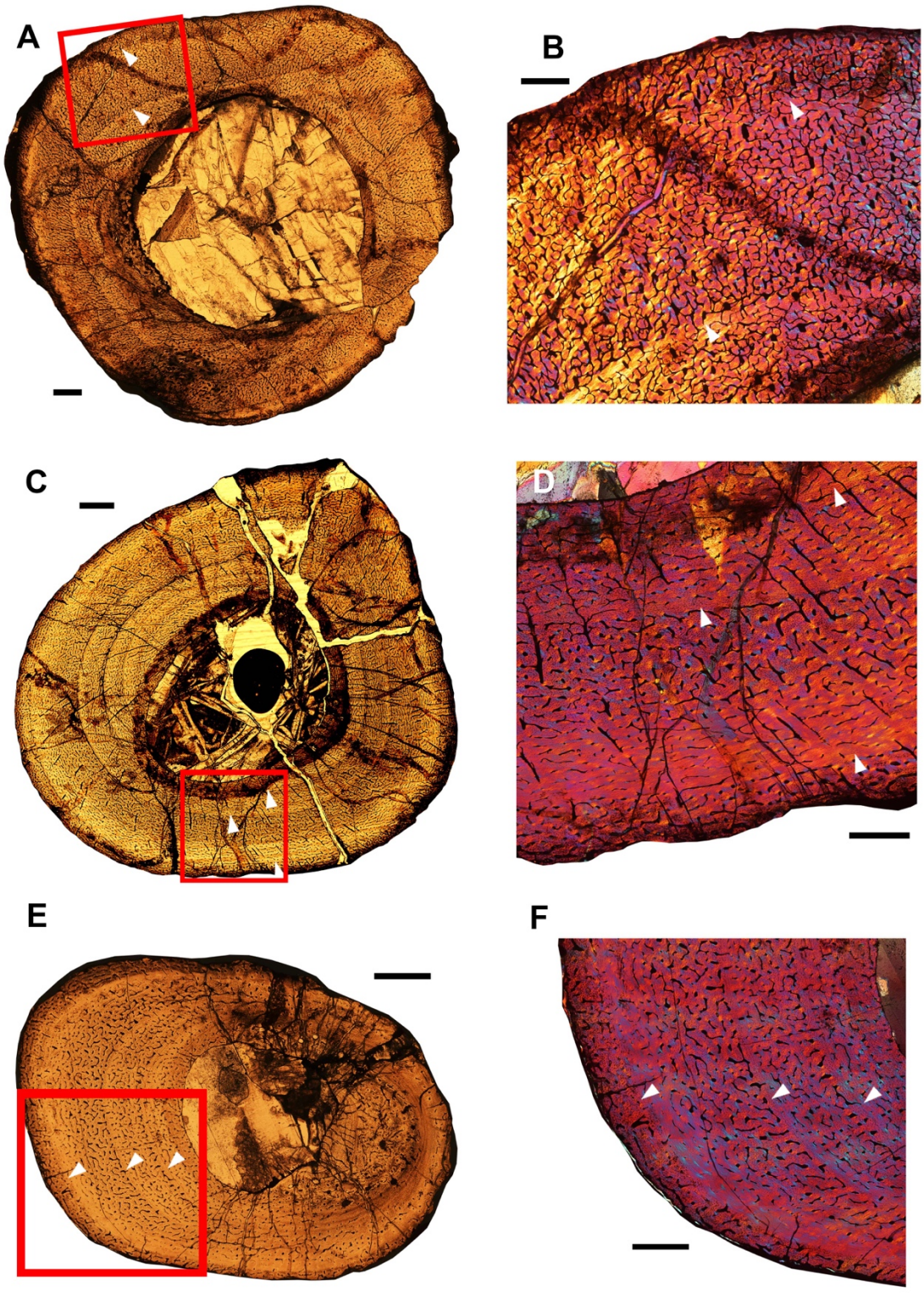
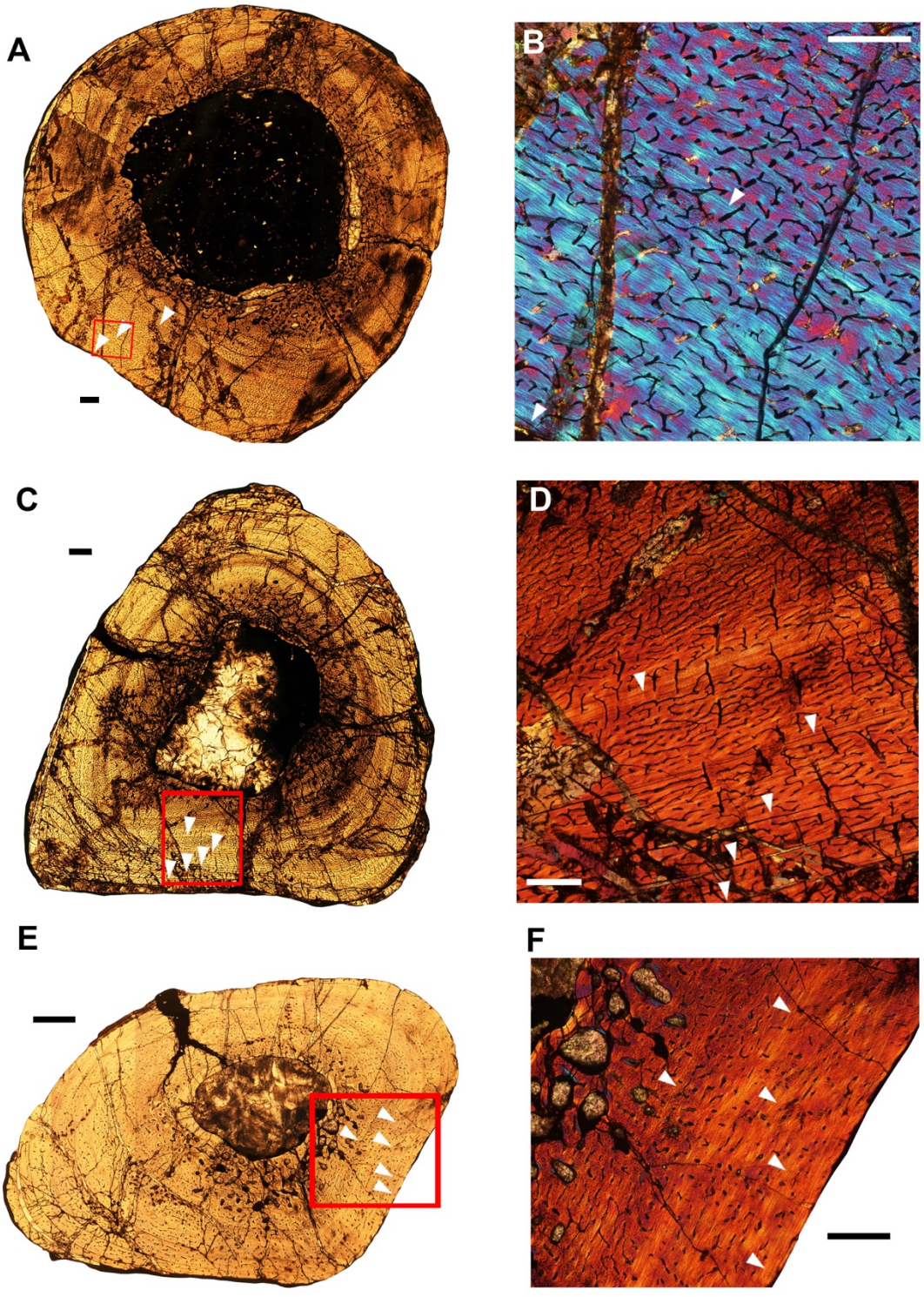

A
B
C
D
E
F

Figure 3.4. Transverse sections of the *P. mongoliensis* hind limb elements from the specimen MPC-D100/619. **A)** femur preserved three LAGs in the cortex; **B)** diaphysis of the femur consists of a combination of reticular and sub-plexiform vascularizations with a parallel-fibered bone matrix; **C)** tibia has five preserved LAGs; **D)** the tibia cortex is composed of more organized tissues consisting of mainly sub-plexiform and small amount of radial tissue. The vascularization density tends to reduce in the outer cortex; **E)** The preserved number of LAGs in the fibula is five; **F)** the fibula cortex shows mainly longitudinally oriented vascular canals and the vascularization density is decreased, some reticular vascularizations were developed in the inner half of the cortex. Red square indicates enlarged views from A) in B), from C) in D), from E) in F). The enlarged views were observed through a full lambda (530nm) plate with polarized light to reveal fiber orientation but this tends to obscure growth marks. White arrows point preserved LAGs in the cortex. The scale bars in A), C), and E) equal to 1mm; B), D), and F) equal to 0.5mm.


A
B
C
D
E
F

Literature Cited

Bouvier, M., and W. L. Hylander. 1996. The mechanical or metabolic function of secondary osteonal bone in the monkey *Macaca fascicularis*. Archives of oral biology 41: 941-950.

Carter, D. R. 1984. Mechanical loading histories and cortical bone remodeling. Calcified tissue international 36: S19-S24.

Chinsamy, A. 1994. Dinosaur bone histology: implications and inferences.; pp. 213-227 *i*n D. Rosenberg, and D. L. Wolberg (eds.), Dino Fest. The Paleontological Society Special Publication No. 7.

Chinsamy, A., and A. Tumarkin-Deratzian. 2009. Pathologic bone tissues in a turkey vulture and a nonavian dinosaur: implications for interpreting endosteal bone and radial fibrolamellar bone in fossil dinosaurs. The Anatomical Record 292: 1478-1484.

Currey, J. 1984. Comparative mechanical properties and histology of bone. American Zoologist 24: 5-12.

Curry, K. A. 1999. Ontogenetic histology of *Apatosaurus* (Dinosauria: Sauropoda): New insights on growth rates and longevity. Journal of Vertebrate Paleontology 19: 654-665.

Enlow, D. H. 1962. Functions of the haversian system. American Journal of Anatomy 110: 269-305.

Erickson, G. M., and C. A. Brochu. 1999. How the 'terror crocodile' grew so big. Nature 398: 205-206.

Erickson, G. M., P. J. Makovicky, P. J. Currie, M. A. Norell, S. A. Yerby, and C. A. Brochu. 2004. Gigantism and comparative life-history parameters of tyrannosaurid dinosaurs. Nature 430: 772-775.

Erickson, G. M., P. J. Makovicky, B. D. Inouye, C. F. Zhou, and K. Q. Gao. 2009. A Life Table for *Psittacosaurus lujiatunensis*: Initial Insights Into Ornithischian Dinosaur Population Biology (vol 292, pg 1514, 2009). Anatomical Record-Advances in Integrative Anatomy and Evolutionary Biology 292: 1684-1684.

Erickson, G. M., and T. A. Tumanova. 2000. Growth curve of *Psittacosaurus mongoliensis* Osborn (Ceratopsia : Psittacosauridae) inferred from long bone histology. Zoological Journal of the Linnean Society 130: 551-566.

Francillon-Vieillot, H., V. De Buffrénil, J. Castanet, J. Géraudie, F. J. Meunier, J. Y. Sire, L. Zylberberg, and A. De Ricqlès. 1990. Microstructure and mineralization of vertebrate skeletal tissues; pp. 471-548 *i*n J. G. Carter (ed.), Skeletal biomineralization: patterns, processes and evolutionary trends. Van Nostrand Reinhold, New York.

Frost, H. M. 1990. Skeletal structural adaptations to mechanical usage (SATMU): 2. Redefining Wolff's Law: The remodeling problem. The Anatomical Record 226: 414-422.

Garcia, B. J. 2011. Skeletochronology of the American Alligator (*Alligator mississippiensis*): Examination of the Utility of Elements for Histological Study. Florida State University.

Horner, J. R., A. de Ricqles, and K. Padian. 1999. Variation in dinosaur skeletochronology indicators: implications for age assessment and physiology. Paleobiology 25: 295-304.

Horner, J. R., A. de Ricqles, and K. Padian. 2000. Long bone histology of the hadrosaurid dinosaur *Maiasaura peeblesorum*: growth dynamics and physiology based on an ontogenetic series of skeletal elements. Journal of Vertebrate Paleontology 20: 115-129.

Horner, J. R., and K. Padian. 2004. Age and Growth Dynamics of *Tyrannosaurus*. Proceedings: Biological Sciences 271: 1875-1880.

Klein, N., T. Scheyer, and T. Tütken. 2009. Skeletochronology and isotopic analysis of a captive individual of *Alligator mississippiensis* Daudin, 1802. Fossil Record 12: 121-131.

Lamm, E.-T. 2013. Preparation and sectioning of specimens. Bone histology of fossil tetrapods: advancing methods, analysis, and interpretation: 55-160.

Parfitt, A. M. 1994. Osteonal and hemi-osteonal remodeling: the spatial and temporal framework for signal traffic in adult human bone. Journal of cellular biochemistry 55: 273-286.

Reizner, J., and J. R. Horner. 2006. An ontogenetic series of the ceratopsid dinosaur *Einiosaurus procurvicornis* as determined by long bone histology.: In *66th Annual Meeting, Society of Vertebrate Paleontology. Program and Abstracts.*, Ottawa, ONT.

Sander, P. M. 2000. Longbone histology of the Tendaguru sauropods: implications for growth and biology. Paleobiology 26: 466-488.

Sander, P. M., and N. Klein. 2005. Developmental plasticity in the life history of a prosauropod dinosaur. Science 310: 1800-1802.

Schweitzer, M. H., R. M. Elsey, C. G. Dacke, J. R. Horner, and E. T. Lamm. 2007. Do egg-laying crocodilian (*Alligator mississippiensis*) archosaurs form medullary bone? Bone 40: 1152-1158.

Varricchio, D. J. 1993. Bone microstructure of the Upper Cretaceous theropod dinosaur *Troodon formosus*. Journal of Vertebrate Paleontology 13: 99-104.

Werning, S. 2012. The ontogenetic osteohistology of *Tenontosaurus tilletti*. PloS one 7: e33539.

Zhao, Q., M. J. Benton, C. Sullivan, P. M. Sander, and X. Xu. 2013. Histology and postural change during the growth of the ceratopsian dinosaur *Psittacosaurus lujiatunensis*. Nature communications 4.

CHAPTER FOUR

ONTOGENETIC HISTOVARIABILITY IN A POPULATION OF *PSITTACOSAURUS MONGOLIENSIS* FROM THE LOWER CRETACEOUS KHULSANGOL FORMATION, UVURKHANGAI PROVINCE, MONGOLIA

Contribution of Authors and Co-Authors

Manuscript in Chapter 4

Author: Badamkhatan Zorigt

Contributions: Conceived the study, obtained and processed specimens, analyzed data, interpreted results, and wrote the manuscript.

Co-author: John R. Horner

Contributions: Provided fieldwork funding, specimen processing facilities and equipment, microscope and photograph equipment. Assisted with the study design, discussed implications of results, and edited earlier drafts of the manuscript.

Manuscript Information Page

Badamkhatan Zorigt, John R. Horner
Journal of Vertebrate Paleontology
Status of Manuscript:
_x_Prepared for submission to a peer-reviewed journal
___Officially submitted to a peer-reviewed journal
___Accepted by a peer-reviewed journal
___Published in a peer-reviewed journal

Published by Society of Vertebrate Paleontology

Abstract

The growth strategies of many dinosaur taxa have been explored using various skeletal elements. A larger sample size consisting of a single skeletal element is crucial to construct robust growth curves for particular dinosaur species. The histology of 58 *Psittacosaurus mongoliensis* tibiae collected from the Early Cretaceous Builst Khudag (BLK) locality in central Mongolia were examined in this study. Due to the presence of a considerable amount of histologic variations in the similar sized tibiae, the growth stages of *P. mongoliensis* are classified based on the tissue types rather than using length or numbers of growth lines. The bone histology suggests accelerated growth of *P. mongoliensis* in the first two years of life. The growth rate increases in individuals ranging in age from 2-5 years old. By the time the animal reached sometime 2-6 years old, the rate slightly decreased and bone tissue shifted to reticular and sub-plexiform. Growth is considerably slowed but still continued at a slower rate when *P. mongoliensis* reached 7-13 years of life. The mortality rate is higher in the first two years until the individual reaches the threshold body size of 65.9 cm in body length and 2.7 kg in mass. The daily bone apposition rate increased to 3.19 μm/day until the animals were seven years old. By the ages of 10-13, the growth rate slowed to 1.6 μm/day and the body size reached 170.2 cm in length and 46.6 kg in mass. The general growth curve for *P. mongoliensis* is sigmoidal, which is consistent with the finding of previous studies.

Introduction

The microstructure of dinosaur bone has been studied since the 1800s (Mantell, 1850; Seitz, 1907; Nopcsa, 1933; Gross, 1934; Enlow and Brown, 1956, 1957; de Ricqlès, 1968, 1972, 1974a, 1974b, 1975). Lines of Arrested Growth ("LAGs") were first reported in dinosaur bone by Reid (1981); as in many extant vertebrates, LAGs in dinosaur bones opened a door to development of skeletochronologic research in this group. Several ontogenetic skeletochronologic studies were conducted on various dinosaur groups including theropods (Horner et al., 2000; Erickson et al., 2001), sauropods (Chinsamy, 1993; Curry, 1999; Sander, 2000; Klein and Sander, 2008), ornithopods (Horner et al., 2000; Werning, 2012; Woodward et al., 2015), and basal ceratopsians (Erickson and Tumanova, 2000; Erickson et al., 2009).

Important ontogenetic studies have been carried out on the basal ceratopsian dinosaur *Psittacosaurus* (Erickson and Tumanova, 2000; Erickson et al., 2009). Erickson and Tumanova (2000) sectioned a total of seventeen skeletal elements consisting of the humerus, femur, and tibia from *Psittacosaurus mongoliensis*. They hypothesized that the growth rate of *P. mongoliensis* started as low as 2.6 g/day then increased up to 12.5 g/day by the age of 7-8. The bone apposition rate decreased (10.5g/day) during the ages of 8-9. The body mass reached up to 19.8 kg at the age of nine. The authors suggested the growth curve of *P. mongoliensis* showed a S-shape using logistic equation.

Another study on *P. lujiatunensis* was published by Erickson et al. (2009). The authors sectioned 26 fibulae for histologic analysis. The general pattern of a survivorship curve for this species reflects Type B_1 pattern that has been observed in moderate to

"large sized" modern species including birds and mammals (Erickson et al., 2009). The study concluded the sexual maturity of *P. lujiatunensis* occurred sometime during the ninth year of life. Juveniles reached their threshold body size between 3-4 years of life.

The skeletochronologic study (Erickson and Tumanova, 2000) on *P. mongoliensis* utilized multiple skeletal elements from various individuals. Since it appears that different skeletal elements from the same individual had different remodeling rates in dinosaur (this is in *Maiasaura* (Horner et al., 1999), conducting a multi-element analysis to construct a population growth curve is unreliable. Moreover, a histologic variation in similar sized individuals has been previously reported (Horner et al., 2000). The most reliable elements for skeletochronology were suggested to be the femur and tibia due to these bones exhibiting the lowest remodeling rate (Horner et al., 1999). In the histologic study of *P. lujiatunensis*, the growth curve was determined using an unconventional element (fibula) that has a different biomechanical function than the tibia or femur (e.g. minor weight bearing function). In order to provide a more comprehensive conclusion, a detailed histologic description of the tissue organization is necessary along with LAG counts, physical measurements that include element length, diaphyseal circumferential perimeter etc.

The purpose of this study is twofold: 1) to conduct a detailed histologic examination of the tissue composition and organization of *P. mongoliensis* tibiae using the largest sample size thus far examined, representing various ontogenetic stages, and 2) to produce a robust growth curve based on a larger sample set of the same skeletal element.

Methods

The specimens used in this study were collected during joint expeditions by the Mongolian Paleontological Center (MPC; Mongolian Academy of Sciences) and the Museum of the Rockies (MOR) over the course of five field seasons (2010-2015). Fieldwork was conducted in the Early Cretaceous Khulsangol Formation (Aptian-Albian) at the Builst Khudag (BLK) locality in Mongolia. The depositional environment of the Khulsangol Formation is interpreted as catastrophic debris flow and sheet-flood deposits that were probably triggered by an intense rainfall or thunderstorm. The BLK bonebed consists of monospecific remains of *P. mongoliensis* (see Chapter 2).

Tibiae were chosen as the focus of the current study as this was the most commonly recovered element at the BLK locality and previous analyses (e.g. Horner et al., 1999) reveal that this bone preserves a robust skeletochronological record. A total of 120 thin sections were made from the 58 *P. mongoliensis* tibiae representing 58 individuals. Over the duration of this project, tibiae were coded NT002 through NT076. The corresponding official MPC specimen numbers are listed in Table 4.1. All tibiae length and diaphyseal perimeters were measured using a caliper and tape measure prior to thin sectioning. For incomplete specimens, the total length of the tibia was estimated using the circumferential length of similar sized complete tibiae (Table 4.2). The tibiae were prepared and thin-sectioned following Lamm (2013). At least two transverse cuts were made from each tibia. However, an additional one or two sections were made from some specimens in order to obtain clear visibility of the microstructure. One slice was used for analysis while the second one was stored as a duplicate.

The slides were examined under 4X or 10X objectives using a Nikon Optiphot-Pol polarizing petrographic microscope. Composite photomicrographs of entire bone cross- section were produced using a combination of Nikon DS-Fi1 digital camera and NIS-Elements BR 3.0 software. Adobe Photoshop CC 2015 was used for digitally tracing the perimeters of diaphysis, medullary cavity, and LAGs. NIH ImageJ v. 1.49 software is used for quantifying perimeters and areas. Only the 36 most complete and well-preserved 36 specimens were used for skeletochronologic analysis.

Bone apposition rate was determined using the average distance between the LAGs along the major and minor axis from the geometric centroid. Daily bone apposition rate is calculated based on the 365 days in order to compare the growth rate with those of extant vertebrates (Table 4.3).

Regression analyses were conducted from the relationship between tibia length and: diaphyseal perimeter, transverse section area, medullary cavity area, medullary cavity perimeter, and cortex thickness. The R^2 values above 0.90 are considered high enough to predict tibia length from the given measurements. All 58 tibiae were used for each regression (Fig. 4.1 and 4.2)

The innermost LAGs in the tibiae longer than 11.5 cm were obliterated by medullary resorption. We used the section stacking method in this study to retro-calculate the missing LAGs following Chinsamy (1993) and Erickson et al. (2001).

Relative body masses of individuals were determined using the Developmental Mass Extrapolation (DME) method introduced by Erickson and Tumanova (2000) (Table 4.4). However, this method is considered one of many untested mass estimations

(Myhrvold, 2013). To use this method, the femur length and circumference length were required to determine individuals' relative mass. Ten tibiae were sampled from the articulated skeletons. The following ratios were calculated from the associated elements: 1) tibia length/femur length (1.08), 2) femur length/femur circumferential perimeter (2.4). These measurements were averaged and used for estimation of the corresponding femur length and femur circumferential perimeter for the rest of the tibiae. The body length was determined in a similar fashion. The averaged ratios of tibia length and body length were calculated from the complete, articulated specimens, and then the corresponding body length was estimated for the rest of the specimens. The ontogenetic mass and body length curves were produced using Microsoft Excel (Fig. 4.3). Additionally, body mass vs. age curve with 95% confidence interval was plotted using logistic function in Minitab Express v.1.4 software (Fig. 4.4).

Results

Individual histologic variation fluctuates greatly between similar sized tibiae. We divided *P. mongoliensis* tibiae into four growth phases based on the tissue organization. *P. mongoliensis* tibiae started with woven tissue and gradually changed to a parallel-fibered bone tissue later in ontogeny.

Growth Phase A

Total of four tibiae represent this growth phase including NT002, NT003, NT004, and NT006 (Fig. 4.5). The smallest tibiae that range from 5.68 to 8.28 cm in length are included in this phase. The cortex thickness ranges between 0.1 and 0.24 cm. The cortex

mostly consists of highly unorganized woven tissue (Fig. 4.6). The cortex is well differentiated from the marrow cavity. All tibiae in this growth phase are densely vascularized. The vascular organization starts with reticular in the smaller individual (NT002). Later, the vascularity gradually changes largely into longitudinal organization. Also woven tissue shifts to parallel-fibered matrix (Fig. 4.7). Some of the tibiae (NT003, NT006) exhibit weak radial vascularization in the mid-cortex (Fig. 4.7). The vascular canals in the outermost cortex are exhibited as weakly anastomosed longitudinal vessels. The longitudinal vascularity predominates on the lateral sides of some tibiae (NT002, NT006); whereas, the combination of reticular and weak radial vascularity is present on the anterior, medial, and posterior sides. The tibiae in this phase present one to two LAGs in the cortices, except one tibia (NT002) which does not exhibit a LAG in the cortex.

Growth Phase B

This phase is represented by following specimens: NT007, NT009, NT015, NT017, NT019, NT020, NT021, NT023, NT024, and NT025 (Fig. 4.8). The tibia length in growth Phase B ranges between 10.41- 16.15 cm. The cortical thickness increases up to 0.38 cm and is consistent on all sides of the bones. Most of the LAGs were preserved in the smaller specimens; whereas the larger specimens lost the innermost 1-2 LAGs. The LAG numbers of this stage range between 2-5 LAGs.

In general, a well-developed reticular vascularization is common in this stage. Half of the specimens (NT020, NT009, NT021, NT023, NT024) exhibit moderate degrees of radial vascularization in their cortices (Fig. 4.9). Radial vessels are moderately anastomosed and are larger in diameter compared to other canals. The extensions of the

radial vascular canals are restricted to the individual zones. These radial canals are distributed evenly on all sides of the cortex. The length of the radial canals is relatively longer than those found in growth Phase A. Between the LAGs, the vascularity of bone tissue changes gradually from reticular to plexiform vascularity producing a distinctive zoning pattern in the larger specimens (NT017; Fig. 4.10). This changing pattern is consistent in most of the specimens of this growth phase, except in NT015, NT019, and NT022.

In NT015, NT019, and NT022, the zoning pattern is changed to a mixture of longitudinal and reticular bone tissue with fewer radial vascularizations. The zones start with densely vascularized reticular and radial vascularization and then gradually change to longitudinally oriented vessels with slight anastomoses. The density of osteocytes gradually decreases when vascularization shifts from reticular to longitudinal orientation. Zone thickness is inconsistent in the larger specimens (NT019, NT021, NT023, NT024, NT025). The bone tissues also become more mature and organized.

Growth Phase C

A total of five tibiae represent this growth phase including NT026, NT027, NT029, NT030, and NT065 (Fig. 4.11). The tibiae in this growth phase are between 16.42 cm and 17.5 cm in length. The cortex thickness is approximately 0.37 cm and there are between two and three LAGs preserved in the tibiae. The total LAG count including retrocalculated LAGs is five to six. This stage largely consists of a sub- to regular plexiform tissue with parallel-fibered bone matrix (Fig. 4.12).

The inner quarter of the cortex (NT026, NT027, NT029; Fig. 4.12) contains reticularly organized vascular canals as observed in previous growth phases (A and B). The rest of the cortex is composed of weakly developed plexiform vascularization. Very few radial vascularizations are observed in the cortices of NT027. The lengths of the radial vessels are relatively shorter than those observed in previous phases and are truncated by LAGs. The tissue change from reticular to plexiform is gradual. In the periosteal region, the density of vascularity is considerably reduced, and the vascularity is becoming more longitudinal. The LAGs were formed as very narrow dark lines. In some regions of the cortex, they are hard to identify. The growth lines are bordered with the non-vascular annuli. The density of the vascularity decreases in the outermost zones. The osteocyte concentration considerably decreases in the outermost zones as well. In the periosteal region, the vascular density of the plexiform tissue greatly decreases.

Two specimens (NT027, NT029) contain partial and weakly developed endosteal linings with multiple lamellae as well as a small number of large resorption cavities surrounding the medullary cavity. One specimen (NT029) preserves a remnant of trabecular structure in the medullary region.

Growth Phase D

Growth phase D is represented by a total of 18 tibiae including NT034, NT037, NT038, NT039, NT040, NT041, NT044, NT071, NT046, NT047, NT050, NT076, NT053, NT054, NT055, NT056, NT057, and NT058 (Fig. 4.13). Tibiae length in this growth phase ranges between 18.9 and 26.9 cm. The cortex thickness reaches up to 0.66 cm. There are a total of 7 to 13 LAGs, out of which, 3-8 actual LAGs were preserved in

the cortex. Along with the preserved LAGs, 2-3 annuli often occur. In general, the cortex mostly consists of a mix of reticular and plexiform tissues with a parallel-fibered matrix. The tissue organization varies among the specimens of this phase. The periosteal region of cortex is weakly vascularized and consists of a combination of longitudinal and weak laminar vascularizations. A small number of weakly developed radial vascularizations occur locally in the cortex (NT039, NT057).

One of the distinctive features of this growth phase is the occurrence of many resorption cavities in 1/3 of inner cortex (Fig. 4.14). These resorption cavities occur usually before the presence of the second LAG. Endosteal regions of the specimens are intensely invaded by osteoclastic resorption cavities without infilling. In several specimens (NT054, NT057, NT058), the resorption cavities were partially filled with lamellae forming secondary osteons (Fig. 4.14). Two specimens (NT071, NT057) possess a large number of resorption cavities that scattered up to their periosteal regions (Fig. 4.15).

In most of the tibiae in this category (NT034, NT036, NT038, NT039, NT037, NT044, NT046, NT047, NT055, NT056), the density of vascularization decreases gradually towards the outer cortex. The inner 1/3 of the cortex consists of a mixture of a small amount of reticular and sub-plexiform bone tissues with parallel-fibered matrix. This tissue combination gradually changes to plexiform immediately after the second or third preserved LAG and is predominant in the rest of the cortex. A considerable decrease in vascularity is observed peripherally in each zone.

In the periosteal region, the vascularity decreases greatly, and some immature laminar vascularity often occurs. LAGs are hard to identify and are represented as a very narrow dark lines. In periosteal regions of some of the larger specimens (NT057, NT058, NT071), a locally developed pack of lines often occurs (Fig. 4.15). We were unable to trace these lines around the entire section due to the incompleteness of the specimen.

Discussion

A histological analysis of a single skeletal element is important in order to obtain the detailed physiological information about an extinct population. A previous study (Erickson and Tumanova, 2000) on *P. mongoliensis* sectioned multiple skeletal elements including the humerus, femur, and tibia. Since different skeletal elements go through a different growth or remodeling rate due to functional or genetic causes (Horner et al., 1999), results of multi-element analyses could lead to an inaccurate conclusion about the animal's physiology. Due to extensive tissue variations in similar sized tibiae, we used tissue types to determine the growth stages of *P. mongoliensis* rather than simply using LAG count or tibiae length.

Histological Analysis of *P. mongoliensis*

The smallest *P. mongoliensis* tibiae in this study (NT002, NT003, NT004) exhibit well-differentiated marrow cavities and moderately organized bone tissue consisting of highly vascular reticular bone tissues with parallel fibered matrix. The combination of reticular/longitudinal vascularization occurred somewhere between the first 2 years of *P. mongoliensis*. Based on the tissue organization, the tibiae in growth Phase A likely

belong to early juveniles (35-49 cm in body length; Table 4.4) in the first or second year of their life. Growth Phase A reflects an occurrence of longitudinally growing bone with a rate of 2.22-3.29 μm/day (Table 4.3). The tissue pattern of Phase A is comparable to the growth stages A (3-5 years) determined by Erickson and Tumanova (2000). However, Zhao et al. (2013a) suggested the same tissue pattern continues to occur until the adult stage in *P. lujiatunensis* (11 years old). This extreme difference in the two sister species of *Psittacosaurus* could have occurred due to misidentification of LAGs.

The presence of reticular tissue without any longitudinal or radial vascularization is probably a transitional phase in *P. mongoliensis*. The reticular tissue occurs somewhere between the ages of 2-4 years, in between the occurrence of reticular/longitudinal and reticular/radial tissue.

In *P. mongoliensis*, the reticular/longitudinal vascularization is retained until the body size reaches approximately 1 meter in length, but the numbers of longitudinal canals decrease at this size. Evenly distributed radial vascularity is frequently visible in the tibiae with 2-5 LAGs (Phase B). The presence of radially oriented canals represents an intensive centrifugal bone growth (Francillon-Vieillot et al., 1990). The bone apposition rate in the Phase B ranges between 1.9- 3.2 μm/day. This radial vascularity does not resemble the highly vascularized radial tissue described by Erickson and Tumanova (2000). Probably, the radial vascularized tissue identified by Erickson and Tumanova (2000) formed in certain individuals due to pathologic cause such as an osteopetrosis as is observed in some fowls (Chinsamy and Tumarkin-Deratzian, 2009). None of the specimens (n=38) in this study exhibit this tissue. Instead, there is a frequent occurrence

of evenly distributed, locally developed radial vascularization during 2-5 years in *P. mongoliensis*. (Fig. 4.9).

Zhao et al. (2013a) reported a postural change (from quadrupedal to bipedal) in *Psittacosaurus* juveniles (1-2 years old). The presence of evenly distributed radial bone tissues in several specimens (NT020, NT009, NT021, NT023, and NT024) may be related to this biomechanical change. As a result of postural change, the weight bearing bones (including the femur and tibia) must have undergone a structural change in order to accommodate the increased stress. The tissue change from reticular/longitudinal to reticular/radial could be a result of this. However, a laminar bone tissue is related to the increased stress in extant vertebrates due to its advanced vascular organization (De Margerie, 2002). Another explanation could be related to a food source change that affected the bone tissue development. The postural change could also facilitate *Psittacosaurus* feeding on a food source located further from the ground; however, there is no direct evidence to support this hypothesis. Based on the reconstructed cranial muscles and teeth microstructure, Sereno et al. (2009) reported that *Psittacosaurus* fed on high caloric food content such as nuts or seeds. Possibly, the nutrition-rich food sources affected the metabolic regime of *Psittacosaurus* by triggering a considerable change in bone tissue such as forming radial tissue.

In growth Phase C, a plexiform bone tissue dominates in all specimens; however, there are small amounts of reticular vascularizations in the inner cortex of the tibiae. In this growth phase, sub-plexiform to plexiform bone tissues begin to form in the tibiae after the fifth year of life. Similar bone tissue occurs in two-year-old *Maiasaura* (Horner

et al., 2000; Woodward et al., 2015). This tissue type has not been reported in *Psittacosaurus* (Erickson and Tumanova, 2000; Erickson et al., 2009; Zhao et al., 2013a). In Phase C, the bone apposition rate of *P. mongoliensis* decreases down to 1.8 - 2.08 μm/day until its seventh year of life. *P. mongoliensis* individuals reached up to 13.41 kg in mass and 127.1 cm in length by the end of the fifth year of life (Table 4.3 and 4.4). The growth Phases B and C exhibit similar rates of bone apposition.

The larger *P. mongoliensis* tibiae (18.9-26.9 cm in length) belong to growth Phase D. The bone apposition rate slows to 1.2 μm/day, especially in larger tibiae 24.2-26.9 cm in length, suggesting considerable decrease of growth. The body sizes of individuals reach up to 170 cm in length and 46.6 kg in mass (Table 4.4). This stage differs from others by presenting a large number of resorption cavities in the inner half of the cortices of the bone. In some specimens (NT071, NT057), the scattered resorption cavities extend up to the outer half of the cortex (Fig. 4.14). The resorption cavities without lamellar infilling are also observed from the tibia of eight-year old individuals by Erickson et al. (2000). The abundant occurrence of resorption cavities indicates a considerable increase of osteoclastic activity in *P. mongoliensis* tibiae. Moreover, several specimens (NT054, NT057, NT058) exhibit the first generation of secondary osteons in their cortices. Interestingly, the same resorption cavities are observed in both smaller (less than a year old) and skeletally matured (at least 9 years old) *Maiasaura* individuals (Horner et al., 2000; Woodward et al., 2015); whereas, it occurs only in larger *P. mongoliensis* individuals. The periosteal regions of tibiae at this stage consist of loosely vascularized parallel-fibered bone tissues indicating a slow bone growth. Tightly packed growth lines

occur locally in avascular periosteal regions of some tibiae cortices (NT057, NT058). Generally, tightly packed growth lines in the periosteum characterize skeletal maturity of an individual and are called an External Fundamental System (EFS) (Cormack, 1987; Castanet et al., 1988; Ponton et al., 2004; Klein et al., 2009; Woodward et al., 2011). We were unable to observe an EFS in any specimen of *P. mongoliensis* tibiae due to the incompleteness of the largest specimens (NT057, NT058). However, if those packed lines in the tibiae represent the beginning of skeletal maturity, *P. mongoliensis* reaches its asymptotic body size soon after its 13th year of life. Perhaps the combined occurrence of extensive resorption cavities with lamellae infilling and tightly packed growth lines may be an indicator of approaching skeletal maturity. To test this, more complete and larger sized specimens are needed.

Regression and Growth Curves

Various measurements were obtained from *P. mongoliensis* tibiae including length, perimeter and area of diaphysis, LAG numbers, perimeter of medullary cavity, bone wall thickness, and LAG number count. There is a strong relationship between tibia length and diaphyseal perimeter (linear-model, R^2= 0.98) as well as tibia length and diaphyseal area (using power-model, R^2= 0.98) (Fig. 4.1). In contrast, predicting medullary cavity perimeter or area from tibia length is less reliable (power-model, and R^2= 0.79 for perimeter, R^2= 0.81 for area) (Fig. 4.2). The relationship between tibia length and area of bone wall appears to be weaker (power-model, R^2= 0.89) compared to the relationship between tibia length and diaphyseal perimeter or area (Fig. 4.1).

P. mongoliensis growth rates are as high as 2.2-3.2 μm/day in earlier years (growth phase A) of ontogeny (Table 4.3). During this growth phase, the body length increases gradually up to 65.9 cm. The body mass at this growth phase increased from 1.7 to 2.7 kg (Table 4.4). This growth phase continued until the third year of life.

The highest growth rate (3.19 μm/day) of body size increase occurred between the third and seventh years of growth (Phases B and C). The increased growth rate could reflect a successful passing of threshold size and further exponential growth of *P. mongoliensis*. A similar growth pattern was reported in the ontogeny of *P. lujiatunensis* (Erickson et al., 2009). During growth Phase B, the occurrence of radial vascularity is commonly observed in the tibiae. The presence of this tissue indicates an extremely fast growing bone tissue (Francillon-Vieillot et al., 1990; De Margerie et al., 2004). A radial bone tissue in the extant vertebrates such as the king penguin (*Aptenodys patagonicus*) correlates with an explosive growth rate of up to 171 μm/day (De Margerie et al., 2004).

The growth rate gradually slowed to 1.6 μm/day after the seventh year of life. During the years seven to nine, the body length reaches between 134.1 and 157.6 cm. Erickson and Tumanova (2000) suggested that the body mass of *P. mongoliensis* exponentially increased up to 20 kg by the age nine. At this point, the results of this study contradict the previous conclusion suggesting the body mass of *P. mongoliensis* reached as high as 40 kg in the ninth year of life. There is a considerable decrease of growth after age of nine. By the age of ten, the body mass of *P. mongoliensis* has reached up to 46.67 kg and body length has increased up to 170.3 cm (Table 4.4).

The oldest individual (13 years old) exhibited the slowest growth rate (1.23 μm/day) and the body mass and length reached 45.9 kg and 169.4 cm, respectively. Presumably, the growth of *P. mongoliensis* continued at this slower rate until it attained the asymptotic body size.

Age Frequency

A total of 36 out of the 58 specimens were used for depicting a frequency graph because of the preservation of the specimens (Fig. 4.16). The smallest (0-2) and the oldest (9-13) individuals were rare in the sample set. Individuals between two and seven years old were common, except a single "three year-old" individual. The most common age range is between five and seven.

The mortality rate appears to be very high during the first two years (Phase A). It appears that mortality is possibly size dependent for smaller *P. mongoliensis* individuals (0-2 years old). The small body size of *P. mongoliensis* could make them easy prey for predators including small-bodied predators such as the dromaeosaurid *Shana*g (Turner et al., 2007) and the triconodont mammal *Repenomamus* (Hu et al., 2005). Meng et al. (2004) suggested that *Psittacosaurus* exhibited parenting behavior based on the discovery of an adult individual associated with 34 juveniles. However, this idea was challenged by Zhao et al. (2013b) who claimed that the adult skull was artificially associated with the juveniles. Instead, *P. lujiatunensis* juveniles (0-2 years old) lived together as a flock (Zhao et al., 2013b). This behavior is observed in extant birds and mammals for protection (Pelletier and Festa-Bianchet, 2004). In addition, several researchers have

noted that juvenile *Psittacosaurus* are usually found in aggregations (Meng et al., 2004; Zhao et al., 2013b).

Individuals between the ages of 2-7 years old are the most abundant (69.4%) in the sample set. Probably the abundance of this age class reflects a threshold age occurring at some point in the second year of *P. mongoliensis*. This result is almost comparable to a previous study (Erickson et al., 2009), however the threshold age of *P. lujiatunensis* was hypothesized to be 3-4 years of life. A slight difference in threshold age between *P. mongoliensis* (2 years old) and *P. lujiatunensis* (3-4 years old) could be taxon specific or it could be data noise due to an observational error.

Larger sized (growth Phase D) *P. mongoliensis* skeletons tend to be found alone rather than in the aggregations. This suggests that an age-related segregation existed in populations of *P. mongoliensis*. Considering histologic features (locally developed packed growth lines) and lower growth rate (1.2-1.6 μm/day), the larger individuals (34.2 – 46.6 kg in mass) were very close to reaching skeletal maturity. The general pattern of the growth curve of *P. mongoliensis* shows the sigmoidal shape as observed in *P. lujiatunensis* population (Erickson et al., 2009) (Fig. 4.4).

Conclusions

This study expands the view of ontogenetic growth of *P. mongoliensis* using a larger sample focusing on a single element from each individual (the tibia). The results of this study partially support the conclusions of previous studies on *Psittacosaurus* population histology (Erickson and Tumanova, 2000; Erickson et al., 2009).

A considerable amount of tissue variations occurs in the histology of similar sized *P. mongoliensis* tibiae. This study shows that tissue type is the most useful feature to draw reliable conclusions about the ontogenetic stage of *P. mongoliensis*. Four different growth phases (A, B, C, and D) are identified and reflect four different growth regimes: (Phase A) fast growing reticular/longitudinal tissue with woven matrix in 0-2 years of life; (Phase B) very fast growing reticular/radial tissues with parallel-fibered matrix occurring in 2-5 years; (Phase C) slightly slowed reticular/plexiform tissues with parallel-fibered matrix occurring in 5-6; and (Phase D) slowed plexiform tissues with parallel-fibered matrix occurring in 7-13 years of life.

Based on the histologic observations, the highly vascularized radial tissue previously described by Erickson and Tumanova (2000) does not commonly occur in this animal, at least in the sample set of tibia in this study (n=38). Therefore, we support the conclusion of Chinsamy and Tumarkin-Deratzian (2009) suggesting this histologic anomaly is related to pathology.

There is a strong relationship (R^2=0.98) between tibia length and diaphyseal measurements including perimeter and area. The threshold age of *P. mongoliensis* was sometime in the second year of life. Once the threshold size is reached the growth rate is increased up to 3.19 μm/day and continues until age seven. After the eighth year, the growth rate gradually slows to 1.6 μm/day, resulting in 36.9 kg in body mass and 157.6 cm in length. By the ages of 10-13, the body mass has reached up to 46.6 kg, and body length ranges between 153.6-170.3 cm. Based on the histologic analysis, *P. mongoliensis* probably reached its skeletal maturity soon after the age of 13. However, this is currently

speculative due to inadequate evidence of EFS presence. The growth curve of *P. mongoliensis* appears to have a sigmoidal shape which is consistent with previous studies including those of Erickson and Tumanova (2000) and Erickson et al. (2009).

Acknowledgements

We thank Rio Tinto Copper Group in Canada, Gerry Ohrstrom, Elizabeth Moore, David Swingle, and Matt Morse for fieldwork funding. We are grateful to Dr. Tsogtbaatar Khishigjav (Mongolian Academy of Sciences) for supporting us to obtain fieldwork permit. We thank E.-T. Lamm (Museum of the Rockies) for thin section preparation. We also grateful to Dr. H. Woodward for the helpful discussion. We also thank Ch. Bayardorj, B. Ganzorig, P. Khatanbaatar, Andi Bennett, Julie Bennett, Matt Morse, and David Fuqua for fieldwork assistance.

Table 4.1. Total specimen (tibiae) list used in this study. Tibia codes are listed with corresponding official institution (MPC) and field numbers. The specimens were collected during the five field seasons (2010-2015).

No.	Tibia code	Field number	MPC number
1	NT002	BLK11-42-4	MPC-D100/620-001
2	NT003	BLK12018A	MPC-D100/620-002
3	NT004	BLK14020	MPC-D100/620-003
4	NT005	BLK11-42-3	MPC-D100/620-004
5	NT006	BLK106-1	MPC-D100/620-005
6	NT007	BLK12010-4	MPC-D100/618-004
7	NT009	BLK11042	MPC-D100/620-006
8	NT008	BLK12021	MPC-D100/620-007
9	NT010	BLK14032-A	MPC-D100/620-008
10	NT011	BLK12010-1	MPC-D100/618-001
11	NT020	BLK12010-2	MPC-D100/618-002
12	NT012	BLK12011	MPC-D100/620-009
13	NT013	BLK14034	MPC-D100/620-010
14	NT014	BLK12020	MPC-D100/620-011
15	NT015	BLK14033	MPC-D100/620-012
16	NT016	BLK12010-3	MPC-D100/618-003
17	NT017	BLK12024	MPC-D100/620-013
18	NT018	BLK14022	MPC-D100/620-014
19	NT019	BLK11-44-1	MPC-D100/620-015
20	NT063	BLK12023	MPC-D100/620-016
21	NT021	BLK14024	MPC-D100/620-017
22	NT022	BLK11-17-2	MPC-D100/620-018
23	NT023	BLK14023	MPC-D100/620-019
24	NT024	BLK14025	MPC-D100/620-020
25	NT025	BLK12010-5	MPC-D100/618-005
26	NT026	BLK12017	MPC-D100/620-021
27	NT027	BLK11-16-1	MPC-D100/620-022
28	NT028	BLK12022	MPC-D100/620-023
29	NT029	BLK11-17-1	MPC-D100/620-024

No.	Tibia number	Field number	MPC number
30	NT030	BLK11-40	MPC-D100/617
31	NT065	BLK12016	MPC-D100/620-025
32	NT067	BLK12019	MPC-D100/620-026
33	NT068	BLK12014	MPC-D100/620-027
34	NT034	BLK11-23-b	MPC-D100/620-028
35	NT069	BLK14033-B	MPC-D100/620-029
36	NT036	BLK14034	MPC-D100/620-030
37	NT037	BLK12008	MPC-D100/620-031
38	NT038	BLK12013	MPC-D100/620-032
39	NT039	BLK14035	MPC-D100/620-033
40	NT040	BLK106	MPC-D100/620-034
41	NT041	BLK12001	MPC-D100/620-035
42	NT042	BLK14028	MPC-D100/620-036
43	NT031	BLK14026	MPC-D100/620-037
44	NT044	BLK11-43	MPC-D100/620-038
45	NT071	BLK14035-B	MPC-D100/620-039
46	NT046	BLK12018B	MPC-D100/620-040
47	NT047	BLK12002	MPC-D100/620-041
48	NT072	BLK14032-B	MPC-D100/620-042
49	NT073	BLK11-24	MPC-D100/620-043
50	NT050	BLK12012	MPC-D100/620-044
51	NT076	BLK14036	MPC-D100/620-045
52	NT053	BLK11-14	MPC-D100/620-046
53	NT032	BLK11-2-1	MPC-D100/620-047
54	NT054	BLK14031	MPC-D100/620-048
55	NT055	BLK12025	MPC-D100/619
56	NT056	BLK11-49-1	MPC-D100/620-049
57	NT057	BLK14030	MPC-D100/620-050
58	NT058	BLK11-19-1	MPC-D100/620-051

Table 4.2. Data collected from 58 histologically sectioned *P. mongoliensis* tibiae.

No.	Tibia code	Length, cm	Diaphyseal area,cm^2	Diaphyseal perimeter,cm	Medullary cavity area,cm^2	Medullary cavity perimeter,cm	Cortical thickness,cm
1	NT002	5.68	0.20625	1.7427	0.071	0.989	0.097
2	NT003	6.30	0.23331	1.7362	0.049	0.796	0.144
3	NT004	7.00	0.28713	1.9281	0.057	0.865	0.162
4	NT005	7.77	0.29541	2.0135	0.140	1.403	0.110
5	NT006	8.28	0.35943	2.1565	0.092	1.094	0.174
6	NT007	10.41	0.52911	2.7121	0.103	1.159	0.240
7	NT009	10.55	0.5484	2.7633	0.176	1.751	0.157
8	NT008	10.63	0.55081	2.7678	0.176	1.770	0.188
9	NT010	11.25	0.53072	2.615	0.083	1.041	0.245
10	NT011	11.54	0.69735	3.0043	0.164	1.465	0.249
11	NT020	11.69	0.71402	3.0439	0.136	1.348	0.273
12	NT012	12.48	0.85423	3.343	0.192	1.662	0.237
13	NT013	12.63	0.85255	3.4334	0.267	2.065	0.228
14	NT014	13.32	0.98963	3.6297	0.178	1.569	0.287
15	NT015	13.32	1.01066	3.6203	0.215	1.693	0.294
16	NT016	13.33	1.0083	3.6229	0.141	1.367	0.347
17	NT017	13.44	1.03773	3.6525	0.235	1.763	0.294
18	NT018	13.82	0.98185	3.6622	0.219	1.830	0.280
19	NT019	14.98	1.29372	4.1422	0.095	1.161	0.466
20	NT063	15.15	1.31046	4.143	0.199	1.603	0.376
21	NT021	15.39	1.38604	4.2545	0.314	2.053	0.359
22	NT022	15.46	1.40003	4.3021	0.287	2.057	0.388
23	NT023	15.66	1.44305	4.3287	0.363	2.220	0.341
24	NT024	15.88	1.44017	4.3312	0.373	2.323	0.327
25	NT025	16.15	1.44337	4.3477	0.249	1.824	0.376
26	NT026	16.42	1.49544	4.421	0.355	2.160	0.364
27	NT027	17.27	1.5963	4.6029	0.359	2.215	0.380
28	NT028	17.29	1.54224	4.5687	0.373	2.336	0.343
29	NT029	17.32	1.61746	4.6548	0.382	2.406	0.335
30	NT030	17.50	1.63953	4.6259	0.391	2.289	0.359
31	NT065	17.76	2.06272	5.2105	0.249	1.826	0.515
32	NT067	18.26	1.7048	4.8733	0.523	2.801	0.313
33	NT068	18.89	1.9618	5.207	0.592	2.967	0.341
34	NT034	18.97	1.95756	5.0985	0.319	2.294	0.497
35	NT069	19.17	2.19021	5.3338	0.474	2.496	0.444
36	NT036	19.25	2.08002	5.1625	0.343	2.138	0.497
37	NT037	19.45	2.45525	5.6205	0.635	2.929	0.432
38	NT038	19.51	2.35163	5.6374	0.265	2.061	0.532
39	NT039	19.84	2.23036	5.412	0.245	1.922	0.581
40	NT040	19.88	2.6996	6.0986	0.443	2.819	0.560
41	NT041	20.10	2.08052	5.2516	0.409	2.483	0.419
42	NT042	20.76	2.66636	6.0012	0.730	3.213	0.420
43	NT031	20.77	2.72305	6.0036	0.474	2.582	0.501
44	NT044	21.19	2.73026	6.0377	0.455	2.722	0.520
45	NT071	21.20	2.73309	5.9949	0.450	2.471	0.525
46	NT046	21.39	2.84886	6.0935	0.429	2.447	0.521
47	NT047	21.44	2.83192	6.0949	0.371	2.233	0.577
48	NT072	21.50	2.96972	6.2391	0.598	2.969	0.479
49	NT073	21.79	2.75245	6.1367	0.783	3.433	0.442
50	NT050	21.95	2.93989	6.2524	0.671	3.024	0.541
51	NT076	22.97	2.88031	6.2331	0.528	2.658	0.529
52	NT053	23.60	3.39355	6.661	0.350	2.258	0.660
53	NT032	23.60	3.06567	6.5196	0.611	2.994	0.470
54	NT054	23.68	3.19065	6.5425	0.703	3.030	0.531
55	NT055	24.27	3.1031	6.5755	0.488	2.620	0.638
56	NT056	24.90	3.48836	6.8776	0.539	2.708	0.639
57	NT057	26.77	4.10849	7.3959	0.880	3.447	0.584
58	NT058	26.91	3.9326	7.4348	0.753	3.296	0.615

Table 4.3. Average daily bone apposition rate for each year of growth based on 365 days to compare modern vertebrates. Asterisk indicates the retro-calculated growth lines

No	Tibia code	LAGs	Thickness,um	Rate, um/day
1	NT002	0	1028.40	2.82
2	NT003	1	1064.80	2.92
3	NT004	1	819.84	2.25
		2	348.90	0.96
4	NT006	1	585.70	1.60
		2	879.96	2.41
5	NT007	1	610.26	1.67
		2	1128.33	3.09
6	NT011	1*	1064.80	2.92
		2*	730.85	2.00
		3	1196.07	3.28
7	NT012	1*	1064.80	2.92
		2	731.37	2.00
		3	1208.98	3.31
8	NT013	1	867.99	2.38
		2	1299.14	3.56
9	NT015	1*	585.70	1.60
		2*	879.96	2.41
		3	1285.50	3.52
		4	810.19	2.22
10	NT016	1	690.12	1.89
		2	583.25	1.60
		3	646.52	1.77
		4	1295.43	3.55
11	NT017	1*	1064.80	2.92
		2*	753.74	2.07
		3	551.26	1.51
		4	807.12	2.21
12	NT019	1	1085.80	2.97
		2	911.12	2.50
		3	1214.61	3.33
		4	775.77	2.13
13	NT021	1*	585.70	1.60
		2*	879.96	2.41
		3	1143.13	3.13
		4	585.40	1.60
		5	1488.57	4.08
14	NT023	1*	1085.80	2.97
		2*	911.12	2.50
		3*	1214.61	3.33
		4*	775.77	2.13
		5	599.24	1.64
15	NT024	1*	585.70	1.60
		2*	879.96	2.41
		3*	1285.50	3.52
		4*	810.19	2.22
		5	596.18	1.63
16	NT025	1	585.70	1.60
		2	879.96	2.41
		3	529.58	1.45
		4	763.94	2.09
		5	1550.17	4.25
17	NT026	1*	585.70	1.60
		2*	879.96	2.41
		3	1285.50	3.52
		4	810.19	2.22
		5	1227.25	3.36
18	NT027	1*	585.70	1.60
		2*	879.96	2.41
		3*	1285.50	3.52
		4*	810.19	2.22
		5	1528.52	4.19
19	NT030	1*	585.70	1.60
		2*	879.96	2.41
		3*	1285.50	3.52
		4	1373.08	3.76
		5	1304.48	3.57
20	NT034	1*	585.70	1.60
		2*	879.96	2.41
		3*	1285.50	3.52
		4*	810.19	2.22
		5	1460.79	4.00
		6	687.35	1.88
21	NT036	1*	585.70	1.60
		2*	879.96	2.41
		3*	1285.50	3.52
		4*	810.19	2.22
		5	1142.32	3.13
		6	1147.33	3.14
22	NT037	1*	585.70	1.60
		2*	879.96	2.41
		3*	1285.50	3.52
		4*	810.19	2.22
		5*	1528.52	4.19
		6	795.08	2.18
		7	1189.28	3.26
23	NT038	1*	585.70	1.60
		2*	879.96	2.41
		3	1369.85	3.75
		4	782.18	2.14
		5	699.99	1.92
		6	786.73	2.16
		7	760.01	2.08
24	NT039	1	686.62	1.88
		2	1269.50	3.48
		3	813.90	2.23
		4	1477.80	4.05
		5	1464.71	4.01
		6	1072.46	2.94
		7	302.69	0.83

Table 4.3 continued.

No	Tibia code	LAGs	Thickness,um	Rate, um/day
25	NT040	1*	585.70	1.60
		2*	879.96	2.41
		3*	1285.50	3.52
		4*	810.19	2.22
		5*	1528.52	4.19
		6	768.20	2.10
		7	776.06	2.13
26	NT041	1*	585.70	1.60
		2*	879.96	2.41
		3*	1285.50	3.52
		4*	810.19	2.22
		5	636.39	1.74
		6	1266.55	3.47
27	NT044	1*	585.70	1.60
		2*	879.96	2.41
		3	1369.85	3.75
		4	938.74	2.57
		5	807.32	2.21
		6	1188.07	3.25
		7	790.42	2.17
28	NT046	1*	686.62	1.88
		2*	1269.50	3.48
		3*	813.90	2.23
		4*	1477.80	4.05
		5	1243.76	3.41
		6	1941.36	5.32
		7	861.18	2.36
29	NT047	1*	585.70	1.60
		2*	879.96	2.41
		3*	1285.50	3.52
		4	1458.69	4.00
		5	1226.70	3.36
		6	1312.24	3.60
30	NT050	1*	585.70	1.60
		2*	879.96	2.41
		3	1285.50	3.52
		4	810.19	2.22
		5	598.17	1.64
		6	1316.19	3.61
		7	1673.72	4.59
31	NT053	1*	585.70	1.60
		2*	879.96	2.41
		3*	1285.50	3.52
		4	1377.21	3.77
		5	1517.25	4.16
		6	1046.59	2.87
		7	568.16	1.56
		8	1049.89	2.88

No	Tibia code	LAGs	Thickness,um	Rate, um/day
32	NT054	1*	585.70	1.60
		2*	879.96	2.41
		3*	1285.50	3.52
		4*	1458.69	4.00
		5	1533.99	4.20
		6	898.36	2.46
		7	845.25	2.32
		8	532.70	1.46
33	NT055	1*	585.70	1.60
		2*	879.96	2.41
		3*	1285.50	3.52
		4*	810.19	2.22
		5	1261.76	3.46
		6	1166.37	3.20
		7	705.07	1.93
		8	694.33	1.90
		9	354.91	0.97
		10	447.63	1.23
34	NT056	1*	686.62	1.88
		2*	1269.50	3.48
		3	813.90	2.23
		4	926.07	2.54
		5	579.07	1.59
		6	1218.39	3.34
		7	575.67	1.58
		8	980.26	2.69
		9	1041.72	2.85
35	NT057	1*	585.70	1.60
		2*	879.96	2.41
		3*	1285.50	3.52
		4*	810.19	2.22
		5*	636.39	1.74
		6	1020.21	2.80
		7	561.15	1.54
		8	591.38	1.62
		9	463.01	1.27
		10	533.89	1.46
		11	367.29	1.01
		12	345.49	0.95
		13	323.68	0.89
36	NT058	1*	585.70	1.60
		2*	879.96	2.41
		3*	1285.50	3.52
		4*	810.19	2.22
		5	1275.14	3.49
		6	678.14	1.86
		7	1043.36	2.86
		8	591.12	1.62
		9	791.93	2.17
		10	308.48	0.85

Table 4.4. Estimates of *P. mongoliensis* femur, body length, and body mass based on regression equation and the Developmental Mass Extrapolation method.

No	Tibia code	LAGs	Femur length, cm	Body length, cm	Mass, kg
1	NT002	0	4.34	30.38	0.31
2	NT003	0	4.34	30.38	0.31
		1	4.95	33.86	0.43
		Surface	5.84	39.90	0.60
3	NT004	0	4.34	30.38	0.31
		1	4.50	30.74	0.32
		2	5.19	35.51	0.50
		Surface	6.48	44.31	0.82
4	NT006	0	4.34	30.38	0.31
		1	4.87	33.32	0.41
		2	6.82	46.63	1.12
		Surface	7.67	52.41	1.36
5	NT007	0	4.34	30.38	0.31
		1	5.37	36.68	0.55
		2	7.80	53.33	1.68
		Surface	9.64	65.91	2.70
6	NT011	0	4.34	30.38	0.31
		1	4.97	33.97	0.43
		2	6.44	43.99	0.94
		3	8.92	61.01	2.51
		Surface	10.68	73.01	3.67
7	NT012	0	4.34	30.38	0.31
		1	4.98	34.03	0.44
		2	7.04	48.11	1.23
		3	9.51	65.04	3.05
		Surface	11.56	79.01	4.66
8	NT013	0	4.34	30.38	0.31
		1	8.55	58.46	2.21
		2	10.89	74.43	4.56
		Surface	11.69	79.94	4.82
9	NT015	0	4.34	30.38	0.31
		1	4.87	33.32	0.41
		2	6.88	47.03	1.15
		3	9.53	65.12	3.06
		4	11.25	76.93	5.04
		Surface	12.34	84.33	5.66
10	NT016	0	4.34	30.38	0.31
		1	5.73	39.16	0.66
		2	6.96	47.60	1.19
		3	8.28	56.58	2.01
		4	10.80	73.83	4.45
		Surface	12.34	76.40	5.67
11	NT017	0	4.34	30.38	0.31
		1	4.97	34.00	0.43
		2	6.41	43.84	0.93
		3	7.60	51.95	1.55
		4	9.37	64.05	2.91
		Surface	12.45	85.08	5.81
12	NT019	0	4.34	30.38	0.31
		1	5.67	38.77	0.64
		2	7.51	51.33	1.50
		3	10.26	70.16	3.82
		4	11.93	81.58	6.01
		Surface	13.87	94.83	8.05
13	NT021	0	4.34	30.38	0.31
		1	4.87	33.32	0.41
		2	6.82	46.63	1.12
		3	9.26	63.34	2.81
		4	10.47	71.57	4.06
		5	13.47	92.06	8.63
		Surface	14.25	97.40	8.72
14	NT023	0	4.34	30.38	0.31
		1	5.67	38.77	0.64
		2	7.51	51.33	1.50
		3	10.26	70.16	3.82
		4	11.36	77.63	5.18
		5	12.63	86.33	7.12
		Surface	14.50	99.10	9.18
15	NT024	0	4.34	30.38	0.31
		1	4.87	33.32	0.41
		2	6.88	47.03	1.15
		3	9.53	65.12	3.06
		4	11.59	79.22	5.50
		5	12.90	88.16	7.58
		Surface	14.70	100.50	9.58

No	Tibia code	LAGs	Femur length, cm	Body length, cm	Mass, kg
16	NT025	0	4.34	30.38	0.31
		1	5.37	36.68	0.55
		2	7.34	50.15	1.40
		3	8.29	56.64	2.01
		4	9.97	68.14	3.50
		5	13.05	89.22	7.86
		Surface	14.95	102.21	10.08
17	NT026	0	4.34	30.38	0.31
		1	4.87	33.32	0.41
		2	6.88	47.03	1.15
		3	9.91	67.77	3.45
		4	11.18	76.43	4.94
		5	13.75	93.98	9.19
		Surface	15.20	103.93	10.60
18	NT027	0	4.34	30.38	0.31
		1	4.87	33.32	0.41
		2	6.88	47.03	1.15
		3	9.53	65.12	3.06
		4	11.33	77.42	5.14
		5	14.42	98.55	10.59
		Surface	15.99	109.34	12.34
19	NT030	0	4.34	30.38	0.31
		1	4.87	33.32	0.41
		2	6.88	47.03	1.15
		3	9.01	61.61	2.59
		4	11.89	81.25	5.94
		5	14.66	100.23	11.14
		Surface	16.20	127.10	12.83
20	NT034	0	4.34	30.38	0.31
		1	4.87	33.32	0.41
		2	6.88	47.03	1.15
		3	9.53	65.12	3.06
		4	11.14	76.16	4.89
		5	14.14	96.63	9.99
		6	15.61	106.73	13.46
		Surface	17.57	120.11	16.35
21	NT036	0	4.34	30.38	0.31
		1	4.87	33.32	0.41
		2	6.88	47.03	1.15
		3	9.53	65.12	3.06
		4	11.72	80.09	5.69
		5	13.90	95.06	9.51
		6	16.18	110.62	14.98
		Surface	17.82	121.83	17.07
22	NT037	0	4.34	30.38	0.31
		1	4.87	33.32	0.41
		2	6.88	47.03	1.15
		3	9.53	65.12	3.06
		4	11.33	77.42	5.14
		5	13.74	93.91	9.17
		6	15.32	104.74	12.72
		7	17.50	119.65	18.96
		Surface	18.01	123.10	19.01
23	NT038	0	4.34	30.38	0.31
		1	4.87	33.32	0.41
		2	8.20	56.07	1.95
		3	11.08	75.72	4.80
		4	12.72	86.98	7.28
		5	14.26	97.50	10.26
		6	15.77	107.80	13.87
		7	17.51	119.69	18.98
		Surface	18.06	123.47	19.36
24	NT039	0	4.34	30.38	0.31
		1	4.87	33.32	0.41
		2	7.37	50.41	1.42
		3	9.01	61.57	2.58
		4	12.23	83.58	6.46
		5	15.24	104.21	12.53
		6	17.39	118.91	18.61
		7	17.93	122.57	20.38
		Surface	18.37	125.57	20.47

Table 4.4 continued.

No	Tibia code	LAGs	Femur length, cm	Body length, cm	Mass, kg
25	NT040	0	4.34	30.38	0.31
		1	4.87	33.32	0.41
		2	6.88	47.03	1.15
		3	9.53	65.12	3.06
		4	11.33	77.42	5.14
		5	15.59	106.61	13.41
		6	17.04	116.50	17.50
		7	18.51	126.56	22.44
		Surface	18.61	126.84	22.61
26	NT041	0	4.34	30.38	0.31
		1	4.87	33.32	0.41
		2	6.88	47.03	1.15
		3	11.18	76.40	4.94
		4	12.02	82.20	6.15
		5	14.09	96.31	9.89
		6	15.46	105.66	13.06
		Surface	18.61	127.23	19.44
27	NT044	0	4.34	30.38	0.31
		1	4.87	33.32	0.41
		2	6.88	47.03	1.15
		3	11.48	78.46	5.35
		4	12.21	83.50	6.44
		5	14.12	96.54	9.96
		6	15.73	107.51	13.75
		7	18.07	123.53	20.87
		Surface	19.62	134.15	22.78
28	NT046	0	4.34	30.38	0.31
		1	4.87	33.32	0.41
		2	7.37	50.41	1.42
		3	9.01	61.57	2.58
		4	11.43	78.17	5.29
		5	13.91	95.08	9.51
		6	17.94	122.61	20.40
		7	19.61	134.07	26.68
		Surface	19.80	135.39	26.92
29	NT047	0	4.34	30.38	0.31
		1	4.87	33.32	0.41
		2	6.88	47.03	1.15
		3	9.90	67.68	3.43
		4	13.05	89.19	7.85
		5	15.57	106.45	13.35
		6	18.22	124.59	21.41
		Surface	19.85	135.73	23.60
30	NT050	0	4.34	30.38	0.31
		1	4.87	33.32	0.41
		2	6.88	47.03	1.15
		3	9.53	65.12	3.06
		4	11.79	80.63	5.80
		5	13.07	89.35	7.90
		6	15.84	108.29	14.05
		7	19.22	131.37	25.10
		Surface	20.32	138.92	25.30
31	NT053	0	4.34	30.38	0.31
		1	4.87	33.32	0.41
		2	6.88	47.03	1.15
		3	9.58	65.49	3.11
		4	12.60	86.16	7.08
		5	15.56	106.36	13.32
		6	17.68	120.89	19.55
		7	18.88	129.07	23.80
		8	20.81	142.23	31.85
		Surface	21.85	149.39	31.96

No	Tibia code	LAGs	Femur length, cm	Body length, cm	Mass, kg
32	NT054	0	4.34	30.38	0.31
		1	4.87	33.32	0.41
		2	6.88	47.03	1.15
		3	9.53	65.12	3.06
		4	12.25	83.73	6.50
		5	15.30	104.60	12.67
		6	17.31	118.32	18.33
		7	18.98	129.76	24.18
		8	19.84	135.61	27.60
		Surface	21.93	149.92	31.80
33	NT055	0	4.34	30.38	0.31
		1	4.87	33.32	0.41
		2	6.88	47.03	1.15
		3	9.53	65.12	3.06
		4	11.33	77.42	5.14
		5	12.97	88.64	7.71
		6	15.42	105.43	12.97
		7	17.08	116.75	17.62
		8	18.51	126.51	22.41
		9	19.30	131.95	25.43
		10	20.13	137.62	28.85
		Surface	22.47	153.60	34.21
34	NT056	0	4.34	30.38	0.31
		1	4.87	33.32	0.41
		2	7.37	50.41	1.42
		3	9.01	61.57	2.58
		4	11.63	79.52	5.56
		5	12.84	87.76	7.48
		6	15.32	104.75	12.72
		7	16.62	113.62	16.23
		8	18.58	127.03	22.69
		9	20.88	142.73	32.18
		Surface	23.05	157.60	36.94
35	NT057	0	4.34	30.38	0.31
		1	4.87	33.32	0.41
		2	6.88	47.03	1.15
		3	11.18	76.40	4.94
		4	12.02	82.20	6.15
		5	14.09	96.31	9.89
		6	16.12	110.19	14.81
		7	17.20	117.56	17.98
		8	18.33	125.29	21.77
		9	19.31	132.04	25.48
		10	20.40	139.44	30.01
		11	21.13	144.45	33.36
		12	21.70	148.35	36.14
		13	22.30	152.45	39.22
		Surface	24.79	169.47	45.94
36	NT058	0	4.34	30.38	0.31
		1	4.87	33.32	0.41
		2	6.88	47.03	1.15
		3	11.18	76.40	4.94
		4	13.35	91.26	8.41
		5	15.89	108.61	14.18
		6	17.48	119.47	18.88
		7	19.67	134.44	26.89
		8	21.06	144.00	33.05
		9	22.55	154.17	40.56
		10	23.63	161.55	46.67
		Surface	24.92	170.37	46.67

Figure 4.1. Relationship graphs between tibia length and A) diaphyseal perimeter, B) diaphyseal area, and C) cortical thickness. There are strong relationships (R^2>0.9) between tibia length and perimeter, as well as area. Relationship between length and cortical thickness is weak (R^2=0.89).

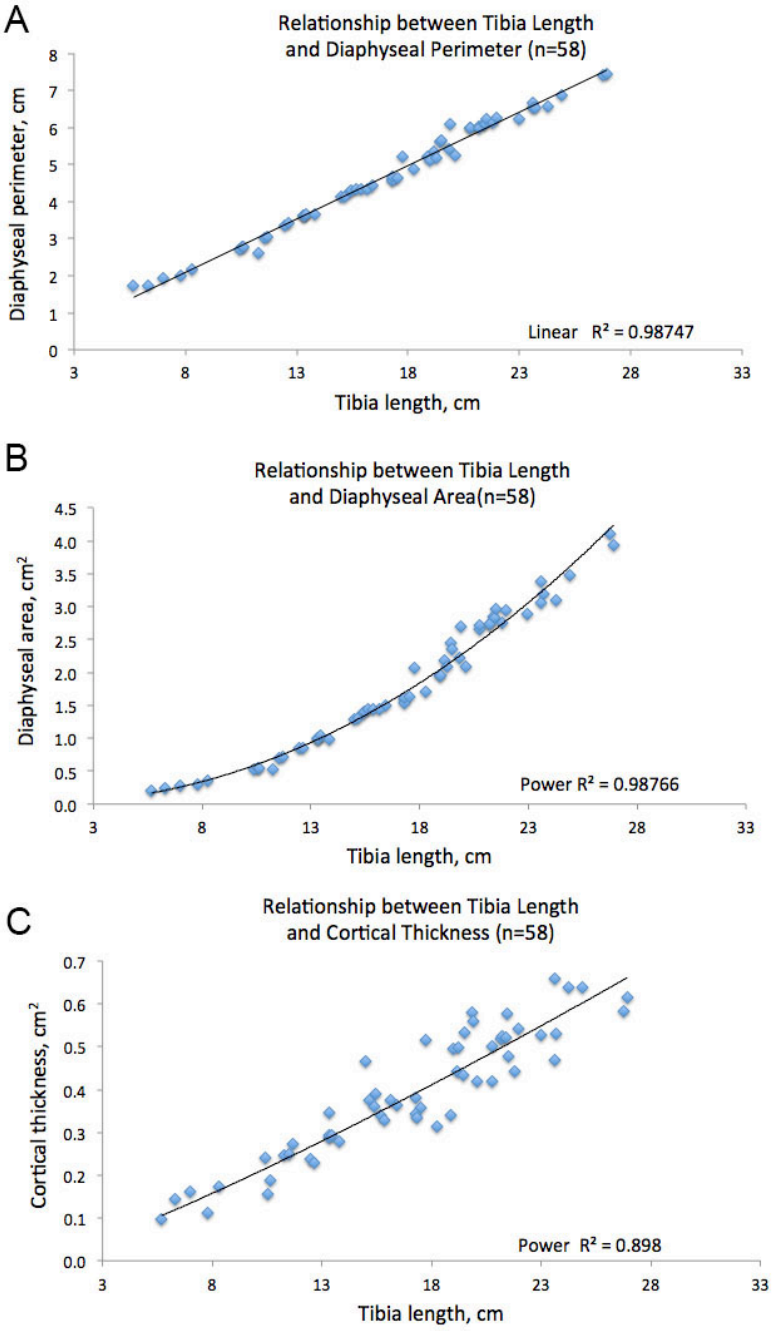


Figure 4.2. Relationship graphs between tibia length and A) medullary cavity perimeter, and B) medullary cavity area. There are weak relationships (R^2<0.9) between tibia length and both the medullary cavity perimeter and area.

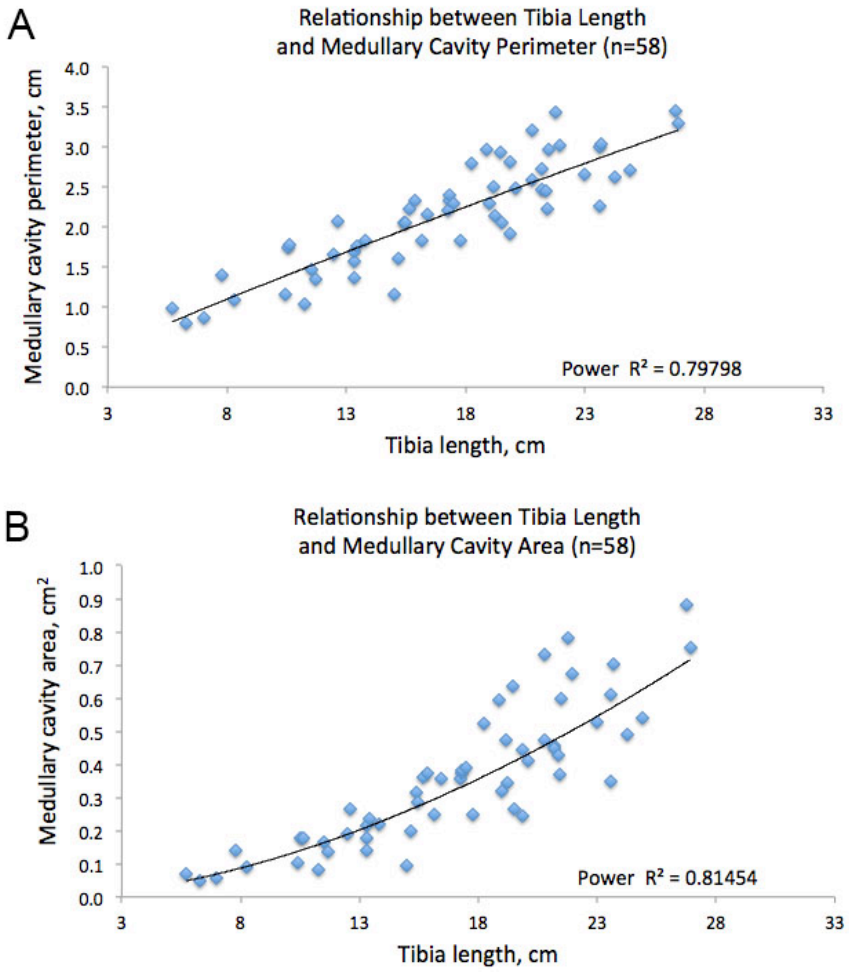


Figure 4.3. Ontogenetic growth curves for ten *P. mongoliensis* individuals. There is an observable body length variation between same-aged individuals. Minimal body growth length occurs in the first year of life. Body length exponentially increases between 2-7 years then gradually decreases. B) Body mass increases in minimal rate during the first 2-3 years, then exponentially increases throughout its life. However, there is an evident bone apposition rate decrease in the later years (after tenth year) of *P. mongoliensis* life (see Table 4.3 and Discussion).

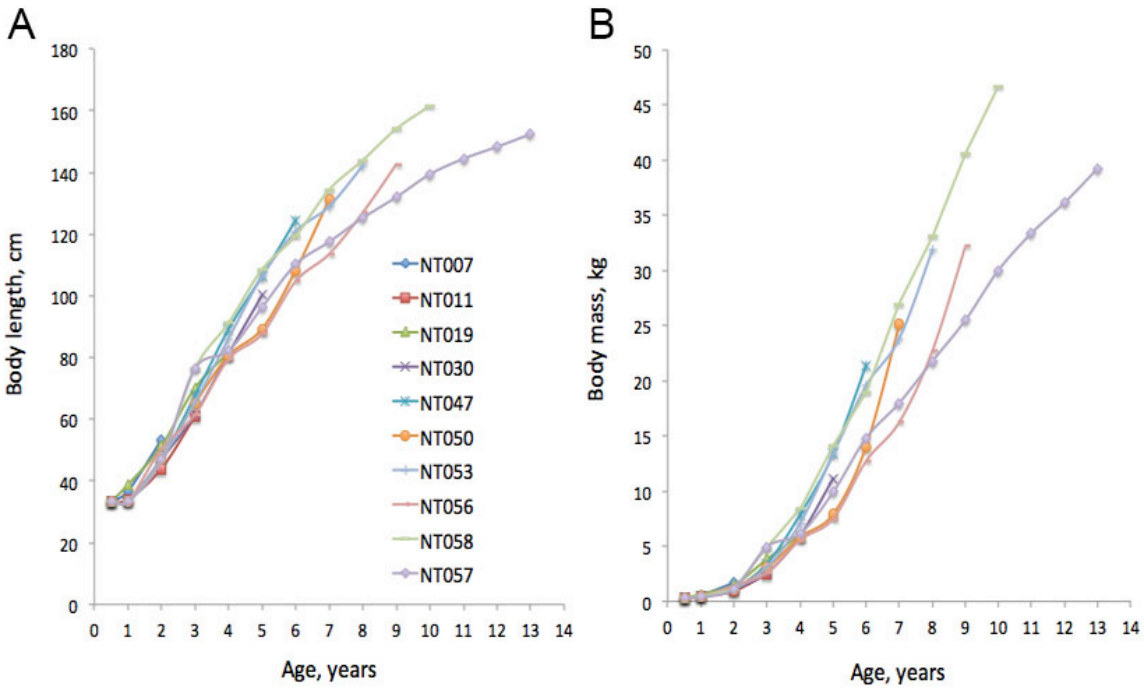


Figure 4.4. Growth curve for *P. mongoliensis*. The growth curve (R^2=0.93) is plotted using a logistic model based on the estimated body mass and relative age. Green dashed line indicates 95% confidence interval.

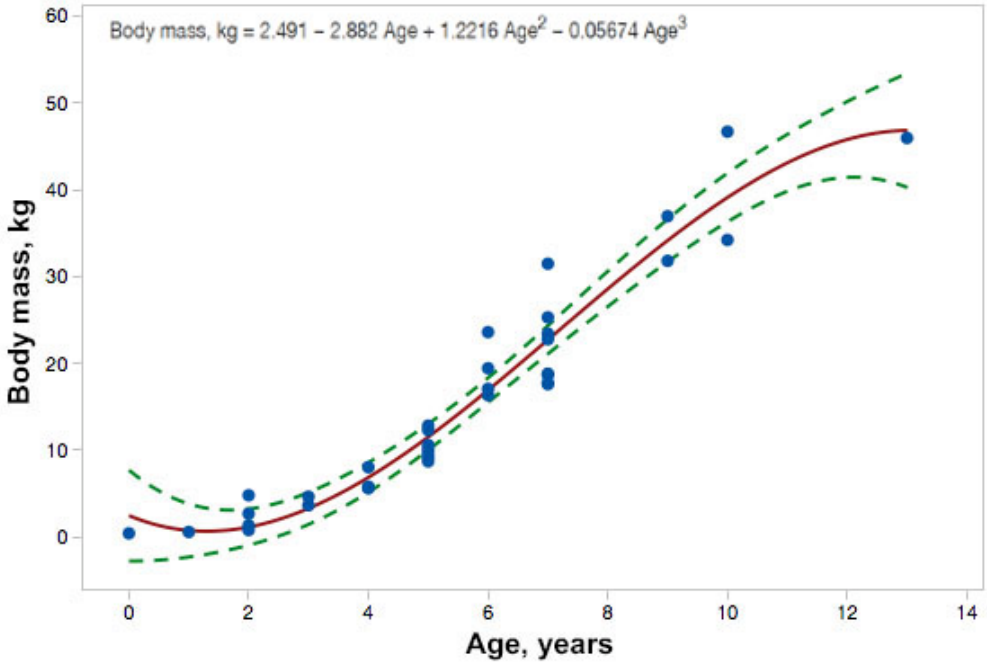


Figure 4.5. Transverse sections from the four *P. mongoliensis* tibiae representing growth Phase A. Upper sides of the sections are orienting to anterior. The lengths of the tibiae range between 5.68 and 8.28 cm. Scale bar equals 5 mm.

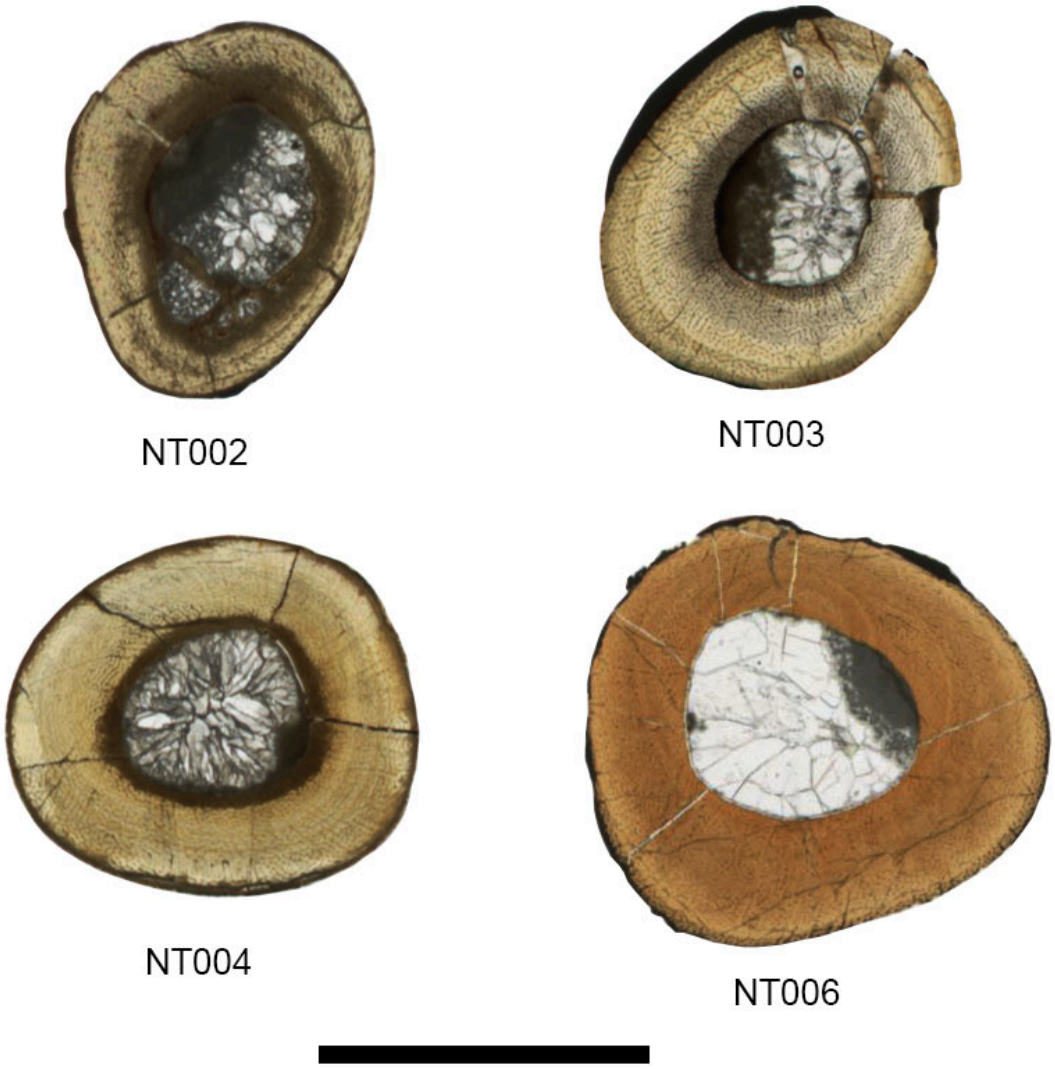


Figure 4.6. Transverse section of the smallest *P. mongoliensis* tibia (NT002) representing growth Phase A in this study. Upper sides of the figures orient to anterior side of the tibia. A) A highly vascularized reticular tissue dominates on the anterior side of the diaphysis of NT002 whereas a longitudinal vascularity is abundant on the posterior side. B) Enlarged view of the red square on A). Tissue composition consists largely of a reticular vascularization with woven matrix. The tissue is observed through full lambda (530nm) plate with polarized light. The scale bar equals 1mm in A), 0.5mm in B).

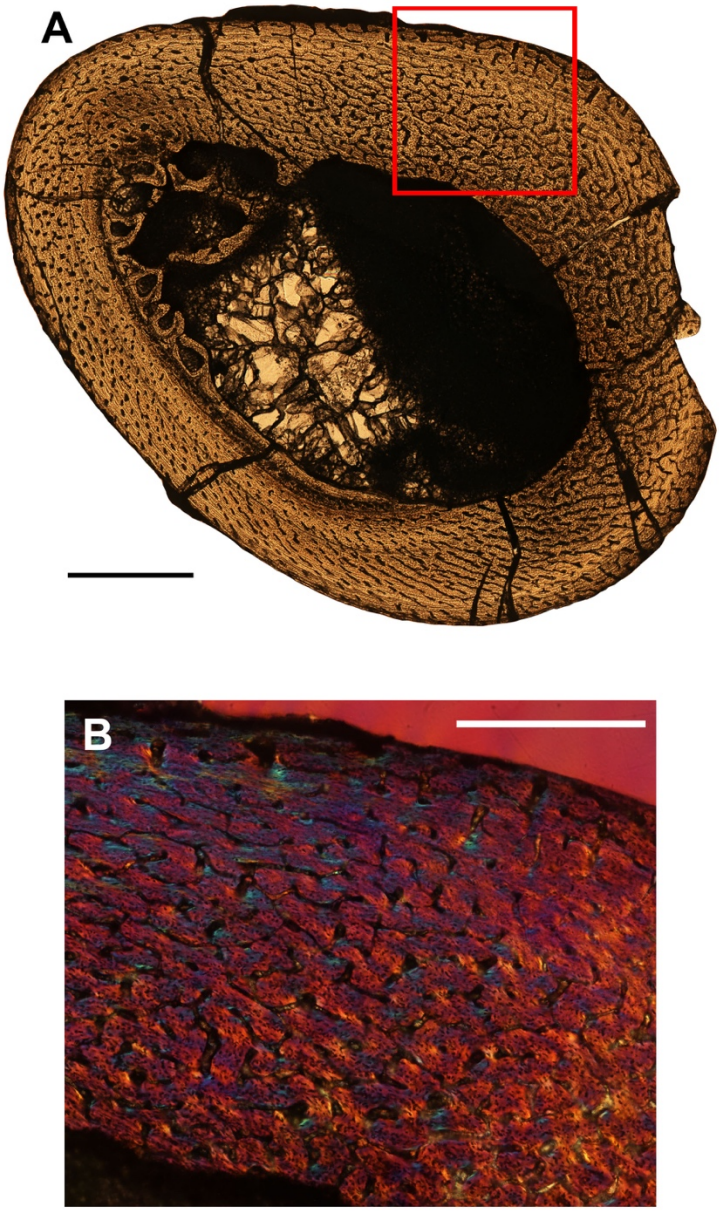


Figure 4.7. Transverse section of the *P. mongoliensis* tibia (NT003) representing growth Phase A. Upper sides of the figures orient to anterior side of the tibia. A) The tissues in the tibia diaphysis consist of a combination of reticular and longitudinal tissues. B) Inner half of the cortex consists of a reticular vascularization with woven matrix. The tissue type changes to parallel-fibered tissue in the outer half of cortex. The tissue is observed through full lambda (530nm) plate with polarized light. Red square indicates an enlarged view from A) showed in B). White arrow points a LAG. The scale bar equals 1mm in A), 0.5mm in B).

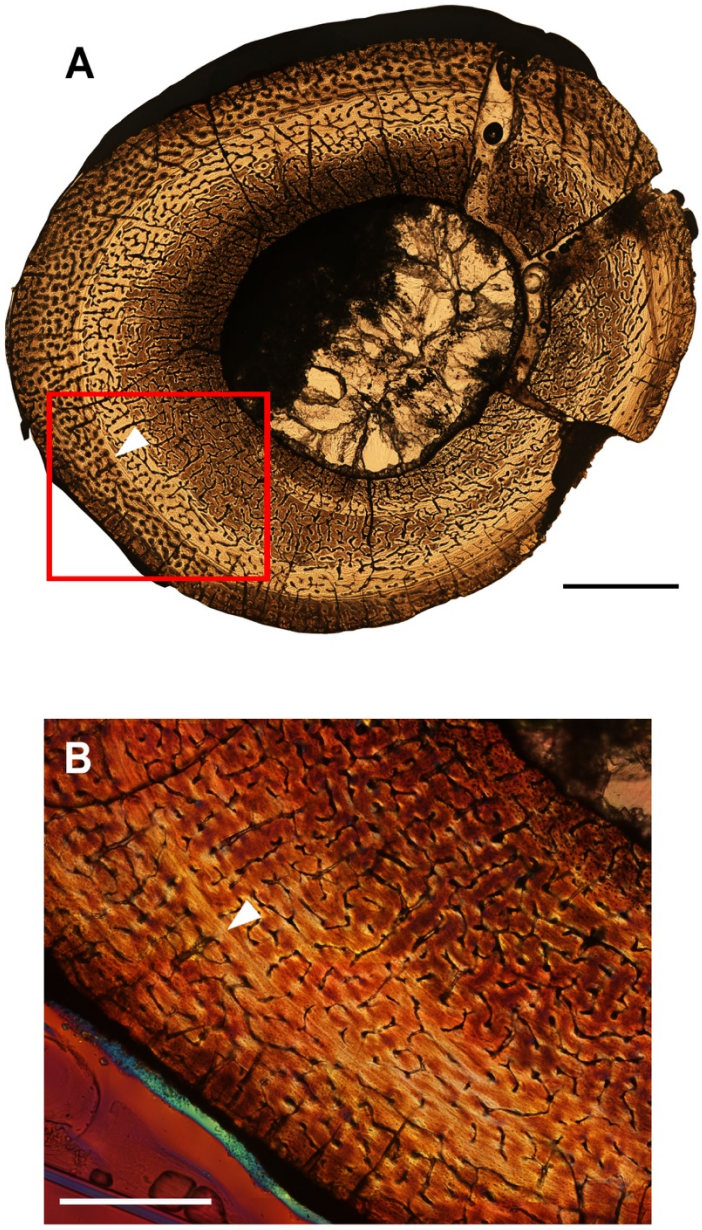


Figure 4.8. Transverse sections from the ten *P. mongoliensis* tibiae representing growth Phase B. Upper sides of the sections are oriented to anterior. The lengths of the tibiae range between 10.41 and 16.15 cm. Scale bar equals 1 cm.

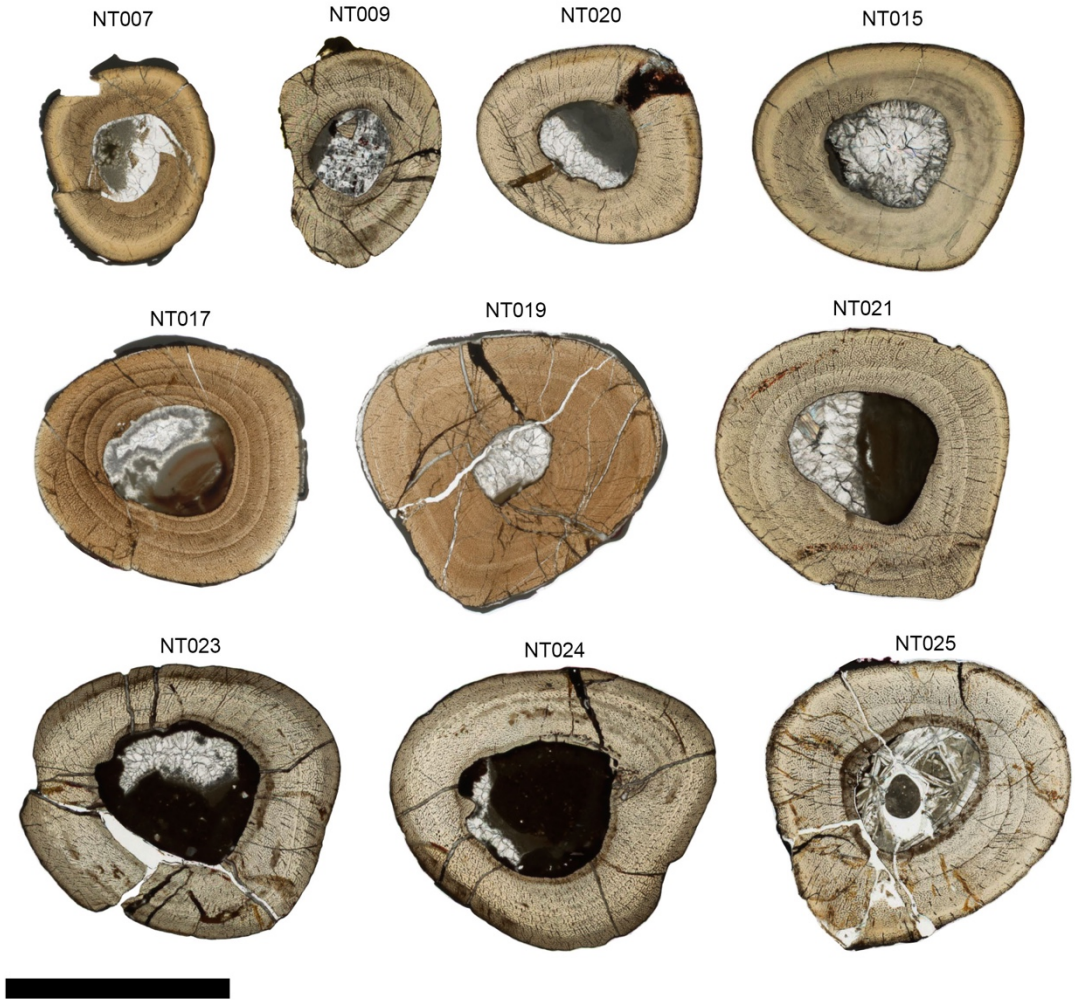


Figure 4.9. Transverse section of the *P. mongoliensis* tibia (NT009) representing growth Phase B. Upper sides of the figures orient to anterior side of the tibia. A) The tissues in the tibia diaphysis consist of a combination of reticular and radial tissues. B) Outer half of the cortex possesses many longer radial canals. The section is observed using polarized light. Red square indicates an enlarged view from A) showed in B). White arrows point LAGs. The scale bars equal 1mm.



Figure 4.10. Transverse section of the *P. mongoliensis* tibia (NT017) representing growth Phase B. Upper sides of the figures orient to anterior side of the tibia. A) The tissues in the tibia diaphysis consist of a combination of reticular and sub-plexiform tissues. B) A reticular tissue occurs innermost cortex, between first and second LAGs. The tissue gradually changes to immature sub-plexiform tissue centrifugally. The section is observed using polarized light. Red square indicates an enlarged view from A) showed in B). White arrows point LAGs. The scale bars equal 1mm.

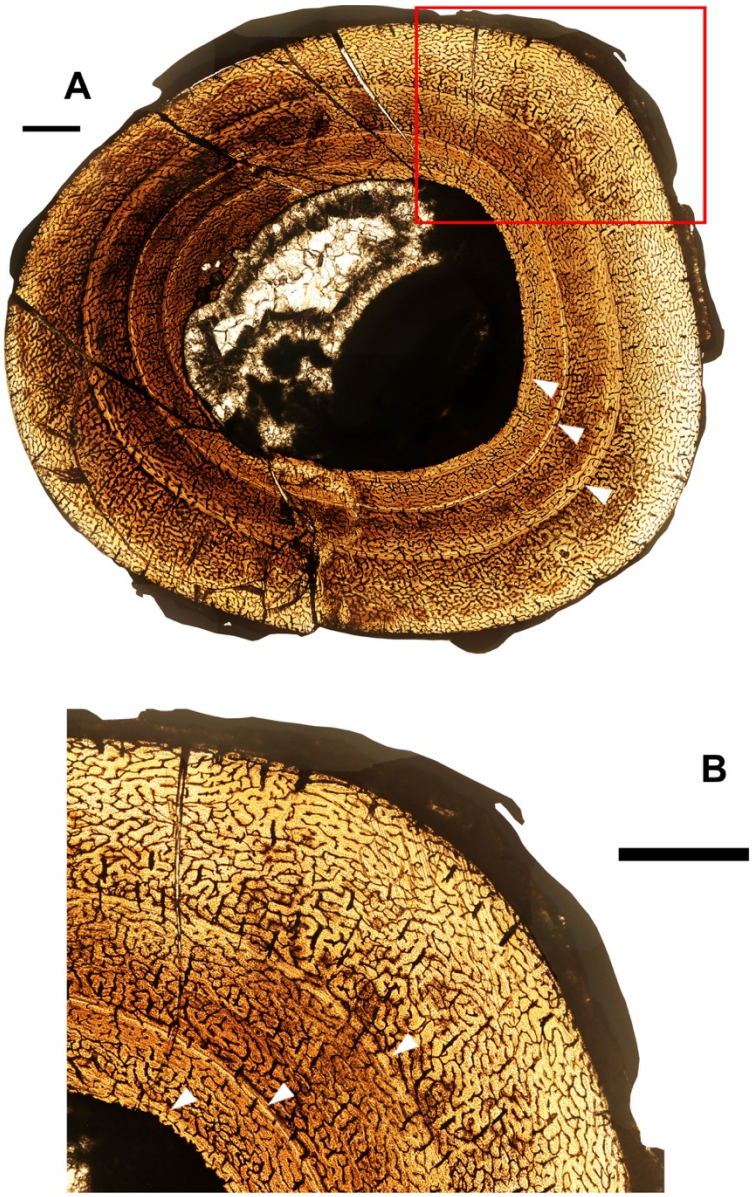


Figure 4.11. Transverse sections from the five *P. mongoliensis* tibiae representing growth Phase C. Upper sides of the sections are oriented to anterior. The lengths of the tibiae range between 16.42 and 17.5 cm. Scale bar equals 1 cm.

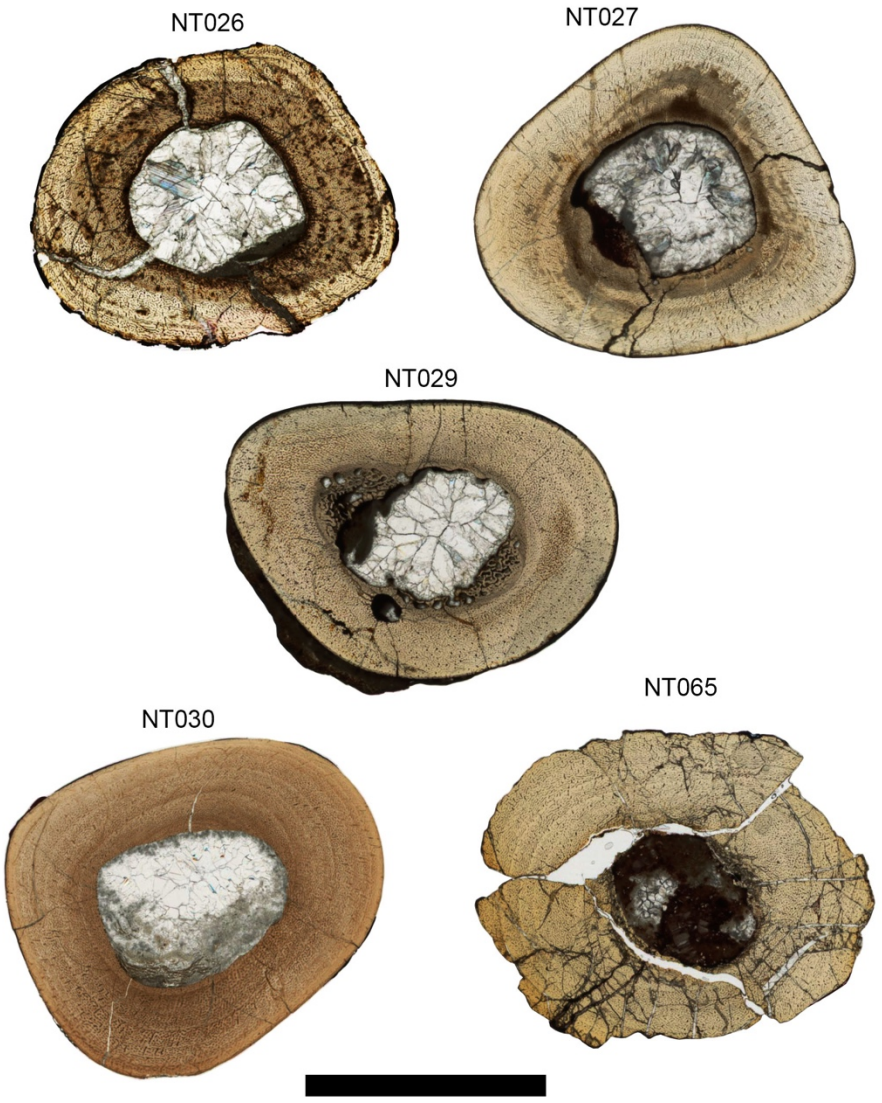


Figure 4.12. Transverse section of the *P. mongoliensis* tibia (NT027) representing growth Phase C. Upper sides of the figures orient to anterior side of the tibia. A) The tissues in the tibia diaphysis consist of a plexiform vascularization. B) The plexiform tissue with parallel-fibered matrix in the outer cortex. The tissue is observed through full lambda (530nm) plate with polarized light. Red square indicates an enlarged view from A) showed in B). White arrows point LAGs. The scale bar equals 1mm in A, 0.5mm in B.

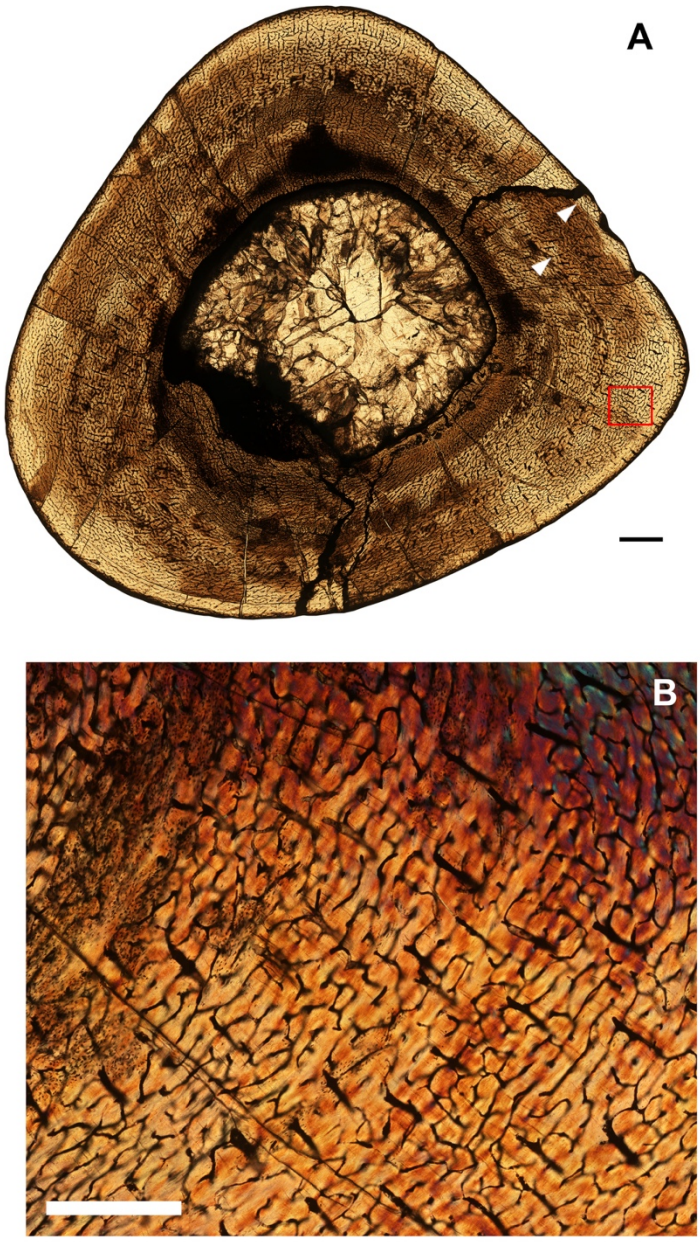


Figure 4.13. Transverse sections from the eighteen *P. mongoliensis* tibiae representing growth Phase D. Upper sides of the sections are oriented to anterior. The lengths of the tibiae range between 18.9 and 26.9 cm. Scale bar equals 1 cm.

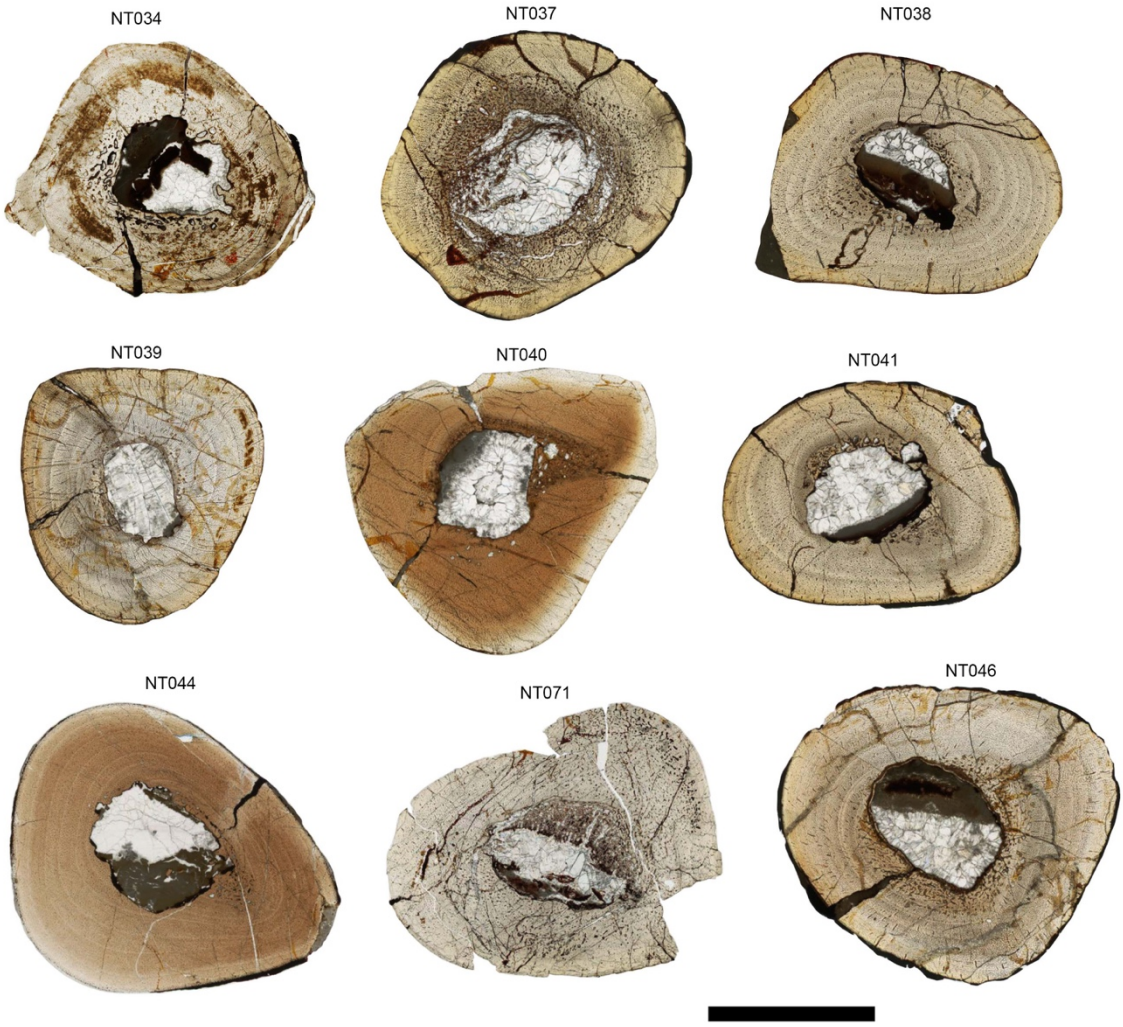


Figure 4.13 continued.

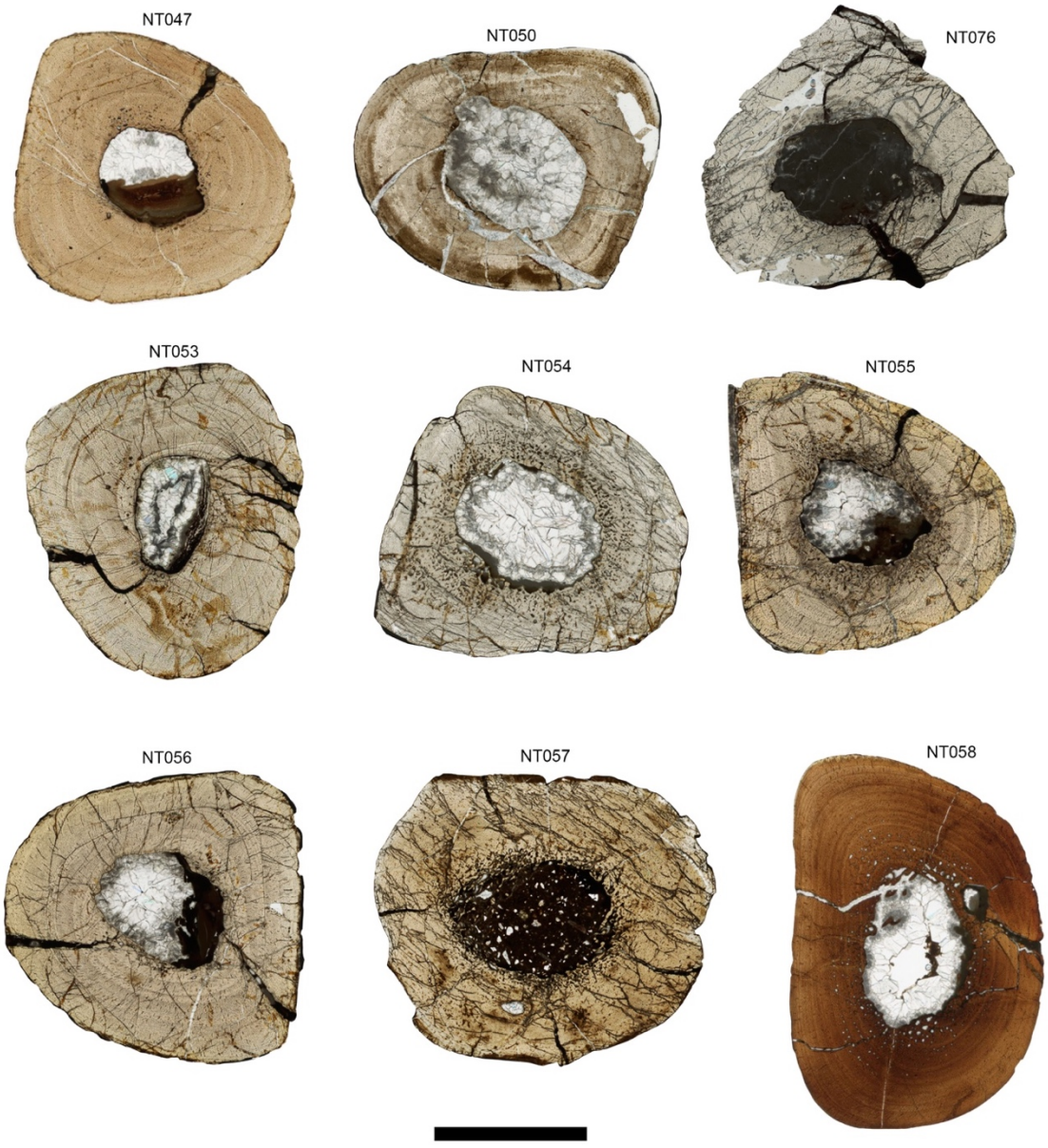


Figure 4.14. Transverse section of the *P. mongoliensis* tibia (NT034) representing growth Phase D. Upper sides of the figures orient to anterior side of the tibia. A) The tibia diaphysis consists of a plexiform tissue. The resorption cavities invaded the inner half of the cortex. B) An abundant number of resorption cavities occur in the inner half of the cortex. Some of the cavities are partially filled with new bone (red circles), starting to form secondary osteons. The section is observed using polarized light. Red square indicates an enlarged view from A) showed in B). White arrows point LAGs. The scale bars equal 1mm

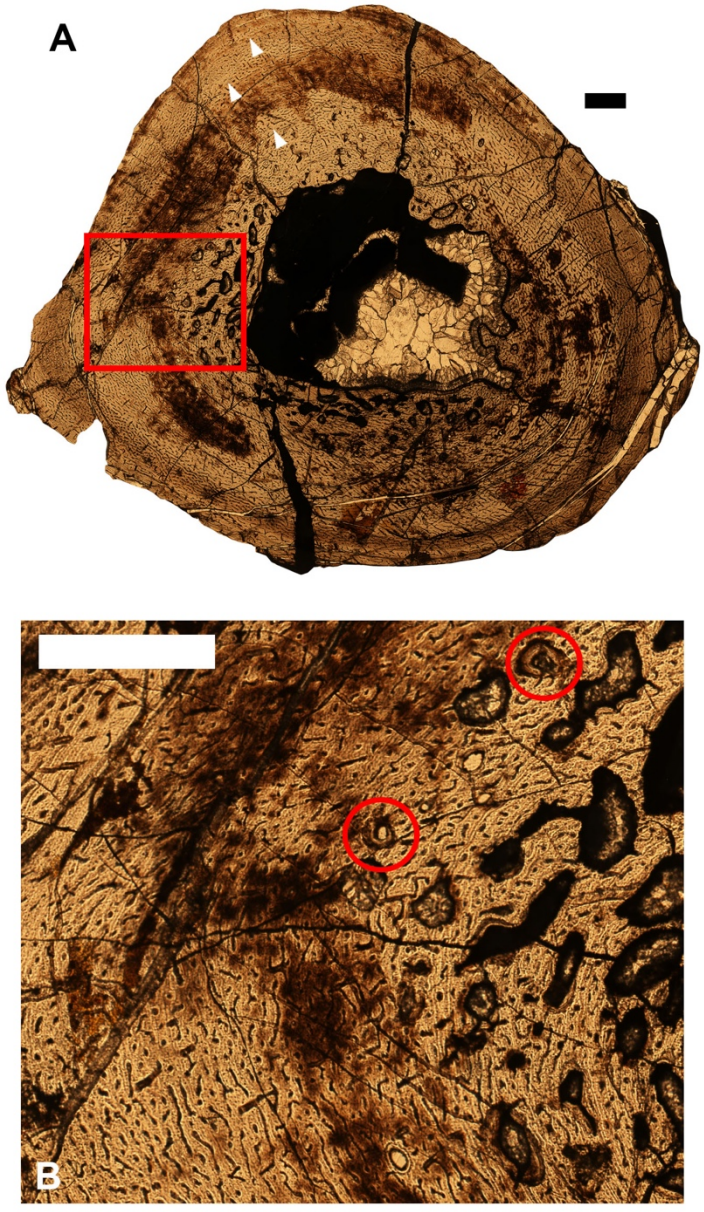


Figure 4.15. Transverse section of the *P. mongoliensis* tibia (NT071) representing growth Phase D. Upper sides of the figures orient to anterior side of the tibia. A) The tibia diaphysis consists of a plexiform tissue. The resorption cavities heavily invaded the anterior and posterior sides of the outer cortex. B) Resorption cavities in outer cortex. Red bracket shows tightly packed growth lines indicating very slowly depositing bone tissue. The section is observed using polarized light. Red square indicates an enlarged view from A) showed in B). The scale bar equals 2 mm in A), 1 mm in B).

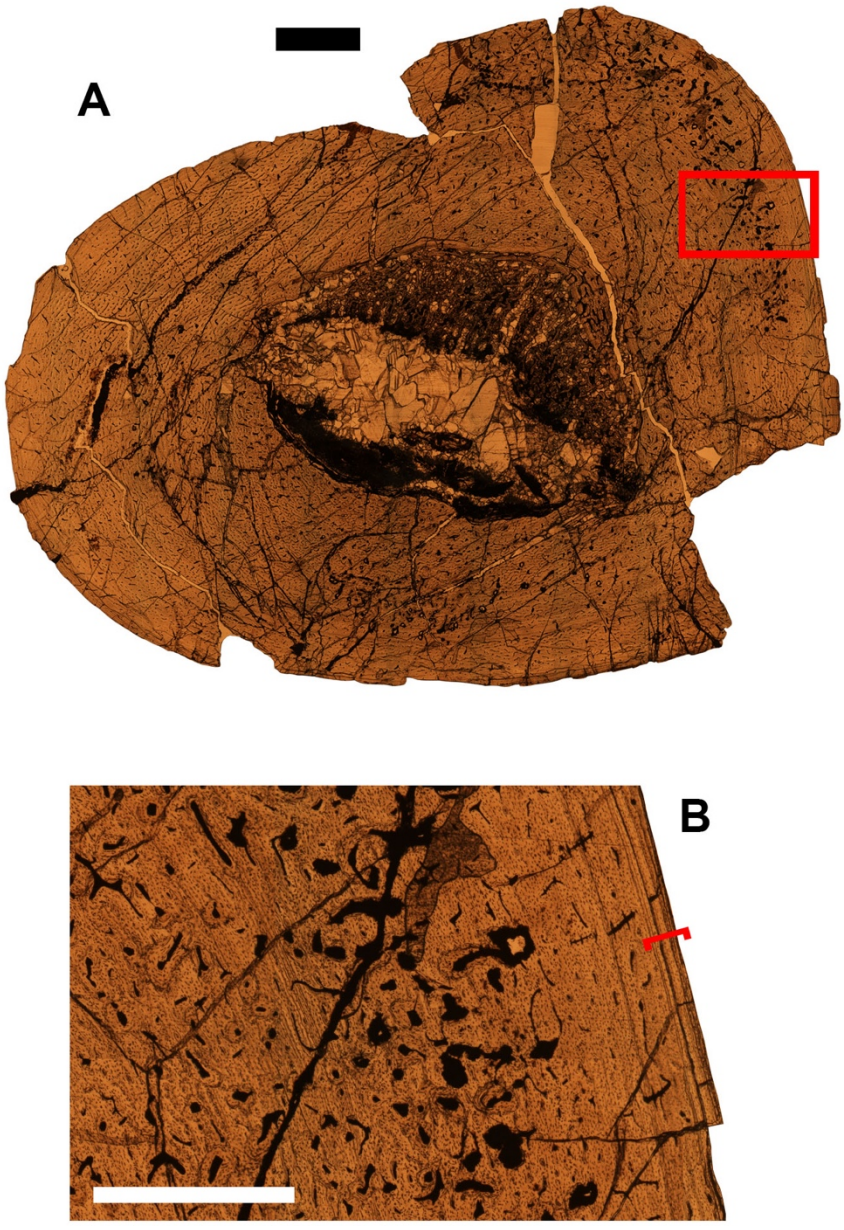
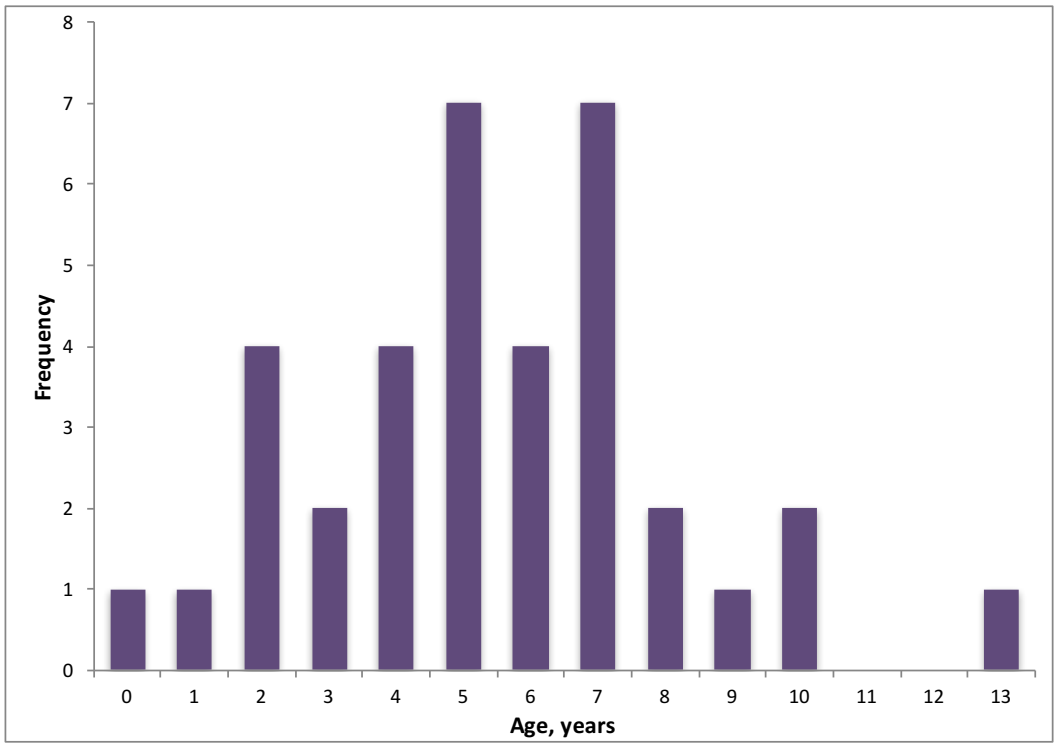


Figure 4.16. An age frequency chart for 36 *P. mongoliensis* individuals. The majority of the sample set consists of the individuals between 2-7 years old. The majority of the sample set consists of the individuals between 2-7 years old. Apparently, the yearlings and older individuals (10 or above) are the rarest. However, there is a complete absence of individuals between 11 and 12 years old.



Literature Cited

Castanet, J., D. G. Newman, and H. S. Girons. 1988. Skeletochronological data on the growth, age, and population structure of the tuatara, *Sphenodon punctatus*, on Stephens and Lady Alice Islands, New Zealand. Herpetologica: 25-37.

Chinsamy, A. 1993. Bone histology and growth trajectory of the prosauropod dinosaur *Massospondylus carinatus* Owen. Modern Geology 18: 319-329.

Chinsamy, A., and A. Tumarkin-Deratzian. 2009. Pathologic bone tissues in a turkey vulture and a nonavian dinosaur: implications for interpreting endosteal bone and radial fibrolamellar bone in fossil dinosaurs. The Anatomical Record 292: 1478-1484.

Cormack, D. 1987. Ham's Histology. 732 pp., Lippincott Williams & Wilkins,, New York.

Curry, K. A. 1999. Ontogenetic histology of *Apatosaurus* (Dinosauria: Sauropoda): new insights on growth rates and longevity. Journal of Vertebrate Paleontology 19: 654-665.

De Margerie, E. 2002. Laminar bone as an adaptation to torsional loads in flapping flight. Journal of Anatomy 201: 521-526.

De Margerie, E., J. P. Robin, D. Verrier, J. Cubo, R. Groscolas, and J. Castanet. 2004. Assessing a relationship between bone microstructure and growth rate: a fluorescent labelling study in the king penguin chick (*Aptenodytes patagonicus*). Journal of Experimental Biology 207: 869-879.

de Ricqlès, A. 1968. Recherches paléohistologiques sur les os longs des tétrapodes: origine du tissu osseux plexiforme des dinosauriens sauropodes. Masson.

de Ricqlès, A. 1972. Recherches paléohistologiques sur les os longs des Tétrapodes: Titanosuchiens, Dinocéphales et Dicynodontes. Masson.

de Ricqlès, A. 1974a. Recherches paléohistologiques sur les os longs des Tétrapodes: Cotylosaures et Mésosaures. Masson.

de Ricqlès, A. 1974b. Recherches paléohistologiques sur les os longs des Tétrapodes: Éothériodontes et Pélycosaures. Masson.

de Ricqlès, A. 1975. Recherches paléohistologiques sur les os longs des Tétrapodes: 7. Sur la classification, la signification fonctionnelle et l'histoire des tissus osseux des Tétrapodes. Masson.

Enlow, D. H., and S. O. Brown. 1956. A Comparative Histological Study of Fossil and Recent Bone Tissues. Part I. The Texas Journal of Science VIII: 405-443.

Enlow, D. H., and S. O. Brown. 1957. A Comparative Histological Study of Fossil and Recent Bone Tissues. Part II. The Texas Journal of Science IX: 186-214.

Erickson, G. M., P. J. Makovicky, B. D. Inouye, C. F. Zhou, and K. Q. Gao. 2009. A Life Table for *Psittacosaurus lujiatunensis*: Initial Insights Into Ornithischian Dinosaur Population Biology (vol 292, pg 1514, 2009). Anatomical Record-Advances in Integrative Anatomy and Evolutionary Biology 292: 1684-1684.

Erickson, G. M., K. C. Rogers, and S. A. Yerby. 2001. Dinosaurian growth patterns and rapid avian growth rates. Nature 412: 429-433.

Erickson, G. M., and T. A. Tumanova. 2000. Growth curve of *Psittacosaurus mongoliensis* Osborn (Ceratopsia : Psittacosauridae) inferred from long bone histology. Zoological Journal of the Linnean Society 130: 551-566.

Francillon-Vieillot, H., V. De Buffrénil, J. Castanet, J. Géraudie, F. J. Meunier, J. Y. Sire, L. Zylberberg, and A. De Ricqlès. 1990. Microstructure and mineralization of vertebrate skeletal tissues; pp. 471-548 *i*n J. G. Carter (ed.), Skeletal biomineralization: patterns, processes and evolutionary trends. Van Nostrand Reinhold, New York.

Gross, W. 1934. Die Typen des mikroskopischen Knochenbaues bei fossilen Stegoccphalen und Reptilien. Anatomy and Embryology 103: 731-764.

Horner, J. R., A. de Ricqles, and K. Padian. 1999. Variation in dinosaur skeletochronology indicators: implications for age assessment and physiology. Paleobiology 25: 295-304.

Horner, J. R., A. de Ricqles, and K. Padian. 2000. Long bone histology of the hadrosaurid dinosaur *Maiasaura peeblesorum*: growth dynamics and physiology based on an ontogenetic series of skeletal elements. Journal of Vertebrate Paleontology 20: 115-129.

Hu, Y., J. Meng, Y. Wang, and C. Li. 2005. Large Mesozoic mammals fed on young dinosaurs. Nature 433: 149-152.

Klein, N., and M. Sander. 2008. Ontogenetic stages in the long bone histology of sauropod dinosaurs. Paleobiology 34: 247-263.

Klein, N., T. Scheyer, and T. Tütken. 2009. Skeletochronology and isotopic analysis of a captive individual of *Alligator mississippiensis* Daudin, 1802. Fossil Record 12: 121-131.

Lamm, E.-T. 2013. Preparation and sectioning of specimens. Bone histology of fossil tetrapods: advancing methods, analysis, and interpretation: 55-160.

Mantell, G. A. 1850. On the Pelorosaurus; An Undescribed Gigantic Terrestrial Reptile Whose Remains are Associated with Those of the Iguanodon and Other Saurians in the Strata of Tilgate Forest, in Sussex. Philosophical Transactions of the Royal Society of London 140: 379-390.

Meng, Q., J. Liu, D. J. Varricchio, T. Huang, and C. Gao. 2004. Palaeontology: Parental care in an ornithischian dinosaur. Nature 431: 145-146.

Myhrvold, N. P. 2013. Revisiting the estimation of dinosaur growth rates. PloS one 8: e81917.

Nopcsa, F. B. 1933: 11. On the Histology of the Ribs in Immature and Half-grown Trachodont Dinosaurs. Paper presented at the Proceedings of the Zoological Society of London, 1933.

Pelletier, F., and M. Festa-Bianchet. 2004. Effects of body mass, age, dominance and parasite load on foraging time of bighorn rams, *Ovis canadensis*. Behavioral Ecology and Sociobiology 56: 546-551.

Ponton, F., A. Elżanowski, J. Castanet, A. Chinsamy, E. De Margerie, A. De Ricqlès, and J. Cubo. 2004. Variation of the outer circumferential layer in the limb bones of birds. Acta Ornithologica 39: 137-140.

Reid, R. H. 1981. Lamellar-zonal bone with zones and annuli in the pelvis of a sauropod dinosaur. Nature 292: 49-51.

Sander, P. M. 2000. Longbone histology of the Tendaguru sauropods: implications for growth and biology. Paleobiology 26: 466-488.

Seitz, A. L. L. 1907. Vergleichende Studien über den mikroskopischen Knochenbau fossiler und rezenter Reptilien und dessen Bedeutung für das Wachstum und Umbildung des Knochengewebes im allgemein. E. Karras.

Sereno, P. C., Z. Xijin, and T. Lin. 2009. A new psittacosaur from Inner Mongolia and the parrot-like structure and function of the psittacosaur skull. Proceedings of the Royal Society B: Biological Sciences.

Turner, A. H., S. H. Hwang, and M. A. Norell. 2007. A small derived Theropod from Oosh, Early Cretaceous, Baykhangor Mongolia. American Museum Novitates 3557: 1-27.

Werning, S. 2012. The ontogenetic osteohistology of *Tenontosaurus tilletti*. PloS one 7: e33539.

Woodward, H. N., E. A. F. Fowler, J. O. Farlow, and J. R. Horner. 2015. *Maiasaura*, a model organism for extinct vertebrate population biology: a large sample statistical assessment of growth dynamics and survivorship. Paleobiology 41: 503-527.

Woodward, H. N., J. R. Horner, and J. O. Farlow. 2011. Osteohistological Evidence for Determinate Growth in the American Alligator. Journal of Herpetology 45: 339-342.

Zhao, Q., M. J. Benton, C. Sullivan, P. M. Sander, and X. Xu. 2013a. Histology and postural change during the growth of the ceratopsian dinosaur *Psittacosaurus lujiatunensis*. Nature communications 4.

Zhao, Q., M. J. Benton, X. Xu, and P. M. Sander. 2013b. Juvenile-only clusters and behaviour of the Early Cretaceous dinosaur *Psittacosaurus*. Acta Palaeontologica Polonica 59: 827-833.

CHAPTER FIVE

CONCLUSIONS

Taphonomic modes dictate the preservation of vertebrate fossils. *Psittacosaurus* fossils have been known mostly from basin margin, lacustrine-margin, and volcanigenic deposits (Brinkman et al., 2001; Zhao et al., 2007; Eberth, 2010; Ford and Martin, 2010; Sereno, 2010). However, the Lujiatun Bed in China was determined to represent a volcaniclastic deposit in an alluvial setting consisting of a debris flow, hyperconcentrated flow, stream and sheet-flood, and lahar deposit composed of volcaniclastic sediments. The sedimentologic and taphonomic data suggest the Builst Khudag (BLK) bonebed was formed in an alluvial setting by debris flows and sheet-flood deposit. Apparently, the sheet-flood deposits in the alluvial setting tend to preserve articulated and three-dimensional psittacosaur fossils; whereas flattened (two-dimensional) fossils are mostly found in lacustrine deposits (Meng et al., 2004; Xing and Norell, 2006). The juvenile *Psittacosaurus* aggregation from the BLK bonebed broadens the age spectrum of juvenile clusters up to the age of five. However, the range of body sizes of the juvenile aggregation from the BLK site is larger than those found in the Lujiatun Bed reflecting a possible taxon-specific growth rate in *P. mongoliensis*.

The ideal choice of bone for the dinosaur growth assessment is still unclear. However, the femur and tibia were suggested to be the best skeletal elements for the histologic analyses due their low remodeling rates (Horner et al., 1999). Previously, the humerus, femur, tibia, and fibula were utilized to determine the growth dynamics of

Psittacosaurus. Since there is a considerable amount of histologic variation between skeletal elements from a single individual (Horner et al., 1999), using a sample set consisting of different bones from each specimen may obscure growth patterns. A comparative histologic analysis of the associated femora, tibiae, and fibulae from four *Psittacosaurus* individuals revealed that the tibia is the ideal element for both the tissue typing and skeletochronology in *Psittacosaurus*.

Determining dinosaur growth strategies at the population level requires larger sample sizes in which each individual is represented by the same bone. Most of the growth studies on various dinosaur taxa have used a very limited number of specimens or multitude of skeletal elements (Erickson and Tumanova, 2000). Since the tibia is the best for both tissue typing and skeletochronology, a large sample set consisting of tibiae from the BLK locality was used for this *Psittacosaurus* growth analysis. This study revealed that there is a considerable amount of histologic variation between similar sized *Psittacosaurus* tibiae. The *P. mongoliensis* growth rate began at a high rate but slowed after the age of ten. Between the ages of 10 and 13, the body size reached 170.3 cm in length and 46.6 kg in mass. Since there was no positively identified External Fundamental System (EFS) in the *P. mongoliensis* specimens of this study, the growth of the *P. mongoliensis* individuals still grew at a very slow rate after the age of ten. However, considerable change in the development of bone tissue was observed in all individuals aged ten and above, and may indicate the initiation of skeletal maturity.

Lastly, prior to conducting a population level growth analysis, it is necessary to examine the histology of multiple elements in order to determine the ideal bone for tissue

typing and relative age assessment. A larger sample size of the same skeletal element is necessary to reduce the influence of variations between bones in the skeleton. Moreover, the specimens must be collected from the same stratigraphic level reflecting a population that lived in the same time period. Dinosaur growth research based on the aforementioned fundamental studies will enable to construction of robust and comprehensive growth curves for any dinosaur taxon.

Literature Cited

Brinkman, D. B., D. A. Eberth, M. Ryan, and P. Chen. 2001. The occurrence of *Psittacosaurus xinjiangensis* Sereno and Chow, 1988 in the Urho area, Junggar Basin, Xinjiang, People's Republic of China. Canadian Journal of Earth Sciences 38: 1781-1786.

Eberth, D. A. 2010. A review of ceratopsian paleoenvironmental associations and taphonomy. New perspectives on horned dinosaurs. Edited by MJ Ryan, BJ Chinnery-Allgeier, and DA Eberth. Indiana University Press, Bloomington, IN: 428-446.

Erickson, G. M., and T. A. Tumanova. 2000. Growth curve of *Psittacosaurus mongoliensis* Osborn (Ceratopsia : Psittacosauridae) inferred from long bone histology. Zoological Journal of the Linnean Society 130: 551-566.

Ford, T. L., and L. D. Martin. 2010: A semi-aquatic life habit for *Psittacosaurus*. Paper presented at the New Perspectives on Horned Dinosaurs: The Royal Tyrrell Museum Ceratopsian Symposium, 2010.

Horner, J. R., A. de Ricqles, and K. Padian. 1999. Variation in dinosaur skeletochronology indicators: implications for age assessment and physiology. Paleobiology 25: 295-304.

Meng, Q., J. Liu, D. J. Varricchio, T. Huang, and C. Gao. 2004. Palaeontology: Parental care in an ornithischian dinosaur. Nature 431: 145-146.

Sereno, P. C. 2010: Taxonomy, cranial morphology, and relationships of parrot-beaked dinosaurs (Ceratopsia: *Psittacosaurus*). Paper presented at the New perspectives on horned dinosaurs: The Royal Tyrrell Museum ceratopsian symposium, 2010.

Xing, X., and M. A. Norell. 2006. Non-avian dinosaur fossils from the Lower Cretaceous Jehol Group of western Liaoning, China. Geological Journal 41: 419-437.

Zhao, Q., P. M. Barrett, and D. A. Eberth. 2007. Social behaviour and mass mortality in the basal ceratopsian dinosaur *Psittacosaurus* (Early Cretaceous, People's Republic of China). Palaeontology 50: 1023-1029.

REFERENCES CITED

Alifanov, V. R. 2008. The tiny horned dinosaur *Gobiceratops minutus* gen. et sp. nov.(Bagaceratopidae, Neoceratopsia) from the Upper Cretaceous of Mongolia. Paleontological Journal 42: 621-633.

Alifanov, V. R., and R. Barsbold. 2009. *Ceratonykus oculatus* gen. et sp. nov., a new dinosaur (? Theropoda, Alvarezsauria) from the Late Cretaceous of Mongolia. Paleontological Journal 43: 94-106.

Averianov, A. O., A. V. Voronkevich, S. V. Leshchinskiy, and A. V. Fayngertz. 2006. A ceratopsian dinosaur *Psittacosaurus sibiricus* from the Early Cretaceous of West Siberia, Russia and its phylogenetic relationships. Journal of Systematic Palaeontology 4: 359-395.

Bagnold, R. A. 1956. The flow of cohesionless grains in fluids. Philosophical Transactions of the Royal Society of London A: Mathematical, Physical and Engineering Sciences 249: 235-297.

Bakker, R. T. 1986. The Dinosaur Heresies, New Theories Unlocking the Mystery of the Dinosaurs and Their Extinction. William Morrow and Co., New York.

Ballance, P. F. 1984. Sheet-flow-dominated gravel fans of the non-marine middle Cenozoic Simmler Formation, central California. Sedimentary Geology 38: 337-359.

Barrett, P. M., and X.-L. Wang. 2007. Basal titanosauriform (Dinosauria, Sauropoda) teeth from the lower cretaceous Yixian formation of liaoning province, China. Palaeoworld 16: 265-271.

Barsbold, R. 1974. Duel of Dinosaurs. Pryroda 2: 81-83.

Barsbold, R. 1979. Opisthopubic pelvis in the carnivorous dinosaurs. Nature 279: 792-793.

Barsbold, R. 1981. Toothless carnivorous dinosaurs of Mongolia. Trudy Sovmestnoi Sovetsko-Mongol'skoi Paleontologicheskoi Ekspeditsii 15: 28-39.

Barsbold, R. 1983. Carnivorous dinosaurs of the Cretaceous of Mongolia. Trudy Sovmestnoi Sovetsko-Mongol'skoi Paleontologicheskoi Ekspeditsii. 13: 50-112.

Barsbold, R. 1986. Raubdinosaurier Oviraptoren. Herpetologische Untersuchungen in der Mongolischen Volksrepublik: 210-223.

Barsbold, R. 1988. A new Late Cretaceous ornithomimid from the Mongolian People's Republic. Paleontological Journal 1: 124-127.

Barsbold, R. 1997. Mongolian dinosaurs; pp. 447-450 *i*n P. J. Currie, and K. Padian (eds.), The encyclopedia of dinosaurs. Academic Press., San Diego.

Barsbold, R. 1998. Fighting dinosaurs—they really fought: In *Encontro Internacional sobre Paleobiologia dos Dinossáurios: Programa de Musealização para Pistas de Dinossáurios em Portugal*, C. M. de Carvalho AMG, Andrade AMPSAF, da Silva CAPFM, dos Santos VAF ed, pp. 74-78. Museu Nacional de História Natural, Lisbon, Portugal.

Barsbold, R., H. Osmólska, M. Watabe, P. J. Currie, and K. Tsogtbaatar. 2000. A new oviraptorosaur [Dinosauria, Theropoda] from Mongolia: the first dinosaur with a pygostyle. Acta Palaeontologica Polonica 45: 97-106.

Barsbold, R., and A. Perle. 1984. On first finding of primitive ornithomimosauria from the Cretaceous of the MPR (Mongolian Peoples-Republic). Paleontologicheskiy Zhurnal: 121-123.

Batalla, R. J., C. De Jong, P. Ergenzinger, and M. Sala. 1999. Field observations on hyperconcentrated flows in mountain torrents. Earth Surface Processes and Landforms 24: 247-253.

Behrensmeyer, A. K. 1975. The taphonomy and paleoecology of Plio-Pleistocene vertebrate assemblages East of Lake Rudolph, Kenya. Bull. Mus. Compar. Zool., Harvard Univ 146: 473-578.

Behrensmeyer, A. K. 1978. Taphonomic and ecologic information from bone weathering. Paleobiology: 150-162.

Berkey, C. P., and F. K. Morris. 1927. Geology of Mongolia; pp. 456, Central Asiatic Expeditions. American Museum of the Natural History, New York.

Beverage, J. P., and J. K. Culbertson. 1964. Hyperconcentrations of suspended sediment. Journal of Hydraulic Div., ASCE 90: 117-128.

Blair, T. C. 1987. Sedimentary processes, vertical stratification sequences, and geomorphology of the Roaring River alluvial fan, Rocky Mountain National Park, Colorado. Journal of Sedimentary Research 57.

Bochkov, S. V. 1986. Geological report No.4276. Ministry of Geology, USSR.

Bohlin, B. 1953. Fossil reptiles from Mongolia and Kansu. Rep. Sino-Swedish Expedition Publication 37: 113.

Bouvier, M., and W. L. Hylander. 1996. The mechanical or metabolic function of secondary osteonal bone in the monkey *Macaca fascicularis*. Archives of oral biology 41: 941-950.

Bratseva, G. M., and I. M. Novodvorskaya. 1975. Spore and pollen from the Early Cretaceous Khuren Dukh locality. Trudy Sovmetstnoi Sovetsko-Mongol'skoi Paleontologicheskoya Ekspeditsii. 2: 205-209.

Bratseva, G. M., and I. M. Novodvorskaya. 1976. Burial conditions of Early Cretaceous fauna and flora in the localities of Builyasutuin-Khuduk and Anda-Khuduk. Trudy Sovmetstnoi Sovetsko-Mongol'skoi Paleontologicheskoya Ekspeditsii. 3: 285-290.

Brinkman, D. B., D. A. Eberth, M. Ryan, and P. Chen. 2001. The occurrence of *Psittacosaurus xinjiangensis* Sereno and Chow, 1988 in the Urho area, Junggar Basin, Xinjiang, People's Republic of China. Canadian Journal of Earth Sciences 38: 1781-1786.

Brown, B. B., and E. M. Schlaikjer. 1940. The structure and relationships of *Protoceratops*. Transactions of the New York Academy of Sciences 2: 99-100.

Brusatte, S. L., T. D. Carr, G. M. Erickson, G. S. Bever, and M. A. Norell. 2009. A long-snouted, multihorned tyrannosaurid from the Late Cretaceous of Mongolia. Proceedings of the National Academy of Sciences 106: 17261-17266.

Bull, W. B. 1972. Recognition of alluvial fan deposits in the stratigraphic record.

Carter, D. R. 1984. Mechanical loading histories and cortical bone remodeling. Calcified tissue international 36: S19-S24.

Castanet, J., D. G. Newman, and H. S. Girons. 1988. Skeletochronological data on the growth, age, and population structure of the tuatara, *Sphenodon punctatus*, on Stephens and Lady Alice Islands, New Zealand. Herpetologica: 25-37.

Charig, A. J., and A. C. Milner. 1986. *Baryonyx*, a remarkable new theropod dinosaur. Nature 324: 359-361.

Charig, A. J., and A. C. Milner. 1997. *Baryonyx walkeri*, a fish-eating dinosaur from the Wealden of Surrey. Bulletin - Natural History Museum Geology Series 53: 11-70.

Chen, P. J. 1987. Cretaceous paleogeography in China. Palaeogeography, Palaeoclimatology, Palaeoecology 59: 49-56.

Chiappe, L. M., M. A. Norell, and J. M. Clark. 1998. The skull of a relative of the stem-group bird *Mononykus*. Nature 392: 275-278.

Chiba, K., M. J. Ryan, D. R. Braman, D. A. Eberth, E. E. Scott, C. M. Brown, Y. Kobayashi, and D. C. Evans. 2015. Taphonomy of a Monodominant *Centrosaurus apertus* (Dinosauria: Ceratopsia) Bonebed from the Upper Oldman Formation of Southeastern Alberta. Palaios 30: 655-667.

Chinsamy, A. 1993. Bone histology and growth trajectory of the prosauropod dinosaur *Massospondylus carinatus* Owen. Modern Geology 18: 319-329.

Chinsamy, A. 1994. Dinosaur bone histology: implications and inferences.; pp. 213-227 *i*n D. Rosenberg, and D. L. Wolberg (eds.), Dino Fest. The Paleontological Society Special Publication No. 7.

Chinsamy, A., and A. Tumarkin-Deratzian. 2009. Pathologic bone tissues in a turkey vulture and a nonavian dinosaur: implications for interpreting endosteal bone and radial fibrolamellar bone in fossil dinosaurs. The Anatomical Record 292: 1478-1484.

Clark, J. M., M. A. Norell, and R. Barsbold. 2001. Two new oviraptorids (Theropoda: Oviraptorosauria), Upper Cretaceous Djadokhta Formation, Ukhaa Tolgod, Mongolia. Journal of Vertebrate Paleontology 21: 209-213.

Colbert, E. H. 1961. Dinosaurs: their discovery and their world. New York, Dutton [1961].

Colbert, E. H. 1965. The Age of Reptiles. Weidenfeld & Nicolson, London.

Colbert, E. H. 2000. Asiatic dinosaur rush; pp. 211-234 *i*n M. J. Benton, M. A. Shishkin, D. M. Unwin, and E. N. Kurochkin (eds.), The age of dinosaurs in Russia and Mongolia. Cambridge University Press.

Cormack, D. 1987. Ham's Histology. 732 pp., Lippincott Williams & Wilkins,, New York.

Currey, J. 1984. Comparative mechanical properties and histology of bone. American Zoologist 24: 5-12.

Currie, P., D. Badamgarav, and E. Koppelhus. 2003. The first Late Cretaceous footprints from the Nemegt locality in the Gobi of Mongolia. Ichnos 10: 1-13.

Currie, P. J. 1997. Gastroliths; pp. 270 *i*n P. J. Currie, and K. Padian (eds.), Encyclopedia of Dinosaurs. Academic Press, San Diego.

Curry, K. A. 1999. Ontogenetic histology of *Apatosaurus* (Dinosauria: Sauropoda): New insights on growth rates and longevity. Journal of Vertebrate Paleontology 19: 654-665.

Dasgupta, P. 2006. Facies characteristics of Talchir Formation, Jharia Basin, India: implications for initiation of Gondwana sedimentation. Sedimentary Geology 185: 59-78.

Dashzeveg, D., M. J. Novacek, M. A. Norell, J. M. Clark, L. M. Chiappe, A. Davidson, M. C. McKenna, L. Dingus, C. Swisher, and P. Altangerel. 1995. Extraordinary preservation in a new vertebrate assemblage from the Late Cretaceous of Mongolia. Nature 374: 446-449.

De Margerie, E. 2002. Laminar bone as an adaptation to torsional loads in flapping flight. Journal of Anatomy 201: 521-526.

De Margerie, E., J. P. Robin, D. Verrier, J. Cubo, R. Groscolas, and J. Castanet. 2004. Assessing a relationship between bone microstructure and growth rate: a fluorescent labelling study in the king penguin chick (*Aptenodytes patagonicus*). Journal of Experimental Biology 207: 869-879.

de Ricqlès, A. 1968. Recherches paléohistologiques sur les os longs des tétrapodes: origine du tissu osseux plexiforme des dinosauriens sauropodes. Masson.

de Ricqlès, A. 1972. Recherches paléohistologiques sur les os longs des Tétrapodes: Titanosuchiens, Dinocéphales et Dicynodontes. Masson.

de Ricqlès, A. 1974a. Recherches paléohistologiques sur les os longs des Tétrapodes: Cotylosaures et Mésosaures. Masson.

de Ricqlès, A. 1974b. Recherches paléohistologiques sur les os longs des Tétrapodes: Éothériodontes et Pélycosaures. Masson.

de Ricqlès, A. 1975. Recherches paléohistologiques sur les os longs des Tétrapodes: 7. Sur la classification, la signification fonctionnelle et l'histoire des tissus osseux des Tétrapodes. Masson.

Devyatkin, E. V., T. V. Nikolaeva, and V. F. Shuvalov. 1990. [Structural geomorphological position and main stages of activity of the basalt magmatism in Mongolia in Mesozoic and Cenozoic]; pp. 126-134, Geodynamics of Intercontinental Mountain Regions. Nauka, Novosibirsk.

Dodson, P. 1976. Quantitative aspects of relative growth and sexual dimorphism in *Protoceratops*. Journal of Paleontology: 929-940.

Eberth, D. 1993. Depositional environments and fades transitions of dinosaur-bearing Upper Cretaceous redbeds at Bayan Mandahu (Inner Mongolia, People's Republic of China). Canadian Journal of Earth Sciences 30: 2196-2213.

Eberth, D. A. 2010. A review of ceratopsian paleoenvironmental associations and taphonomy. New perspectives on horned dinosaurs. Edited by MJ Ryan, BJ Chinnery-Allgeier, and DA Eberth. Indiana University Press, Bloomington, IN: 428-446.

Eberth, D. A., M. Shannon, and B. G. Noland. 2010. A Bonebeds Database: Classification, Biases, and Patterns of Occurrence. Bonebeds: Genesis, analysis, and paleobiological significance: 103.

Elzanowski, A. 1983. Birds in Cretaceous ecosystems. Acta Palaeontologica Polonica 28: 75-92.

Enlow, D. H. 1962. Functions of the haversian system. American Journal of Anatomy 110: 269-305.

Enlow, D. H., and S. O. Brown. 1956. A Comparative Histological Study of Fossil and Recent Bone Tissues. Part I. The Texas Journal of Science VIII: 405-443.

Enlow, D. H., and S. O. Brown. 1957. A Comparative Histological Study of Fossil and Recent Bone Tissues. Part II. The Texas Journal of Science IX: 186-214.

Erickson, G. M., and C. A. Brochu. 1999. How the 'terror crocodile' grew so big. Nature 398: 205-206.

Erickson, G. M., P. J. Makovicky, P. J. Currie, M. A. Norell, S. A. Yerby, and C. A. Brochu. 2004. Gigantism and comparative life-history parameters of tyrannosaurid dinosaurs. Nature 430: 772-775.

Erickson, G. M., P. J. Makovicky, B. D. Inouye, C. F. Zhou, and K. Q. Gao. 2009. A Life Table for *Psittacosaurus lujiatunensis*: Initial Insights Into Ornithischian Dinosaur Population Biology (vol 292, pg 1514, 2009). Anatomical Record-Advances in Integrative Anatomy and Evolutionary Biology 292: 1684-1684.

Erickson, G. M., K. C. Rogers, and S. A. Yerby. 2001. Dinosaurian growth patterns and rapid avian growth rates. Nature 412: 429-433.

Erickson, G. M., and T. A. Tumanova. 2000. Growth curve of *Psittacosaurus mongoliensis* Osborn (Ceratopsia : Psittacosauridae) inferred from long bone histology. Zoological Journal of the Linnean Society 130: 551-566.

Esteban, M. 1976. Vadose Pisolite and Caliche: GEOLOGIC NOTES. AAPG Bulletin 60: 2048-2057.

Esteban, M., and C. F. Klappa. 1983. Subaerial exposure environment; pp. 1-54, Carbonate depositional environments. American Association of Petroleum Geologists Tulsa, Okla.

Estes, R. 1991. The behavior guide to African mammals. University of California Press Berkeley.

Fastovsky, D., D. Weishampel, M. Watabe, R. Barsbold, K. Tsogtbaatar, and P. Narmandakh. 2011. A nest of *Protoceratops andrewsi* (Dinosauria, Ornithischia). Journal of Paleontology 85: 1035-1041.

Fastovsky, D. E., D. Badamgarav, H. Ishimoto, M. Watabe, and D. B. Weishampel. 1997. The paleoenvironments of Tugrikin-Shireh (Gobi Desert, Mongolia) and aspects of the taphonomy and paleoecology of *Protoceratops* (Dinosauria: Ornithishichia). Palaios: 59-70.

Fernandez-Jalvo, Y. 1988. Tafonomia de Microvertebrados en Gran Dolina, Atapuerca (Burgos). Ph. D. Thesis, Facultad de Ciencias Geologicas, Universidad Complutense de Madrid, 1988, unpublished.

Fiorillo, A. R. 1988. Taphonomy of Hazard Homestead Quarry (Ogallala Group), Hitchcock County, Nebraska. Rocky Mountain Geology 26: 57-97.

Flowerdew, J. R., and M. A. Sleigh. 1987. Mammals: their reproductive biology and population ecology. Edward Arnold Baltimore.

Ford, T. L., and L. D. Martin. 2010: A semi-aquatic life habit for *Psittacosaurus*. Paper presented at the New Perspectives on Horned Dinosaurs: The Royal Tyrrell Museum Ceratopsian Symposium, 2010.

Fowler, D. W., H. N. Woodward, E. A. Freedman, P. L. Larson, and J. R. Horner. 2011. Reanalysis of "*Raptorex kriegsteini*": a juvenile tyrannosaurid dinosaur from Mongolia. PloS one 6: e21376.

Fox, R. C. 1978. Upper Cretaceous terrestrial vertebrate stratigraphy of the Gobi Desert (Mongolian People's Republic) and western North America. Geological Association of Canada Special Paper 18: 571-594.

Francillon-Vieillot, H., V. De Buffrénil, J. Castanet, J. Géraudie, F. J. Meunier, J. Y. Sire, L. Zylberberg, and A. De Ricqlès. 1990. Microstructure and mineralization of vertebrate skeletal tissues; pp. 471-548 *i*n J. G. Carter (ed.), Skeletal biomineralization: patterns, processes and evolutionary trends. Van Nostrand Reinhold, New York.

Frost, H. M. 1990. Skeletal structural adaptations to mechanical usage (SATMU): 2. Redefining Wolff's Law: The remodeling problem. The Anatomical Record 226: 414-422.

Garcia, B. J. 2011. Skeletochronology of the American Alligator (*Alligator mississippiensis*): Examination of the Utility of Elements for Histological Study. Florida State University.

Gilmore, C. W. 1933. Two new dinosaurian reptiles from Mongolia with notes on some fragmentary specimens. American Museum Novitates 679: 1-20.

Gradziński, R. 1970. Sedimentation of dinosaur-bearing Upper Cretaceous deposits of the Nemegt Basin, Gobi Desert. Palaeontologia Polonica 21: 147-229.

Gradziński, R., and T. Jerzykiewicz. 1972. Additional geographical and geological data from the Polish-Mongolian Palaeontological Expeditions. Palaeontologia Polonica 22: 17-32.

Gradziński, R., and T. Jerzykiewicz. 1974. Dinosaur and mammal-bearing aeolian and associated deposits of the Upper Cretaceous in the Gobi Desert (Mongolia). Sedimentary Geology 12: 249-278.

Gradziński, R., Z. Kielan-Jaworowska, and T. Maryańska. 1977. Upper Cretaceous Djadokhta, Barun Goyot and Nemegt formations of Mongolia, including remarks on previous subdivisions. Acta Geologica Polonica 27: 281-318.

Granger, W., and W. K. Gregory. 1923. *Protoceratops andrewsi*, a pre-ceratopsian dinosaur from Mongolia. American Museum Novitates 42: 1-9.

Gregory, W. K., and C. C. Mook. 1925. On *Protoceratops*, a primitive ceratopsian dinosaur from the Lower Cretaceous of Mongolia. American Museum of Natural History.

Gross, W. 1934. Die Typen des mikroskopischen Knochenbaues bei fossilen Stegoccphalen und Reptilien. Anatomy and Embryology 103: 731-764.

Harland, W. B., R. L. Armstrong, A. V. Cox, L. E. Craig, A. G. Smith, and D. G. Smith. 1990. A geologic time scale. Cambridge: Cambridge University Press: 263.

Hartley, A. J. 1993. Sedimentological response of an alluvial system to source area tectonism: the Seilao Member of the Late Cretaceous to Eocene Purilactis Formation of northern Chile. Alluvial Sedimentation: 489-500.

Hasegawa, H., R. Tada, N. Ichinnorov, and C. Minjin. 2009. Lithostratigraphy and depositional environments of the Upper Cretaceous Djadokhta Formation, Ulan Nuur basin, southern Mongolia, and its paleoclimatic implication. Journal of Asian Earth Sciences 35: 13-26.

Haynes, G. 1983. Frequencies of spiral and green-bone fractures on ungulate limb bones in modern surface assemblages. American antiquity: 102-114.

Horner, J., K. Padian, and A. de Ricqlès. 1997. Histological analysis of a dinosaur skeleton: evidence of skeletal growth variation. Journal of Morphology 232: 267.

Horner, J. R., A. de Ricqles, and K. Padian. 1999. Variation in dinosaur skeletochronology indicators: implications for age assessment and physiology. Paleobiology 25: 295-304.

Horner, J. R., A. de Ricqles, and K. Padian. 2000. Long bone histology of the hadrosaurid dinosaur *Maiasaura peeblesorum*: growth dynamics and physiology based on an ontogenetic series of skeletal elements. Journal of Vertebrate Paleontology 20: 115-129.

Horner, J. R., and M. B. Goodwin. 2006. Major cranial changes during *Triceratops* ontogeny. Proceedings of the Royal Society of London B: Biological Sciences 273: 2757-2761.

Horner, J. R., and M. B. Goodwin. 2009. Extreme cranial ontogeny in the Upper Cretaceous dinosaur *Pachycephalosaurus*. PloS one 4: e7626.

Horner, J. R., and R. Makela. 1979. Nest of juveniles provides evidence of family structure among dinosaurs.

Horner, J. R., and K. Padian. 2004. Age and Growth Dynamics of *Tyrannosaurus*. Proceedings: Biological Sciences 271: 1875-1880.

Hu, Y., J. Meng, Y. Wang, and C. Li. 2005. Large Mesozoic mammals fed on young dinosaurs. Nature 433: 149-152.

Ishigaki, S., M. Watabe, K. Tsogtbaatar, and M. Saneyoshi. 2010. Dinosaur footprints from the Upper Cretaceous of Mongolia. Geological Quarterly 53: 449-460.

Jerzykiewicz, T. 1989: Upper Cretaceous dinosaur-bearing eolianites in the Mongolian Basin. Paper presented at the Sixth Symposium on Mesozoic Terrestrial Ecosystems: abstracts, 1989.

Jerzykiewicz, T. 2000. Lithostratigraphy and sedimentary settings of the Cretaceous dinosaur beds of Mongolia.; pp. 279-296 *i*n M. J. Benton, M. A. Shishkin, and D. M. Unwin (eds.), The age of dinosaurs in Russia and Mongolia. Cambridge University Press.

Jerzykiewicz, T., P. Currie, D. Eberth, P. Johnston, E. Koster, and J.-J. Zheng. 1993. Djadokhta Formation correlative strata in Chinese Inner Mongolia: an overview of the stratigraphy, sedimentary geology, and paleontology and comparisons with the type locality in the pre-Altai Gobi. Canadian Journal of Earth Sciences 30: 2180-2195.

Jerzykiewicz, T., and D. A. Russell. 1991. Late Mesozoic stratigraphy and vertebrates of the Gobi Basin. Cretaceous Research 12: 345-377.

Jiang, B., and J. Sha. 2007. Preliminary analysis of the depositional environments of the Lower Cretaceous Yixian Formation in the Sihetun area, western Liaoning, China. Cretaceous Research 28: 183-193.

Kalandadze, N. N., and S. M. Kurzanov. 1974. Lower Cretaceous localities of terrestrial vertebrates of Mongolia. Trudy Sovmestnoi Sovetsko-Mongol'skoi Paleontologicheskoi Ekspeditsii 1: 9-18.

Karhu, A. A., and A. S. Rautian. 1996. A new family of Maniraptora (Dinosauria: Saurischia) from the Late Cretaceous of Mongolia. Paleontological journal c/c of paleontologicheskii zhurnal 30: 583-592.

Khand, Y., D. Badamgarav, Y. Ariunchimeg, and R. Barsbold. 2000. Cretaceous System in Mongolia and its depositional environments. Cretaceous Environments of Asia. 17: 49-79.

Klein, N., and M. Sander. 2008. Ontogenetic stages in the long bone histology of sauropod dinosaurs. Paleobiology 34: 247-263.

Klein, N., T. Scheyer, and T. Tütken. 2009. Skeletochronology and isotopic analysis of a captive individual of *Alligator mississippiensis* Daudin, 1802. Fossil Record 12: 121-131.

Ksepka, D. T., and M. A. Norell. 2006. Erketu ellisoni, a long-necked sauropod from Bor Guvé (Dornogov Aimag, Mongolia). American Museum Novitates: 1-16.

Kurochkin, E. N., R. Barsbold, M. J. Benton, M. A. Shishkin, D. M. Unwin, and E. N. Kurochkin. 2000. The Russian-Mongolian expeditions and research in vertebrate paleontology. The age of dinosaurs in Russia and Mongolia: 235-255.

Kurzanov, S. M. 1976. A new late Cretaceous carnosaur from Nogon-Tsav, Mongolia. Results of the Soviet-Mongolian Paleontological Expedition 3: 93-104.

Kurzanov, S. M. 1981. An unusual theropod from the Upper Cretaceous of Mongolia. Joint Soviet-Mongolian Paleontological Expedition 15: 39-49.

Kurzanov, S. M. 1992. A giant protoceratopsid from the Upper Cretaceous of Mongolia. Paleontologicheskii Zhurnal: 81-93.

Kurzanov, S. M., and H. Osmólska. 1991. *Tochisaurus nemegtensis* gen. et sp. n., a new troodontid (Dinosauria, Theropoda) from Mongolia. Acta Palaeontologica Polonica 36.

Lacovara, K., M. Lamanna, J. Smith, B. Grandstaff, and J. Smith. 2002. Concentration and preservation potential of vertebrate fossils within coastal lithosomes:

examples from the Upper Cretaceous Bahariya Formation of Egypt. Journal of Vertebrate Paleontology 22.

Lamm, E.-T. 2013. Preparation and sectioning of specimens. Bone histology of fossil tetrapods: advancing methods, analysis, and interpretation: 55-160.

Lee, Y.-N., R. Barsbold, P. J. Currie, Y. Kobayashi, H.-J. Lee, P. Godefroit, F. Escuillié, and T. Chinzorig. 2014. Resolving the long-standing enigmas of a giant ornithomimosaur *Deinocheirus mirificus*. Nature 515: 257-260.

Leeder, M. R. 1975. Pedogenic carbonates and flood sediment accretion rates: a quantitative model for alluvial arid-zone lithofacies. Geological Magazine 112: 257-270.

Lefeld, J. 1971. Geology of the Djadokhta Formation at Bayn Dzak (Mongolia). Palaeontologia Polonica 25: 101-127.

Lillegraven, J. A., and M. C. McKenna. 1986. Fossil mammals from the" Mesaverde" Formation (late Cretaceous, Judithian) of the Bighorn and Wind River basins, Wyoming: with definitions of late Cretaceous North American land-mammal" ages". American Museum novitates; no. 2840.

Lockley, M. G., K. Carpenter, K. F. Hirsch, and J. R. Horner. 1994. Dinosaur ontogeny and population structure: interpretations and speculations based on fossil footprints. Dinosaur eggs and babies: 347-370.

Lockley, M. G., D. D. Gillette, D. D. Gillette, and M. G. Lockley. 1989. Dinosaur tracks and traces: an overview. Dinosaur tracks and traces: 3-10.

Longrich, N. 2010: The function of large eyes in *Protoceratops*: a nocturnal ceratopsian. Paper presented at the New perspectives on horned dinosaurs: The Royal Tyrrell Museum Ceratopsian Symposium. Indiana University Press, Bloomington, 2010.

Loope, D. B., L. Dingus, C. C. Swisher, and C. Minjin. 1998. Life and death in a Late Cretaceous dune field, Nemegt basin, Mongolia. Geology 26: 27-30.

Lowe, D. R. 1982. Sediment gravity flows: II Depositional models with special reference to the deposits of high-density turbidity currents. Journal of Sedimentary Research 52.

Lü, J. C., Y. Tomida, Y. Azuma, Z. M. Dong, and Y.-N. Lee. 2004. New oviraptorid dinosaur (Dinosauria: Oviraptorosauria) from the Nemegt Formation of southwestern Mongolia. Bulletin of the National Science Museum of Tokyo Series C (Geology & Paleontology) 30: 95-130.

Mack, G. H., W. C. James, and H. C. Monger. 1993. Classification of paleosols. Geological Society of America Bulletin 105: 129-136.

Makovicky, P., R. Sadleir, P. Dodson, G. E. Erickson, and M. Norell. 2007. Life history of *Protoceratops andrewsi* from Bayn Zag, Mongolia.: In *67th Annual Meeting, Society of Vertebrate Paleontology. Program and Abstracts*, Austin, TX.

Makovicky, P. J., B. M. Kilbourne, R. W. Sadleir, and M. A. Norell. 2011. A new basal ornithopod (Dinosauria, Ornithischia) from the Late Cretaceous of Mongolia. Journal of Vertebrate Paleontology 31: 626-640.

Makovicky, P. J., and M. A. Norell. 2006. *Yamaceratops dorngobiensis*, a new primitive ceratopsian (Dinosauria: Ornithischia) from the Cretaceous of Mongolia. American Museum Novitates: 1-42.

Maleev, E. A. 1952. A new family of armored dinosaurs from the Upper Cretaceous of Mongolia. Doklady Akademii Nauk SSSR 87: 1-134.

Maleev, E. A. 1954. New turtle-like reptile in Mongolia. Priroda 3: 106-108.

Maleev, E. A. 1955. New carnivorous dinosaurs from the Upper Cretaceous of Mongolia. Doklady Akademii Nauk SSSR 104: 779-782.

Mantell, G. A. 1850. On the Pelorosaurus; An Undescribed Gigantic Terrestrial Reptile Whose Remains are Associated with Those of the Iguanodon and Other Saurians in the Strata of Tilgate Forest, in Sussex. Philosophical Transactions of the Royal Society of London 140: 379-390.

Martin, C. A., and B. R. Turner. 1998. Origins of massive-type sandstones in braided river systems. Earth-Science Reviews 44: 15-38.

Martinson, G. G. 1982. The Upper Cretaceous mollusks of Mongolia; pp. 5-76 *i*n L. A. Nevesskaya (ed.), Sovmestnaya Sovetsko-Mongolskaya Paleontologicheskaya Ekspeditsia.

Martinson, G. G., and V. F. Shuvalov. 1976. Stratigraphy and fossil molluscs of the Lower Cretaceous lacustrine deposits of the Trans-Altai Gobi in Mongolia. Nauka, Leningrad.

Maryanska, T. 1977. Ankylosauridae (Dinosauria) from Mongolia. Palaeontologia Polonica 37: 85-151.

Maryanska, T., and H. Osmolska. 1974. Pachycephalosauria, a new suborder of ornithischian dinosaurs. Palaeontologia Polonica 30: 45-102.

Maryanska, T., and H. Osmólska. 1975. Protoceratopsidae (Dinosauria) of Asia. Palaeontologia Polonica 33: 133-181.

Maryanska, T., and H. Osmólska. 1981. First lambeosaurine dinosaur from the Nemegt formation, Upper Cretaceous, Mongolia. Acta Palaeontologica Polonica 26.

Matsukawa, M., H. Nagata, Y. Taketani, Y. Khanda, P. Khosbajar, D. Badamgarav, and I. Obata. 1997. Dinosaur bearing Lower Cretaceous deposits in the Choir Basin, S.E. Mongolia-Stratigraphy and Sedimentary Environments. Journal of the Geological Society of the Philippines. 52: 99-114.

Matthew, W. D., H. F. Osborn, and B. Brown. 1915. Dinosaurs with Special Reference to the American Museum: Collections. American museum of natural history.

Meng, Q., J. Liu, D. J. Varricchio, T. Huang, and C. Gao. 2004. Palaeontology: Parental care in an ornithischian dinosaur. Nature 431: 145-146.

Meyer, G. A., and S. G. Wells. 1997. Fire-related sedimentation events on alluvial fans, Yellowstone National Park, USA. Journal of Sedimentary Research 67.

Miall, A. D. 1977. Lithofacies types and vertical profile models in braided river deposits: a summary.

Miall, A. D. 2006. The Geology of Fluvial Deposits: Sedimentary Facies, Basin Analysis, and Petroleum Geology. 582 pp., Springer-Verlag.

Middleton, G. V., and M. Hampton. 1976. Subaqueous sediment transport and deposition by sediment gravity waves.

Mikhailov, K. E. 1997. How Dinosaurs Nested. Nauka Zhizn': 73-79.

Mook, C. C. 1918. The habitat of the sauropod dinosaurs. The Journal of Geology: 459-470.

Mulder, T., and J. Alexander. 2001. The physical character of subaqueous sedimentary density flows and their deposits. Sedimentology 48: 269-299.

Munsell Color, C. O. 2000. Munsell soil color charts. Gretabacbeth.

Myhrvold, N. P. 2013. Revisiting the estimation of dinosaur growth rates. PloS one 8: e81917.

Nadon, G. C. 1993. The association of anastomosed fluvial deposits and dinosaur tracks, eggs, and nests: Implications for the interpretation of floodplain environments and a possible survival strategy for ornithopods. Palaios: 31-44.

Namnandorzhi, O. 1957. Traces of huge lizards in Mongolia. Priroda 44: 110-111.

Nemec, W., and R. J. Steel. 1984. Alluvial and coastal conglomerates: their significant features and some comments on gravelly mass-flow deposits.

Nesbitt, S. J., J. A. Clarke, A. H. Turner, and M. A. Norell. 2011. A small alvarezsaurid from the eastern Gobi Desert offers insight into evolutionary patterns in the Alvarezsauroidea. Journal of Vertebrate Paleontology 31: 144-153.

Newton, I. 1989. Lifetime reproduction in birds. Academic Press.

Niedźwiedzki, G., T. Singer, G. D. Gierliński, and M. G. Lockley. 2012. A protoceratopsid skeleton with an associated track from the Upper Cretaceous of Mongolia. Cretaceous Research 33: 7-10.

Nopcsa, F. B. 1933: 11. On the Histology of the Ribs in Immature and Half-grown Trachodont Dinosaurs. Paper presented at the Proceedings of the Zoological Society of London, 1933.

Norell, M. A., J. M. Clark, L. M. Chiappe, and D. Dashzeveg. 1995. A nesting dinosaur. Nature 378: 774-776.

Norell, M. A., J. M. Clark, D. Demberelyin, B. Rhinchen, L. M. Chiappe, A. R. Davidson, M. C. McKenna, P. Altangerel, and M. J. Novacek. 1994. A theropod dinosaur embryo and the affinities of the Flaming Cliffs dinosaur eggs. Science 266: 779-782.

Norell, M. A., J. M. Clark, A. H. Turner, P. J. Makovicky, R. Barsbold, and T. Rowe. 2006. A new dromaeosaurid theropod from Ukhaa Tolgod (Ömnögov, Mongolia). American Museum Novitates: 1-51.

Norell, M. A., P. J. Makovicky, G. S. Bever, A. M. Balanoff, J. M. Clark, R. Barsbold, and T. Rowe. 2009. A review of the Mongolian Cretaceous dinosaur *Saurornithoides* (Troodontidae: Theropoda). American Museum Novitates: 1-63.

Norman, D. B. 1998. On Asian ornithopods (Dinosauria: Ornithischia). 3. A new species of iguanodontid dinosaur. Zoological Journal of the Linnean Society 122: 291-348.

Novacek, M. J. 1996. Dinosaurs of the Flaming Cliff. 369, Doubleday, New York.

Novacek, M. J., M. Norell, M. C. McKenna, and J. Clark. 1994. Fossils of the Flaming Cliffs. Scientific American 271: 60-69.

Obata, I., and M. Matsukawa. 1996. Kyouryuu no michi (Road of dinosaur). Catalogue for the Special Exhibit. Nakazato Village, Gunma Prefecture, Japan.

Osborn, H. F. 1923. Two Lower Cretaceous dinosaurs of Mongolia. American Museum Novitates 95: 10.

Osborn, H. F. 1924a. *Psittacosaurus* and *Protiguanodon*: two Lower Cretaceous iguanodonts from Mongolia. American Museum Novitates 127: 16.

Osborn, H. F. 1924b. Sauropoda and Theropoda of the Lower Cretaceous of Mongolia. American Museum Novitates 128: 7.

Osborn, H. F., P. C. Kaisen, and G. Olsen. 1924. Three new theropoda, *Protoceratops* zone, central Mongolia. American Museum of Natural History.

Osmólska, H. 1981. Coossified tarsometatarsi in theropod dinosaurs and their bearing on the problem of bird origins. Palaeontologica Polonica 42: 79-95.

Osmólska, H. 1982. *Hulsanpesperlei* ng, n. sp.(Deinonychosauria, Saurischia, Dinosauria) from the Upper Cretaceous Barun Goyot Formation of Mongolia. Neues Jahrbuchfur Geologie und Palaontologie, Monatshefte 1982: 440-448.

Osmólska, H., and E. Roniewicz. 1970. Deinocheiridae, a new family of theropod dinosaurs. Palaeontologica Polonica 21: 5-19.

Osmólska, H., E. Roniewicz, and R. Barsbold. 1972. A new dinosaur, *Gallimimus bullatus* n. gen., n. sp.(Ornithomimidae) from the Upper Cretaceous of Mongolia. Palaeontologia Polonica 27: 103-143.

Parfitt, A. M. 1994. Osteonal and hemi-osteonal remodeling: the spatial and temporal framework for signal traffic in adult human bone. Journal of cellular biochemistry 55: 273-286.

Pelletier, F., and M. Festa-Bianchet. 2004. Effects of body mass, age, dominance and parasite load on foraging time of bighorn rams, *Ovis canadensis*. Behavioral Ecology and Sociobiology 56: 546-551.

Perle, A. 1979. Segnosauridae - the new family of Theropoda from Lower Cretaceous of Mongolia. Trudy, Sovmestnaâ Sovetsko− Mongol'skaâ paleontologičeskaâ èkspediciâ 8: 45-55.

Perle, A. 1981. Nova segnozavrid iz verchnego mela Mongolii. Trudy - Sovmestnaya Sovetsko-Mongol'skaya Paleontologicheskaya Ekspeditsiya 15: 50-59.

Perle, A., L. M. Chiappe, and R. Barsbold. 1994. Skeletal morphology of *Mononykus olecranus* (Theropoda: Avialae) from the late Cretaceous of Mongolia. American Museum Novitates/American Museum of natural history.

Perle, A., T. Maryanska, and H. Osmólska. 1982. *Goyocephale lattimorei* gen. et sp. n., a new flat-headed pachycephalosaur (Ornlthlschia, Dinosauria) from the Upper Cretaceous of Mongolia. Acta Palaeontologica Polonica 27.

Perle, A., M. Norell, and J. M. Clark. 1999. A New Maniraptoran Theropod, *Achillobator giganticus* (Dromaeosauridae), from the Upper Cretaceous of Burkhant, Mongolia. Geology and Mineralogy Chair, National University of Mongolia.

Pierson, T. C., and J. E. Costa. 1987. A rheologic classification of subaerial sediment-water flows. Reviews in Engineering Geology 7: 1-12.

Pierson, T. C., and K. M. Scott. 1985. Downstream dilution of a lahar: transition from debris flow to hyperconcentrated streamflow. Water resources research 21: 1511-1524.

Ponton, F., A. Elżanowski, J. Castanet, A. Chinsamy, E. De Margerie, A. De Ricqlès, and J. Cubo. 2004. Variation of the outer circumferential layer in the limb bones of birds. Acta Ornithologica 39: 137-140.

Prieto-Márquez, A. 2011. A reapprisal of *Barsboldia sicinskii* (Dinosauria: Hadrosauridae) from the Late Cretaceous of Mongolia. Journal of Paleontology 85: 468-477.

Reid, R. H. 1981. Lamellar-zonal bone with zones and annuli in the pelvis of a sauropod dinosaur. Nature 292: 49-51.

Reizner, J., and J. R. Horner. 2006. An ontogenetic series of the ceratopsid dinosaur *Einiosaurus procurvicornis* as determined by long bone histology.: In *66th Annual Meeting, Society of Vertebrate Paleontology. Program and Abstracts.*, Ottawa, ONT.

Rogers, R. R. 1990. Taphonomy of three dinosaur bone beds in the Upper Cretaceous Two Medicine Formation of northwestern Montana: evidence for drought-related mortality. Palaios: 394-413.

Rozhdestvensky, A. K. 1952. A new representative of duckbilled dinosaurs from the Upper Cretaceous deposits of Mongolia. Doklady Akademii SSSR 86: 405-408.

Rozhdestvensky, A. K. 1955a. The first discovery of a dinosaur in the USSR in the indigenous locality. Byuleten' Moskovskogo Obschestva Ispytate lei Prirody, Otdel Geologicheskii 30: 118.

Rozhdestvensky, A. K. 1955b. New data on *Psittacosaurus* - Cretaceous ornithopods. Questions on the Geology of Asia 2: 783-788.

Rozhdestvensky, A. K. 1965. Growth changes in Asian dinosaurs and some problems of their taxonomy. Paleontologičeskij žurnal 3: 95-109.

Rozhdestvensky, A. K. 1970. Giant claws of enigmatic Mesozoic reptiles. Paleontol. J 1970: 117-125.

Russell, D. A., and X.-J. Zhao. 1996. New psittacosaur occurrences in Inner Mongolia. Canadian Journal of Earth Sciences 33: 637-648.

Sampson, S. D., M. J. Ryan, and D. H. Tanke. 1997. Craniofacial ontogeny in centrosaurine dinosaurs (Ornithischia: Ceratopsidae): taxonomic and behavioral implications. Zoological Journal of the Linnean Society 121: 293-337.

Sander, P. M. 2000. Longbone histology of the Tendaguru sauropods: implications for growth and biology. Paleobiology 26: 466-488.

Sander, P. M., and N. Klein. 2005. Developmental plasticity in the life history of a prosauropod dinosaur. Science 310: 1800-1802.

Scannella, J. B., and J. R. Horner. 2010. *Torosaurus* Marsh, 1891, is *Triceratops* Marsh, 1889 (Ceratopsidae: Chasmosaurinae): synonymy through ontogeny. Journal of Vertebrate Paleontology 30: 1157-1168.

Schweitzer, M., J. Watt, R. Avci, L. Knapp, L. Chiappe, M. Norell, and M. Marshall. 1999. Beta-keratin specific immunological reactivity in feather-like structures of the Cretaceous Alvarezsaurid, *Shuvuuia deserti*. Journal of Experimental Zoology 285: 146-157.

Schweitzer, M. H., R. M. Elsey, C. G. Dacke, J. R. Horner, and E. T. Lamm. 2007. Do egg-laying crocodilian (*Alligator mississippiensis*) archosaurs form medullary bone? Bone 40: 1152-1158.

Scott, K. M. 1988. Origins, behavior, and sedimentology of lahars and lahar-runout flows in the Toutle-Cowlitz River system, Report 2330-7102.

Seitz, A. L. L. 1907. Vergleichende Studien über den mikroskopischen Knochenbau fossiler und rezenter Reptilien und dessen Bedeutung für das Wachstum und Umbildung des Knochengewebes im allgemein. E. Karras.

Sereno, P. C. 1987. The Ornithischian Dinosaur *Psittacosaurus* from the Lower Cretaceous of Asia and the Relationships of the Ceratospia. Columbia University New York.

Sereno, P. C. 2000. The fossil record, systematics and evolution of pachycephalosaurs and ceratopsians from Asia. The Age of Dinosaurs in Russia and Mongolia. Cambridge University Press, Cambridge: 480-516.

Sereno, P. C. 2010: Taxonomy, cranial morphology, and relationships of parrot-beaked dinosaurs (Ceratopsia: *Psittacosaurus*). Paper presented at the New perspectives on horned dinosaurs: The Royal Tyrrell Museum ceratopsian symposium, 2010.

Sereno, P. C., Z. Xijin, and T. Lin. 2009. A new psittacosaur from Inner Mongolia and the parrot-like structure and function of the psittacosaur skull. Proceedings of the Royal Society B: Biological Sciences.

Shipman, P. 1981. Life History of a Fossil and Introduction To Taphonomy and Paleoecology. 222.

Shultz, A. W. 1984. Subaerial debris-flow deposition in the upper Paleozoic Cutler Formation, western Colorado. Journal of Sedimentary Research 54.

Shuvalov, V. F. 1974. On the geology and age of the Khobur and Khuren Dukh localities in Mongolia. Trudy Sovmetstnoi Sovetsko-Mongol'skoi Paleontologicheskoya Ekspeditsii. 1: 296-304.

Shuvalov, V. F. 1975a. A new Early Cretaceous dinosaur locality Builyasutuin Khuduk; pp. 210-213 *i*n N. N. Kramarenko (ed.), Fossil Fauna and Flora of Mongolia. Trudy Sovmest. Soviet-Mongol. Nauka, Moscow.

Shuvalov, V. F. 1975b. The Stratigraphy of Mesozoic of Central Mongolia. Trudy Sovmestnoi Sovetsko-Mongol'skoi Geologicheskoi Ekspeditsii. 13: 50-112.

Shuvalov, V. F. 1994. Paleogeography of the lakes of Mongolia in the Mesozoic; pp. *i*n D. V. Sevastyanov, V. F. Shuvalov, and I. Neustrueva, Yu (eds.), Limnology and Paleolimnology of Mongolia. Nauka, Leningrad.

Shuvalov, V. F. 2000. The Cretaceous stratigraphy and palaeobiography of Mongolia.; pp. 256-279 *i*n M. J. Benton, M. A. Shishkin, D. M. Unwin, and E. N. Kurochkin (eds.), The age of dinosaurs in Russia and Mongolia. Cambridge University Press.

Shuvalov, V. F., and T. V. Nikolaeva. 1985. On the age and territorial distribution of Cenozoic basalts in the south of Mongolia. Vestnik Leningradskogo Universiteta: Geologiya, Geografiya 7: 52-59.

Sinitsa, S. M. 1993. Jurassic and Lower Cretaceous of Central Mongolia. Trudy Sovmetstnoi Sovetsko-Mongol'skoi Paleontologicheskoya Ekspeditsii. 42: 3-238.

Smith, G. A. 1986. Coarse-grained nonmarine volcaniclastic sediment: terminology and depositional process. Geological Society of America Bulletin 97: 1-10.

Sochava, A. V. 1975. Stratigraphy and lithology of the Upper Cretaceous deposits of South Mongolia. Trudy Sovmestnoi Sovetsko-Mongol'skoi Paleontologicheskoi Ekspeditsii. 13: 113-182.

Sohn, Y. K., C. W. Rhee, and B. C. Kim. 1999. Debris flow and hyperconcentrated flood-flow deposits in an alluvial fan, northwestern part of the Cretaceous Yongdong basin, central Korea. The Journal of Geology 107: 111-132.

Solovyev, N. S., G. A. Shatkov, and L. N. Yakobson. 1977. [The Pri-Argun Mongolian volcanic belt]. Geology and Geophysics 3: 20-31.

Spinage, C. A. 1972. African ungulate life tables. Ecology: 645-652.

Stauffer, P. H. 1967. Grain-flow deposits and their implications, Santa Ynez Mountains, California. Journal of Sedimentary Research 37.

Stewart, D. J. 1981. A meander-belt sandstone of the Lower Cretaceous of Southern England. Sedimentology 28: 1-20.

Suslov, Y. V. 1983. The burial of psittacosaurs at Khamryn-Us (Eastern Gobi, MPR). Trudy Sovmetstnoi Sovetsko-Mongol'skoi Paleontologicheskoya Ekspeditsii.: 118-120.

Tereschenko, V. 2008. Adaptive features of protoceratopsoids (Ornithischia: Neoceratopsia). Paleontological Journal 42: 273-286.

Tereschenko, V. S., and V. R. Alifanov. 2003. *Bainoceratops efremovi*, a new protoceratopid dinosaur (Protoceratopidae, Neoceratopsia) from the Bain-Dzak locality (south Mongolia). Paleontological journal c/c of paleontologicheskii zhurnal 37: 293-302.

Todd, S. P. 1989. Stream-driven, high-density gravelly traction carpets: possible deposits in the Trabeg Conglomerate Formation, SW Ireland and some theoretical considerations of their origin. Sedimentology 36: 513-530.

Tooruul, N. 1986. Geological report N. 3912. Ministry of Geology and Mining, Mongolia.

Tsuihiji, T., R. Barsbold, M. Watabe, K. Tsogtbaatar, T. Chinzorig, Y. Fujiyama, and S. Suzuki. 2014. An exquisitely preserved troodontid theropod with new information on the palatal structure from the Upper Cretaceous of Mongolia. Naturwissenschaften 101: 131-142.

Tsuihiji, T., M. Watabe, K. Tsogtbaatar, T. Tsubamoto, R. Barsbold, S. Suzuki, A. H. Lee, R. C. Ridgely, Y. Kawahara, and L. M. Witmer. 2011. Cranial osteology of a juvenile specimen of *Tarbosaurus bataar* (Theropoda, Tyrannosauridae) from the Nemegt Formation (Upper Cretaceous) of Bugin Tsav, Mongolia. Journal of Vertebrate Paleontology 31: 497-517.

Tumanova, T. A. 1983. The first ankylosaur from the Lower Cretaceous of Mongolia. Transactions from the Joint Soviet–Mongolian Palaeontological Expedition 24: 110-118.

Tumanova, T. A. 1993. On A New Armored Dinosaur from Southeastern Gobi. Paleontologicheskii Zhurnal: 92.

Turner, A. H., S. H. Hwang, and M. A. Norell. 2007a. A small derived Theropod from Oosh, Early Cretaceous, Baykhangor Mongolia. American Museum Novitates 3557: 1-27.

Turner, A. H., S. J. Nesbitt, and M. A. Norell. 2009. A large alvarezsaurid from the Late Cretaceous of Mongolia. American Museum Novitates: 1-14.

Turner, A. H., D. Pol, J. A. Clarke, G. M. Erickson, and M. A. Norell. 2007b. A basal dromaeosaurid and size evolution preceding avian flight. Science 317: 1378-1381.

Varricchio, D. J. 1993. Bone microstructure of the Upper Cretaceous theropod dinosaur *Troodon formosus*. Journal of Vertebrate Paleontology 13: 99-104.

Verzilin, N. N. 1979a. Cretaceous deposits of Khar Hotol and the problem of Sainshand svita. Bulletin Moskovskogo Obshchestva Ispytatelei Prirody, Otdel Geologicheskii 54: 123.

Verzilin, N. N. 1979b. Genesis of the Upper Cretaceous deposits of South Mongolia on the basis of taphonomic observations. Vestnik Leningradskogo Universiteta: Geologiya, Geografiya 12: 7-13.

Verzilin, N. N. 1980. Special features of deposition of sediments in the territory of South Mongolia in Late Cretaceous time. Vestnik Leningradskogo Universiteta: Geologiya, Geografiya 14: 18-27.

Verzilin, N. N. 1982. Palaeolimnological significance of a peculiarity in the texture of the Upper Cretaceous deposits of Mongolia; pp. 81-100 *i*n G. G. Martinson (ed.), Mesozoic Lake Basins of Mongolia. Nauka, Leningrad.

Wan, Z., Z. Wang, and P. Julien. 1994. Hyperconcentrated flow. Journal of Hydraulic Engineering 120: 1234-1234.

Watabe, M., and S. Suzuki. 2000. Report on the Japan− Mongolia Joint Paleontological expedition to the Gobi desert, 1996. Hayashibara Museum of Natural Sciences Research Bulletin 1: 58-68.

Watabe, M., K. Tsogtbaatar, and R. Barsbold. 2008. First discovery of a theropod (Dinosauria) from the Upper Jurassic in Mongolia and its stratigraphy. Paleontological Research 12: 27-36.

Watabe, M., K. Tsogtbaatar, and R. M. Sullivan. 2011. A new pachycephalosaurid from the Baynshire Formation (Cenomanian-late Santonian), Gobi Desert, Mongolia. Bulletin of the New Mexico Museum of Natural History & Science 53: 489-497.

Webster, D. 1996. Dinosaurs of the Gobi: Buried by desert sandstorms 80 million years ago, wondrous creatures reveal themselves in well-preserved fossils of parents and nestlings. National Geographic 190: 70-89.

Weishampel, D. B., D. E. Fastovsky, M. Watabe, D. J. Varricchio, F. D. Jackson, K. Tsogtbaatar, and R. Barsbold. 2008. New oviraptorid embryos from Bugin-Tsav, Nemegt Formation (Upper Cretaceous), Mongolia, with insights into their habitat and growth. Journal of Vertebrate Paleontology 28: 1110-1119.

Werning, S. 2012. The ontogenetic osteohistology of *Tenontosaurus tilletti*. PloS one 7: e33539.

Woodward, H. N., E. A. F. Fowler, J. O. Farlow, and J. R. Horner. 2015. *Maiasaura*, a model organism for extinct vertebrate population biology: a large sample statistical assessment of growth dynamics and survivorship. Paleobiology 41: 503-527.

Woodward, H. N., J. R. Horner, and J. O. Farlow. 2011. Osteohistological Evidence for Determinate Growth in the American Alligator. Journal of Herpetology 45: 339-342.

Wright, V. P., and M. E. Tucker. 1991. Calcretes. Blackwell Scientific Publications.

Xing, X., and M. A. Norell. 2006. Non-avian dinosaur fossils from the Lower Cretaceous Jehol Group of western Liaoning, China. Geological Journal 41: 419-437.

Zhao, Q., P. M. Barrett, and D. A. Eberth. 2007. Social behaviour and mass mortality in the basal ceratopsian dinosaur *Psittacosaurus* (Early Cretaceous, People's Republic of China). Palaeontology 50: 1023-1029.

Zhao, Q., M. J. Benton, C. Sullivan, P. M. Sander, and X. Xu. 2013a. Histology and postural change during the growth of the ceratopsian dinosaur *Psittacosaurus lujiatunensis*. Nature communications 4.

Zhao, Q., M. J. Benton, X. Xu, and P. M. Sander. 2013b. Juvenile-only clusters and behaviour of the Early Cretaceous dinosaur *Psittacosaurus*. Acta Palaeontologica Polonica 59: 827-833.

Zhou, C.-F., K.-Q. Gao, R. C. Fox, and S.-H. Chen. 2006. A new species of *Psittacosaurus* (Dinosauria: Ceratopsia) from the Early Cretaceous Yixian Formation, Liaoning, China. Palaeoworld 15: 100-114.

Zhou, Z. 2006. Evolutionary radiation of the Jehol Biota: chronological and ecological perspectives. Geological Journal 41: 377-393.